

UNIVERSITÀ DEL PIEMONTE ORIENTALE

Department of Translational Medicine

PhD Program in Science & Medical Biotechnology

XXXII cycle

**From sunshine to hunger: impact of Vitamin D  
and Ghrelin on muscle homeostasis.**

SSD: MED/50

PhD coordinator:

Prof. Marisa Gariglio

PhD supervisor:

Prof. Nicoletta Filigheddu

PhD candidate:

Marilisa De Feudis

Academic years 2016-2019



## Table of contents

Summary .....	1
Skeletal muscle homeostasis.....	3
Sarcopenia.....	5
Cachexia .....	7
Vitamin D .....	10
Vitamin D and skeletal muscle .....	13
Vitamin D in sarcopenia .....	14
Vitamin D in cachexia .....	15
Introduction to the paper “Opposing effects of 25-hydroxy- and 1 $\alpha$ ,25-dihydroxy-vitamin D3 on pro-cachectic cytokine-and cancer conditioned medium-induced atrophy in C2C12 myotubes” .....	16
Introduction to the paper “Cholecalciferol (vitamin D3) has a direct protective activity against interleukin 6-induced atrophy in C2C12 myotubes” .....	28
Vitamin D and muscle homeostasis - Unpublished data .....	52
Ghrelin .....	55
Ghrelin and skeletal muscle.....	56
Ghrelin in cachexia .....	57
Ghrelin in sarcopenia.....	58
Introduction to the paper “Both ghrelin deletion and unacylated ghrelin overexpression preserve muscles in aging mice” .....	59
References.....	96
Appendix.....	110

## Summary

Skeletal muscle wasting occurs in several physio-pathological conditions and represents one of the main overlapping features between the physiological age-related sarcopenia and cachexia, which often associates with an underlying disease, such as cancer.

The physiopathology of both sarcopenia and cancer cachexia is complex and multifactorial, however hormonal network dysregulation co-occurs in both these muscle wasting-inducing conditions, where it might participate to prompt skeletal muscle decline. Vitamin D (VD) and Ghrelin came up among the dysregulated hormones in sarcopenia as well as in cancer cachexia.

Vitamin D (VD) is a pleiotropic hormone that, besides its well-known role in regulation of calcium and phosphate homeostasis, impacts on skeletal muscle homeostasis as well, and VD deficiency has been correlated with decrease in muscle mass, function, and performance in various conditions, including sarcopenia. Notably, in elderly subjects, VD supplementation was able to restore muscle strength and prevent muscle mass loss. Since VD deficiency is highly prevalent also among advanced cancer patients with cachexia, the encouraging results of VD supplementation on frail elderly subjects led to the hypothesis that VD supplementation could be used as an anti-cachexia treatment. However, VD administration was ineffective to counteract cancer cachexia associated-muscle wasting both in patients and in animal models.

We show how variously hydroxylated VD metabolites and the differential regulation of VD hydroxylases may trigger contrasting effects on skeletal muscle in vitro, thus explaining the opposite outcome of VD supplementation in vivo and paving the way to new drugs with restricted hydroxylability to overcome the limitations of VD supplementation in some pathological conditions.

Ghrelin is a gastric hormone peptide circulating in both acylated (AG) and unacylated (UnAG) forms. AG is the endogenous ligand of the growth hormone secretagogue receptor (GHSR-1a), and it is involved in metabolic regulation and energetic balance through induction of appetite, food intake, and adiposity. UnAG does not induce GH release and has no direct effects on food intake, but it shares

with AG several biological activities, in particular both AG and UnAG have direct biological activities in vitro on skeletal muscle.

Low ghrelin circulating levels have been observed in elderly subjects, and this condition could participate in the establishment of sarcopenia by facilitating the progression of muscle atrophy and limiting skeletal muscle regeneration capability.

Administration of AG analogues has been explored in several conditions characterized by muscle wasting, including cancer cachexia and aging. However, in sarcopenia, conversely to the beneficial effects observed in cancer cachexia, the administration of AG display scarce effect on skeletal muscle accompanied by an increase in adiposity that might worsen age-related insulin resistance and metabolic dysfunction.

We show that not only lifelong overexpression of UnAG in mice, but also the deletion of ghrelin gene attenuated the age-associated muscle atrophy and functionality decline, as well as systemic inflammation, prompting the design of UnAG mimetics which could be more useful than AG analogs for the treatment of sarcopenia.

## **Skeletal muscle homeostasis**

Skeletal muscle, which account for about half of mammals body weight, has evolved to allow movement in animals, indeed it has primarily characterized by its mechanical activity required for posture, movement, and breathing (Janessen et al. 2000).

The functional unit of skeletal muscle is a long cylindrical multinucleated myofibers composed by myofibrils made up of thousands of sarcomeres, containing the actin and myosin filaments that interact to produce contraction. Multinucleated myofibers originate from the fusion of many myoblasts during embryonic and foetal development, and post-natal growth (Mintz and Baker, 1967). Since skeletal muscle consists of the largest pool of proteins in the whole organism, this specific tissue is highly sensitive under conditions that alter protein balance. Indeed, skeletal muscle mass reflects protein turnover, depending on the balance between pathways favouring protein synthesis or breakdown. The best characterized anabolic pathway involves activation of the serine/threonine kinase Akt which results in downstream amplification of mammalian target of rapamycin (mTOR) that induces protein synthesis (Bodine et al, 2001). A variety of stimuli activate this pathway, such as insulin-like growth factor-1 (IGF-1), branched chain amino acids, exercise, and testosterone. On the other side, the ubiquitin proteasome pathway and autophagy-lysosome system are the major pathways driving muscle protein breakdown. These degradation systems are controlled by the transcription factors forkhead O (Fox-O) and nuclear factor (NF)- $\kappa$ B (Fig. 1). Among the ubiquitin-proteasome proteolytic system two genes, atrogin-1/MAFbx and MuRF1, have been observed dramatically upregulated prior the onset of muscle loss in multiple experimental models (Bodine et al., 2001; Taillandier et al., 2019). Both these genes encode proteins that are referred to as E3 ubiquitin ligases, which are responsible for substrate specificity of ubiquitin conjugation. The autophagy-lysosome system activation determines the formation of double-membrane vesicles named autophagosomes, which are able to engulf a portion of the cytosol and fuse with lysosomes, where their content is completely degraded by lytic enzymes. Although basal autophagy is crucial for the maintenance of muscle homeostasis, the overactivation of autophagic flux leads to muscle atrophy (Bonaldo and

Sandri, 2013). LC3, Gabarap and CathepsinL are autophagy-related genes upregulated in a variety of muscle wasting-associated conditions (Lecker et al., 2004; Satchek et al., 2007).

Myostatin, member of the transforming growth factor  $\beta$  (TGF $\beta$ ) family, is another negative regulator of muscle mass, downregulating the Akt/mTOR pathway and by decreasing the number of satellite cells (Sandri et al., 2008, 2010, 2013).

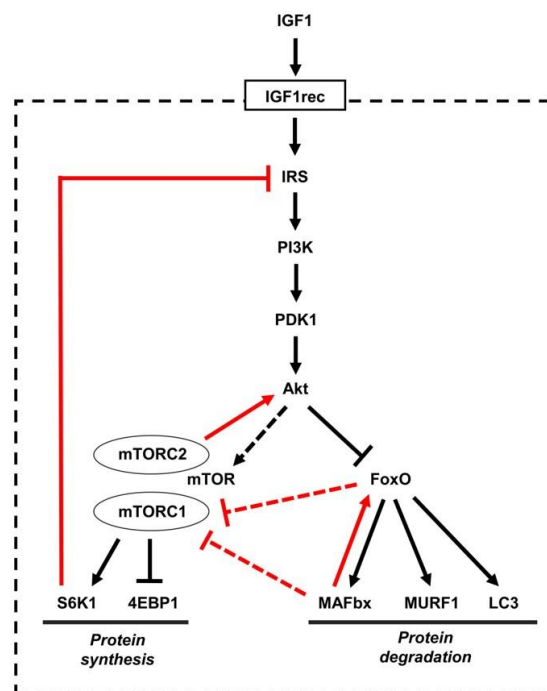


**Figure 1. Overview of IGF-1/Akt signalling pathway.** Scheme representing how IGF1/Akt pathway induces muscle growth by acting on mTOR and FoxO (Schiaffino and Mammucari, 2011).

The alteration of the balance between synthetic and degradation pathways results in muscle atrophy. Skeletal muscle impairment occurs in several conditions and represents one of the main overlapping features between cachexia, where is due to an underlying disease, and the physiologic sarcopenia (Fig. 2).

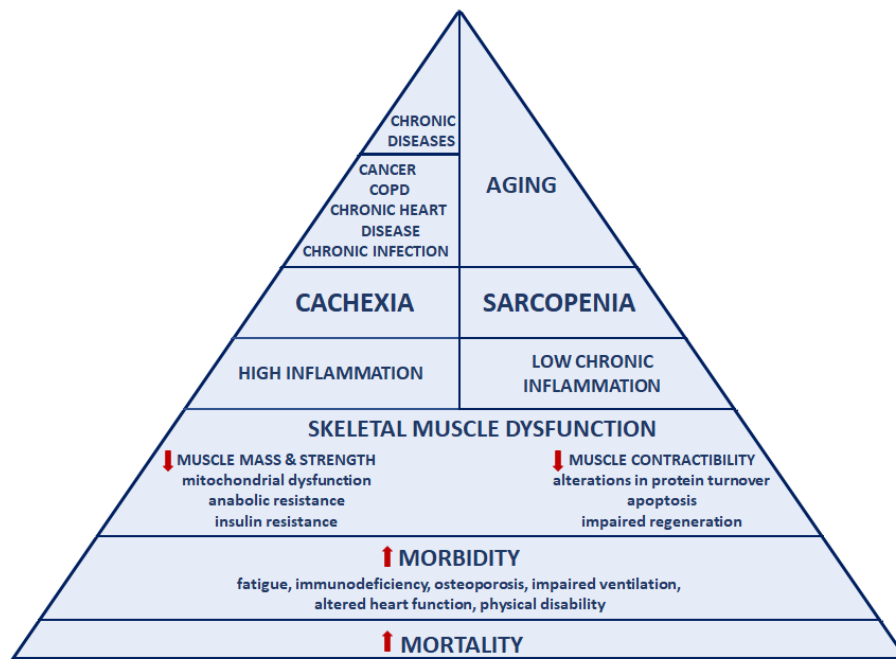


**Figure 2. Representation of the main feature of both cachexia and sarcopenia** (Adapted by Argilés et al., 2015)

## Sarcopenia

Sarcopenia is a multifactorial age-related process defined as a *progressive and generalized loss of muscle mass and strength with the risk of adverse outcome* (Cruz-Jentoft AJ et al., 2010). Starting from the fifth decade of life, this progressive age-related muscle wasting affects up to 33% of individuals and correlates with increased risk of physical frailty, functional impairment, poor health-related quality of life, disability and premature death (Visser M et al., 2011; Van Kan GA 2009; Bunout D et al., 2011, Cruz-Jentoft AJ et al., 2014).

Cellular, hormonal, metabolic, and molecular mechanisms trigger the development of sarcopenia, including impaired insulin signaling, imbalance anabolic and catabolic energy metabolism, upregulation of cytokine expression, immune dysfunction, systemic inflammation, and increased oxidative stress (Sayer et al., 2010). Aging disturbs the homeostasis of skeletal muscle, causing an imbalance between muscle protein anabolic and catabolic pathways, that in turn lead to muscle wasting. Cellular changes in sarcopenic muscle include a reduction in the size and number of



myofibers, which particularly affects type II fibers, partly due to and fewer type II fiber satellite cells. Additionally, a transition of muscle fibers from type II to type I occurs with age, together with fat infiltration (myosteatosis). Moreover, mitochondrial integrity in myocytes is altered and molecular changes, involving alterations to the IGF-1/Akt signaling pathway, ensue (Cruz-Jentoft and Sayer, 2019).

Even if the pathophysiology of sarcopenia is complex and multifactorial, among the causes triggering skeletal muscle decline could be included the alteration in several hormonal networks. The endocrine system regulation is smashed up during aging, in fact hormones involved in inflammatory processes, muscle regeneration and protein synthesis result dysregulated (Vitale G., 2013).

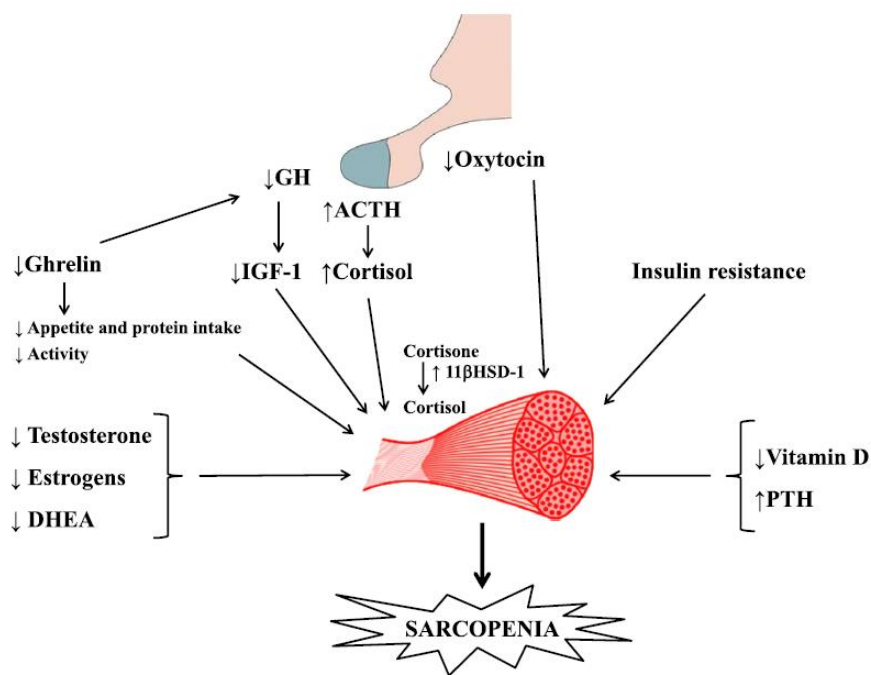


**Fig. 3. Representation of a general deregulation of trophic hormones that impact skeletal muscle and could contribute to the onset of sarcopenia.** 11βHSD-1: 11β-hydroxysteroid dehydrogenase type 1. ACTH: adrenocorticotropin hormone. DHEA: Dehydroepiandrosterone. GH: growth hormone. IGF-1: insulin-like growth factor type 1. PTH: parathyroid hormone. (Vitale et al., 2016).

Actually, a variety of circulating hormones result deregulated during aging, and most of them display effects on both muscle growth and muscle function. However, albeit evidence suggesting the involvement of trophic hormones impairment in the establishment of sarcopenia, data about the efficacy of hormone replacement therapy in elderly sarcopenic subjects are still partial and unclear.

## **Cachexia**

Cachexia is a life-threatening multifactorial syndrome often seen in progressive illnesses, such as cancer, chronic heart failure, chronic kidney disease, chronic obstructive pulmonary disease (COPD), and multiple sclerosis. Particularly in cancer, the prevalence of cachexia varies from 50% to 85% depending on the tumor type (Dodson et al., 2011). Cachexia is a marker of unfavorable prognosis, and it is directly responsible for at least 20% of cancer-related deaths (Vaughan et al., 2013).

Cancer cachexia has been defined *as a multifactorial syndrome characterized by an ongoing loss of skeletal muscle mass (with or without loss of fat mass) that cannot be fully reversed by conventional nutritional support and leads to progressive functional impairment. The pathophysiology is characterized by a negative protein and energy balance driven by a variable combination of reduced food intake and abnormal metabolism* (Fearon et al., 2011). Cancer cachexia is characterized by systemic inflammation, negative protein and energy balance, progressive weight and skeletal muscle loss. Moreover, cachexia has a detrimental impact on cancer therapy, as cachectic patients are usually less tolerant to radio- and chemotherapy because of general weakness and discomfort (Fearon et al., 2010).

Several mechanisms participate in the establishment and development of cachexia, including anorexia, decreased physical activity, decreased secretion of host anabolic hormones, and an altered host metabolic response. (Mantovani and Madeddu, 2010). Systemic inflammation is considered a cancer cachexia hallmark, as pro-inflammatory cytokine activity increases during cancer progression Argilés et al., 2009; MacDonald et al., 2003). Numerous cytokines, including tumor necrosis factor-

alpha (TNF- $\alpha$ ), interleukin-1 (IL-1), IL-6, and interferon-gamma (IFN- $\gamma$ ), play a role in the etiology of cancer cachexia (Fearon et al., 2012; DoDson et al., 2011). Specifically, TNF- $\alpha$  and IL-6 induce myofibrillar breakdown by activation of the ubiquitin-proteasome pathway, via NF- $\kappa$ B-dependent and independent mechanisms (Ali and Garcia, 2014). Moreover, downregulation of IGF-1 anabolic pathway, androgens and satellite cell proliferation, and increases in catabolic processes such as apoptosis (Busquets et al., 2007), autophagy (Penna et al., 2013), mitochondrial dysfunction (Kang et al., 2013) and the myostatin pathway (Padrao et al., 2013) contribute to muscle mass and function loss in this setting.

Although the underlying causes of cachexia are still largely unknown, the emerging thesis that cancer cachexia-associated muscle wasting could contribute to tumor growth and progression (Luo et al., 2014) on one side, and the demonstration that prevention of skeletal muscle wasting in tumor-bearing animals is sufficient to markedly prolong their survival (Zhou et al., 2010) on the other hand, prompted the search for suitable approaches to protect muscle wasting in cancer patients.

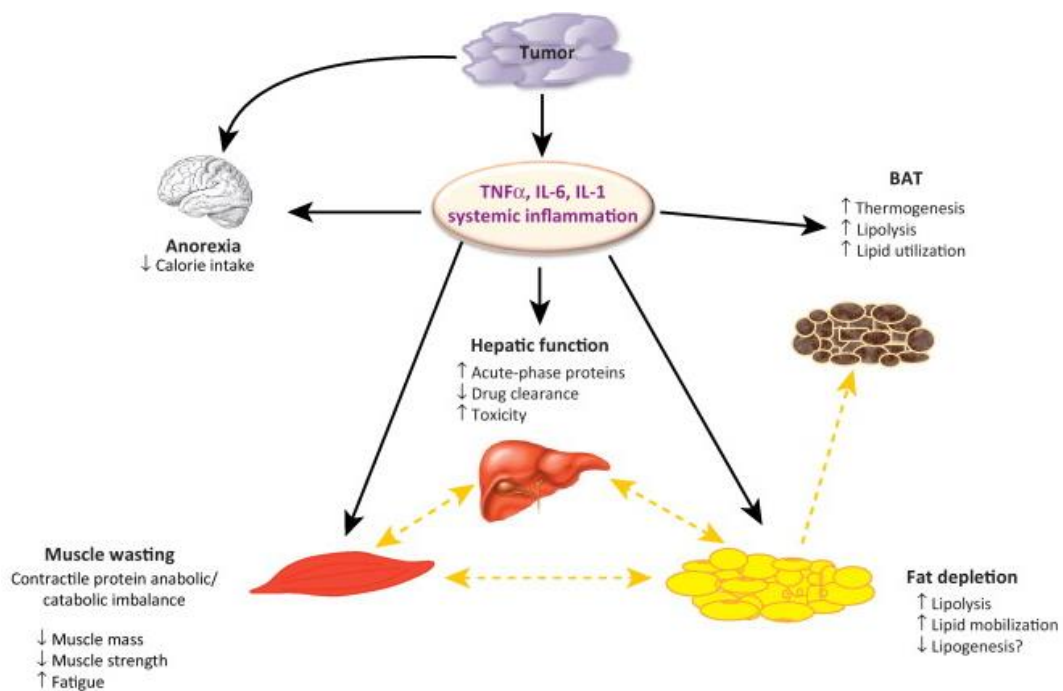


**Figure 4. Mechanisms involved in cancer cachexia.** Tumor-derived catabolic factors such as proinflammatory cytokines act on target tissues to elicit excess catabolism. Alteration of the central nervous system results in reduced food intake. Proteolysis is induced in skeletal muscle through up-regulation of the ubiquitin-proteasome system and autophagy, and protein synthesis is reduced. Loss of adipose tissue results from increased lipolysis, decreased lipogenesis and adipogenesis and white adipose tissue browning. (Tsoli et al., 2013)

As previously reported, alterations in several hormonal networks co-occur in skeletal muscle wasting and are regarded as possible causes triggering skeletal muscle decline. During my PhD internship, I particularly focused on vitamin D and ghrelin, analyzing the relationship between these hormones and skeletal muscle homeostasis.

## Vitamin D

Vitamin D (VD) is a group of fat-soluble secosteroids that includes two compounds: vitamin D3 (also known as cholecalciferol, hereafter VD3) and vitamin D2 (ergocalciferol, hereafter VD2).

VD2 originates from the UV irradiation of the yeast sterol ergosterol and is found naturally in sun-exposed mushrooms, whereas VD3 come either from endogenous synthesis in the skin or from food, as oil-rich fish like salmon, mackerel, and herring. Since humans synthesize VD3 but not VD2, the first one is considered the most “natural” form. Moreover, VD2 is chemically different from, and less physiologically active than, VD3 (Nair et al., 2012; Hymøller et al., 2016).

In humans, VD3 synthesis begins with skin exposure to ultraviolet B radiation and the consequent photochemical conversion of the precursor, 7-dehydrocholesterol (pro-vitamin D), in pre-VD3. Through thermal isomerization, pre-VD3 is converted to VD3 (cholecalciferol) which reaches the liver where it is converted in 25-hydroxyvitamin D3 (25 VD) mainly by cytochrome P450 cyp2R1. Successively, 25 VD is transported to kidney where is converted in 1,25-dihydroxyvitamin D3 (1,25VD) by cytochrome P450 cyp27b1. While 25-hydroxylation generally is not rate limiting, 1 $\alpha$ -hydroxylation step is strictly regulated. Lastly, cyp24a1 catalyzes the conversion of both 25 VD and 1,25 VD into 24-hydroxylated products targeted for inactivation and excretion. 1,25 VD is considered the active form that, through the binding to Vitamin D receptor (VDR), exerts its biological activity in target tissues (Girgis et al, 2014) (Fig. 5).

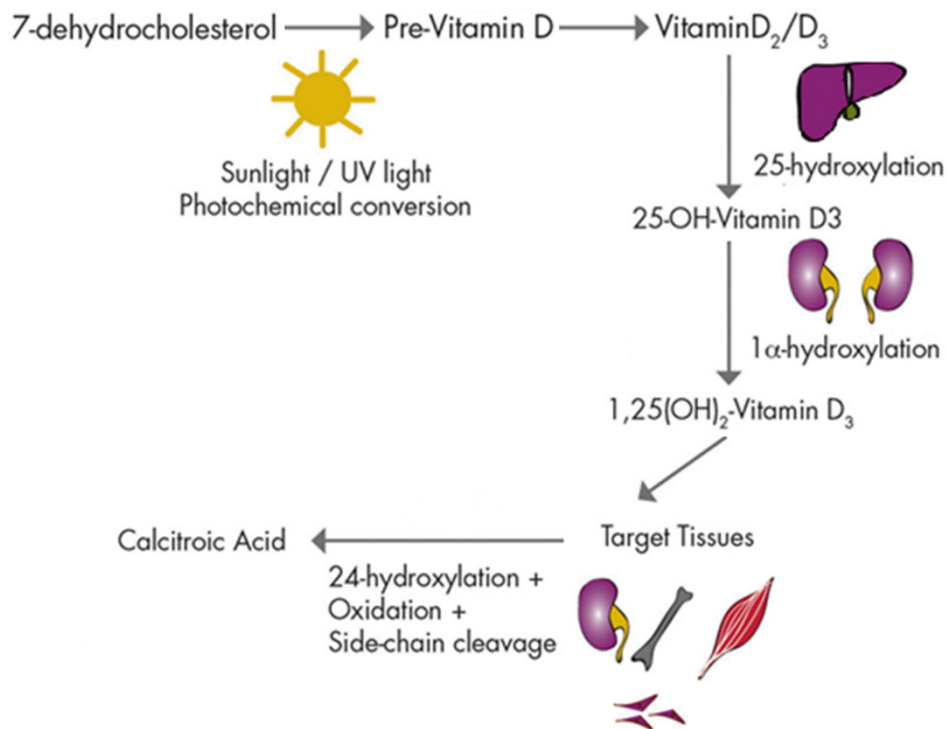


**Figure 5. VD metabolism representation.** (Adapted by Girgis et al., 2013).

VD plays an essential role in regulating calcium and phosphate metabolism and maintaining a healthy mineralized skeleton. Thus, VD promotes intestinal calcium absorption and maintains adequate serum calcium and phosphate concentrations to enable bone mineralization. Moreover, VD is also needed for bone growth and remodeling driven by osteoblasts and osteoclasts. A longstanding VD deficiency has been associated with growth retardation and rickets in children, and osteoporosis or, in the most severe cases, osteomalacia in adults (Bischoff-Ferrari et al., 2009).

Apart its consolidate role in bone metabolism, VD system regulates cell differentiation, cell cycle, and exerts pleiotropic effects on extra-skeletal target tissues, such as immune and cardiovascular system, pancreatic endocrine cells, adipose tissue, and muscle (Caprio et al., 2017; Christakos et al., 2016) (Fig.6).

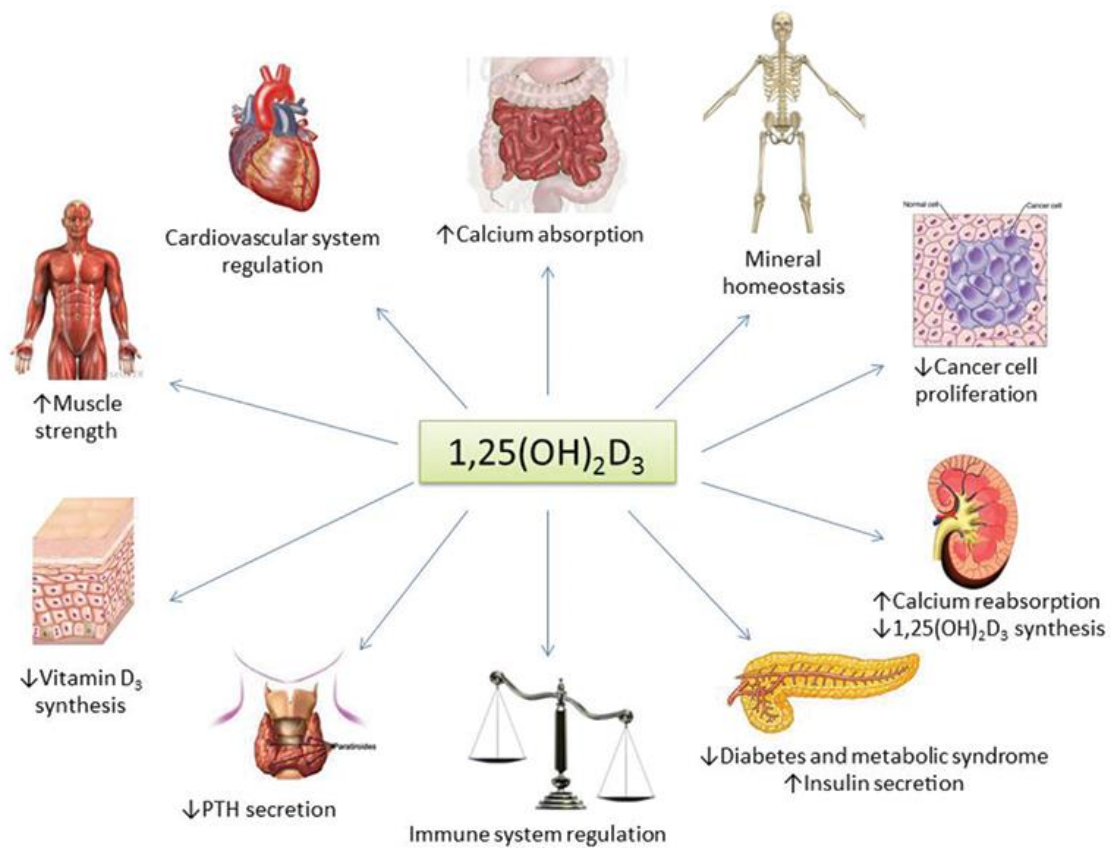


**Figure 6. VD is a pleiotropic hormone.** Representation of principal VD target tissues and actions (Casado et al., 2017).

VD modulates B and T lymphocyte function (Tsoukas et al., 1984; Drozdenko et al., 2014), and VD deficiency has been associated with conditions such as multiple sclerosis, type 1 diabetes (T1D), rheumatoid arthritis, systemic lupus erythematosus, dermatomyositis, inflammatory bowel disease, hepatitis, asthma and respiratory infections (reviewed by Marino and Misra, 2019).

Besides, 1,25(OH)<sub>2</sub>D<sub>3</sub> has a direct action on myocardial cells, smooth muscle fibers, and vascular endothelial cells by stimulating the calcium ATPase activity, promoting the calcium transfer to the intracellular space (Wolden-Kirk et al., 2012). VD deficiency has been associated with inflammation and endothelial and platelet dysfunction, which favors the risk of cardiovascular complications (Kunadian et al., 2014). VDR is also expressed in pancreatic cells and VD affects glucose homeostasis as well, with a direct effect on the β-cell function and insulin secretion (Alvarez and Ashraf, 2010).

Several studies have suggested that low VD status contributes to insulin resistance (Teegarden and Donkin, 2009) and is associated with markers of impaired glucose metabolism, such as glycosylated hemoglobin (Kositsawat et al., 2010).

VD metabolizing enzymes and VDR are expressed also in adipose tissue, then VD regulates adipogenesis, adipocyte apoptosis, affects energy metabolism by controlling the expression of uncoupling proteins, and the appetite suppressing leptin. Furthermore, VD reduces adipose tissue inflammation and VD deficiency is associated with obesity (Abbas, 2017).

### **Vitamin D and skeletal muscle**

Among its extra-skeletal target tissue, VD impacts on skeletal muscle as well. The description of a reversible myopathy associated with VD deficiency leads to recognize a potential association between VD and muscle (Boland, 1986). The identification of the VD receptor (VDR) on muscle cells (Zanello et al., 1997; Bischoff et al., 2001) provided a solid evidence of the direct effect of VD on muscle tissue. Moreover, the expression in skeletal muscle of  $1\alpha$ -hydroxylase, the enzyme responsible for the hydroxylation of 25 VD to 1,25 VD, gave another evidence of the direct action of VD on muscle (Srikuea et al., 2012).

VD deficiency has been correlated with decrease in muscle mass, function, and performance in various pathologies, such as chronic kidney disease (Jean et al., 2017), inflammatory bowel diseases (Mager et al., 2018), COPD (Graumam et al., 2018), and myasthenia gravis (Kang et al., 2018), as well as in elderly subjects (Snijder et al., 2006; Suzuki et al., 2008).

Despite VD clearly impacts on muscle homeostasis, the mechanisms through which it acts and its effects are still controversial. Some studies indicated that treatment of C2C12 myoblasts with 1,25 VD resulted in increased VDR expression, inhibition of cell differentiation and proliferation, and down-regulation of myogenin (Srikuea et al., 2012; Girgis et al., 2014). In contrast, other studies reported that 1,25-(OH)<sub>2</sub>-VD stimulates myogenesis in satellite cells and C2C12 myocytes (Buitrago



et al. 2012; Braga et al., 2017). Others demonstrate that both 1,25-(OH)<sub>2</sub>-VD and 25-OH-VD stimulate VDR mRNA expression and reduce C2C12 cell proliferation without affecting myotube size or myogenin mRNA expression (van der Meijden et al., 2016).

## **Vitamin D in sarcopenia**

25 VD circulating levels drop off with aging and VD deficiency is common amongst elderly subjects. This condition could be due to a decreased dietary intake, limited sunlight exposure, decreased capacity of human skin to produce VD<sub>3</sub>, reduced intestinal absorption, and impaired hydroxylation in the liver and kidneys (Janssen et al., 2002; Mosekilde, 2005). Likewise, an age-dependent decrease in VDR expression has been observed in skeletal muscle (Bischoff-Ferrari et al., 2004). Notably, a significant correlation was found between serum levels of VD metabolites and muscle strength and physical performance (Janssen et al., 2002). Randomized controlled trials and meta-analyses support the role of VD in improving age-related declines in muscle function as well (Wagatsuma et al., 2014; Caristia et al., 2019). Moreover, observational data have suggested the presence of a relationship between low 25 VD serum levels and impaired physical function in elderly populations (Bischoff-Ferrari et al., 2004). Anyway, it has been reported that VD supplementation have beneficial effects to restore muscle strength, without affect muscle mass in the elderly, but preventing muscle loss (Mosekilde, 2005; Beaudart et al., 2014; Cangussu et al., 2015; Iolascon et al. 2017). The risk of falls and hip fractures increases in older people, owing to a loss of skeletal muscle mass and strength, and low vitamin D status plays a central role in the risk of falls in older people (Kim et al., 2011; Domingues-Faria et la., 2017). Actually, VD supplementation has been shown to reduce falls and fractures within elderly subjects affected by VD deficiency (Bischoff-Ferrari HA, 2012; Scott el al., 2015).

Nevertheless, the molecular mechanisms trough which VD acts in sarcopenia context remains to be fully elucidated.

## **Vitamin D in cachexia**

Decreased circulating VD levels have been observed in 47% of oncologic patients (Dev et al, 2011), and reduction in mortality was reported in patients with colorectal cancer who presented adequate levels of vitamin D, suggesting the importance of maintaining vitamin D status (Mohr et al., 2015). Despite the well-established role of VD in muscle homeostasis, few studies have been performed on the efficacy of adequate VD levels in cachectic cancer patients.

A phase II trial in which VD was supplemented to 6 patients with advanced prostate cancer showed an improvement of muscle strength (Van Veldhuizen et al., 2000). Moreover, data from 308 patients who underwent chemotherapy for breast cancer show higher disease-free survival in patients supplemented with vitamin D (Zeichner et al., 2015). However, a phase III trial with 953 patients was prematurely stopped after an interim analysis showed greater mortality in the supplemented versus placebo arm (Scher et al., 2011). The lack of effectiveness of VD supplementation in preventing cancer cachexia-associated muscle wasting was demonstrated also in tumor-bearing animals (Camperi et al., 2017). Nonetheless, another recent study showed that treatment with 1,25 prevented the changes in myoblasts induced by Lewis Lung carcinoma, suggesting that the treatment may be effective in counteracting cancer cachexia-associated muscle weakness (Ryan et al., 2018).

The contrasting data about the effect of VD supplementation highlighted the urgency to elucidate the mechanisms by which VD system impact on skeletal muscle in cancer cachexia.

**Introduction to the paper “Opposing effects of 25-hydroxy- and 1 $\alpha$ ,25-dihydroxy-vitamin D3 on pro-cachectic cytokine-and cancer conditioned medium-induced atrophy in C2C12 myotubes”**

Sustova H, De Feudis M, Reano S, Alves Teixeira M, Valle I, Zaggia I, Agosti E, Prodám F, Filigheddu N.

Acta Physiol (Oxf). 2019 Jul;226(3):e13269. doi: 10.1111/apha.13269.


Subjects affected by muscle wasting-associated conditions, as sarcopenia and cancer cachexia, often display VD deficiency (Snijder et al., 2006; Suzuki et al., 2008; Dev et al., 2011), which correlates with decrease in muscle function and performance and increase in disability, especially in elderly subjects. Since VD supplementation was able to restore muscle strength and prevent muscle mass loss in frail aged subjects, it has been hypothesized that VD supplementation could be used as an anti-cachexia treatment. However, despite encouraging results on elderly, VD supplementation was ineffective against cancer cachexia-associated muscle wasting both in patients and in animal models (Scher et al., 2011; Camperi et al., 2017).

In order to understand the underlying causes of contrasting effect of VD administration in sarcopenia and cancer cachexia, we explored the biological effects and mechanisms of different VD metabolites on C2C12 myotubes undergoing cancer cell conditioned medium- or cytokines-mediated atrophy as a model of *in vitro* cachexia-associated muscle wasting.

Although 1,25 VD is considered the active form, we demonstrated that also the other VD metabolites can directly affect skeletal muscle derived cells. Interestingly, we showed that 25VD and 1,25VD have antithetical effects. 25 VD exerts a protective effect against cytokine-induced atrophy *in vitro*, while 1,25 VD induces atrophy, highly likely due to a differential modulation of 24-hydroxylase. Accordingly, we proved that 24,25 VD affects C2C12 myotube size as well.

Altogether, our data show how variously hydroxylated VD metabolites and the differential regulation of VD hydroxylases may trigger contrasting effects in C2C12 myotubes, thus explaining the opposite outcome of VD supplementation in different condition *in vivo*.

# Opposing effects of 25-hydroxy- and 1 $\alpha$ ,25-dihydroxy-vitamin D<sub>3</sub> on pro-cachectic cytokine- and cancer conditioned medium-induced atrophy in C2C12 myotubes

Hana Sustova<sup>1,2</sup> | Marilisa De Feudis<sup>1,2</sup> | Simone Reano<sup>1,2</sup> | Maraiza Alves Teixeira<sup>1,2</sup> |  
Ilaria Valle<sup>1</sup> | Ivan Zaggia<sup>1</sup> | Emanuela Agosti<sup>1,2</sup> | Flavia Prodam<sup>3</sup> |  
Nicoletta Filigheddu<sup>1,2</sup> 

<sup>1</sup>Department of Translational Medicine, University of Piemonte Orientale, Novara, Italy

<sup>2</sup>Istituto Interuniversitario di Miologia (IIM)

<sup>3</sup>Department of Health Sciences, University of Piemonte Orientale, Novara, Italy

## Correspondence

Nicoletta Filigheddu, Department of Translational Medicine, University of Piemonte Orientale, Novara, Italy.  
Email: nicoletta.filigheddu@med.uniupo.it

## Present Address

Hana Sustova, Pharmakologisches Institut am BPC, Philipps-Universität Marburg, Marburg, Germany

## Funding information

Fondazione Cariplo, Grant/Award Number: 2015\_0634 to N.F.; Compagnia di San Paolo, Grant/Award Number: Ph.D. fellowship to M.A.T.

## Abstract

**Aim:** Loss of skeletal muscle is one of the main features of cancer cachexia. Vitamin D (VD) deficiency is associated with impairment of muscle mass and performance and is highly prevalent in cachectic patients; therefore, VD supplementation has been proposed to counteract cancer cachexia-associated muscle loss. However, in both cachectic cancer patients and tumour-bearing animals, VD supplementation led to disappointing results, urging the need for a better understanding of VD activity on skeletal muscle.

**Methods:** Cancer-associated muscle wasting was reproduced in vitro by treating C2C12 myotubes with cancer cell conditioned medium, a combination of TNF- $\alpha$  and IFN $\gamma$  or IL-6 pro-cachectic cytokines. The biological effects and mechanisms of action of 1,25-dihydroxy VD (1,25 VD) and its precursor 25-hydroxy VD (25 VD) on myotubes were explored.

**Results:** We demonstrated that only 25 VD was able to protect from atrophy by activating Akt signalling, inducing protein synthesis, and stimulating the autophagic flux, while 1,25 VD had an atrophic activity per se, increasing FoxO3 levels, inducing the expression of atrogenes, and blocking the autophagic flux. Furthermore, we showed that the contrasting activities of these VD metabolites on C2C12 myotubes depend on a differential induction of VD-24-hydroxylase and transformation of VD metabolites in pro-atrophic 24-hydroxylated products, as silencing of VD-24-hydroxylase reduced the atrophic activity of 1,25 VD.

**Conclusions:** Altogether these data might explain the lack of efficacy of VD treatment in vivo for the protection of muscle mass in cancer.

## KEYWORDS

atrogenes, autophagy, cancer cachexia, *Cyp24a1* 24-hydroxylase, *Cyp27b1* 1 $\alpha$ -hydroxylase, skeletal muscle atrophy

Sustova, De Feudis and Reano contributed equally to this work.

Prodam and Filigheddu contributed equally to this work.

## 1 | INTRODUCTION

Cachexia is a life-threatening multifactorial syndrome often seen in progressive illnesses, such as cancer, chronic heart failure, chronic kidney disease, chronic obstructive pulmonary disease (COPD), and multiple sclerosis. Particularly in cancer, the prevalence of cachexia varies from 50% to 85% depending on the tumour type.<sup>1</sup> Cachexia is a marker of unfavourable prognosis, and it is directly responsible for at least 20% of cancer-related deaths.<sup>2</sup> Cancer cachexia is characterized by systemic inflammation, negative protein and energy balance, progressive weight and skeletal muscle loss. Moreover, cachexia has a detrimental impact on cancer therapy, as cachectic patients are usually less tolerant to radio- and chemotherapy because of general weakness and discomfort.<sup>3</sup> To date, the underlying causes of cachexia are still largely unknown; but the emerging thesis that cancer cachexia-associated muscle wasting could contribute to tumour growth and progression<sup>4</sup> on one side, and the demonstration that prevention of skeletal muscle wasting in tumor-bearing animals is sufficient to markedly prolong their survival<sup>5</sup> on the other hand, prompted the search for suitable approaches to protect muscle wasting in cancer patients.

Vitamin D<sub>3</sub> (cholecalciferol, VD hereafter for brevity), besides its well-known role in regulation of calcium and phosphate homeostasis, impacts on skeletal muscle homeostasis as well, and VD deficiency has been correlated with decrease in muscle mass, function, and performance in various pathologies, such as chronic kidney disease,<sup>6</sup> inflammatory bowel diseases,<sup>7</sup> COPD,<sup>8</sup> and myasthenia gravis,<sup>9</sup> as well as in elderly subjects.<sup>10,11</sup> Notably, in these latter subjects, VD supplementation was able to restore muscle strength and prevent muscle mass loss.<sup>12,13</sup> Since VD deficiency is highly prevalent also among advanced cancer patients with cachexia,<sup>14</sup> the encouraging results of VD supplementation on frail elderly subjects led to the hypothesis that VD supplementation could be used as an anti-cachexia treatment. A phase II trial in which VD was supplemented to six patients with advanced prostate cancer showed indeed an improvement of muscle strength.<sup>15</sup> However, the follow-up phase III trial with 953 patients was prematurely stopped after an interim analysis showed greater mortality in the supplemented versus placebo arm.<sup>16</sup> The lack of effectiveness of VD supplementation in preventing cancer cachexia-associated muscle wasting was recently demonstrated also in tumour-bearing animals.<sup>17</sup>

VD metabolism initiates in the skin with the conversion of 7-dehydrocholesterol to VD upon ultraviolet exposure. VD is hydroxylated in the liver to 25-hydroxy-VD (25 VD), the major circulating form. 25 VD undergoes another hydroxylation in the kidney to 1 $\alpha$ ,25-dihydroxy-VD (1,25 VD), commonly considered the biologically active form. However, 1 $\alpha$ -hydroxylase (encoded by the *Cyp27b1* gene),

the enzyme responsible for the hydroxylation of 25 VD to 1,25 VD, is expressed in various tissues, including the skeletal muscle,<sup>18</sup> providing support for the direct action of both 25 VD and 1,25 VD on muscle. Indeed, on skeletal muscle-derived cells, both forms have been reported to be active, although sometimes with contrasting results. For example, 1,25 VD treatment of C2C12 myoblasts resulted in increased VD receptor (VDR) expression, inhibition of cell differentiation and proliferation and down-regulation of myogenin.<sup>17-19</sup> In contrast, other studies reported that 1,25 VD stimulates myogenesis in satellite cells and C2C12 myocytes.<sup>20,21</sup>

Therefore, further investigation is needed on the effect of VD metabolites on skeletal muscle, and here, in particular, we explored the biological effects and mechanisms of action of 25 VD and 1,25 VD on myotubes undergoing cancer cell conditioned medium- or cytokines-mediated atrophy as a model of in vitro cachexia-associated muscle wasting.

## 2 | RESULTS

### 2.1 | 25 VD, but not 1,25 VD protects C2C12 myotubes from cytokine- and cancer cell conditioned medium-induced atrophy

C2C12 are a widely used system to model in vitro skeletal muscle atrophy.<sup>22</sup> In particular, treatments of C2C12 myotubes for 24 hours with a combination of TNF- $\alpha$  and IFN $\gamma$  or IL-6 mimic cancer-induced muscle wasting, leading to the reduction of myotubes diameters up to 20%. Co-treatment with 25 VD prevented the decrease in myotube diameter, while 1,25 VD had no protective effects (Figure 1A). As a matter of fact, administration of 1,25 VD alone induced a 20% reduction in myotube diameters, on the contrary, 25 VD had a mild hypertrophic effect, in accordance with previously published results.<sup>23</sup> Likewise, 25 VD protected C2C12 myotubes from the atrophy induced by treatment with conditioned medium from Lewis lung carcinoma (LLC) cells (Figure 1B).

### 2.2 | 1,25 VD induces atrophy by increasing FoxO3 expression and atrogene induction

In skeletal muscle, excessive activation of ubiquitin-proteasome leads to muscle loss. Forkhead box O (FoxO) proteins play a central role in regulating the activation of these atrophic pathways, in particular by inducing the transcription of muscle-specific E3 ubiquitin ligases, collectively known as atrogenes, and of autophagy-related genes.<sup>24</sup> Notably, 1,25 VD increased FoxO3a protein level (Figure 2A) that, in turn, upregulated mRNA expression of Atrogin-1 and MuRF-1 atrogenes (Figure 2B).

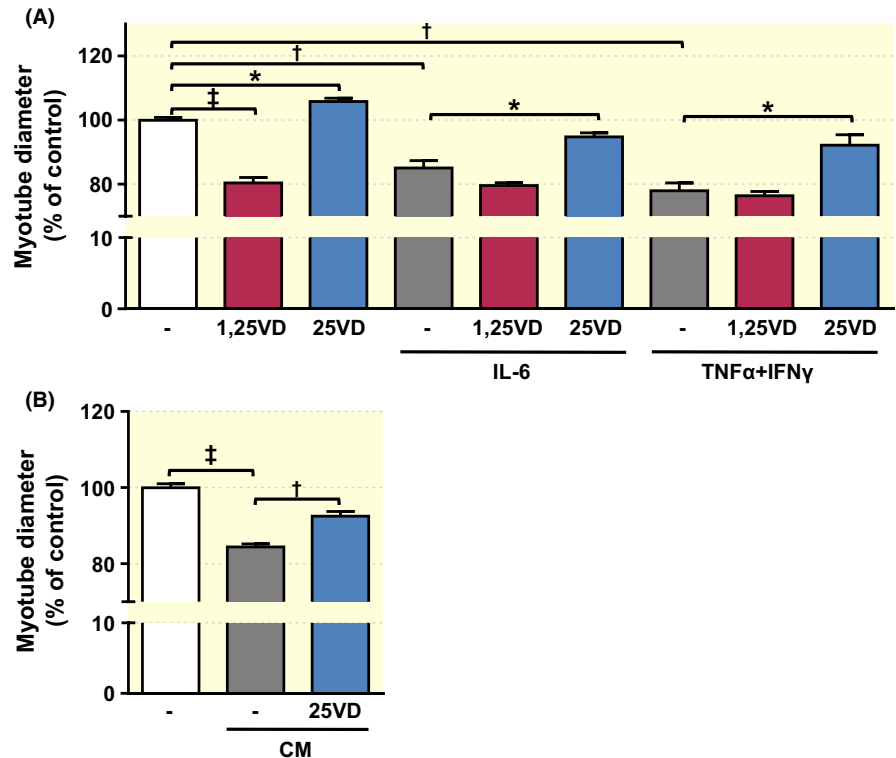


**FIGURE 1** 25 VD, but not 1,25 VD, protects C2C12 myotubes from cytokine-induced atrophy. Myotube diameters were measured after 24 h treatment in differentiation medium (DM) with (A) 100 nmol/L 1,25 VD or 25 VD together with 20 ng/mL IL-6 or 10 ng/mL TNF $\alpha$ /IFN $\gamma$ , and (B) 100 nmol/L 25 VD together with conditioned medium (CM). Data are presented as means  $\pm$  SEM of three independent experiments. \* $P$  < 0.05; † $P$  < 0.01; ‡ $P$  < 0.001

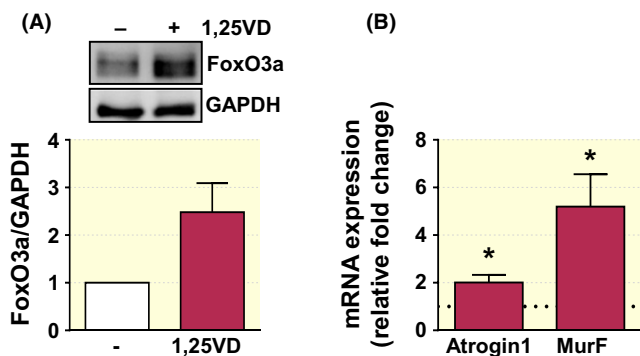


**FIGURE 2** 1,25 VD atrophic activity involves FoxO3a/atrogenes induction. (A) Representative western blot (top) and densitometry (bottom) of FoxO3a protein levels in C2C12 myotubes treated with 100 nmol/L 1,25 VD for 24 h. Expression of atrogenes (B) was assessed by real-time RT-PCR. Reference line represents the control (vehicle-treated cells). \* $P$  < 0.05 vs. control. All treatments were in serum-free medium. Data are presented as means  $\pm$  SEM of three independent experiments

### 2.3 | 25 VD induces activation of Akt signalling pathway and protein synthesis

In agreement with the anti-atrophic and hypertrophic effect of 25 VD (Figure 1), an antibody array detecting the relative expression of phosphorylated proteins showed, within 10 minutes of 25 VD treatment, an increase in the activation of Akt/mTOR protein network associated with protein synthesis.

This anti-atrophic signalling persisted, although attenuated, also after 24 h of treatment (Figure 3A). We confirmed the phosphorylation of Akt by western blotting (Figure 3B) and verified if the early activation of Akt was necessary for the effect of 25 VD on myotubes by adding to the treatments the pharmacologic inhibitor of PI3K/Akt pathway LY294002. The complete abrogation of the protective activity of 25 VD upon LY294002 treatment (Figure 3C) demonstrated indeed the requirement of early activation of Akt pathway for the anti-atrophic effect of 25 VD on myotubes. In addition, coherently with 25 VD-induced activation of Akt signalling, 25 VD treatment increased protein synthesis, measured as puromycin incorporation in SUNSET assay (Figure 3D), and promoted FoxO3a phosphorylation (Figure 3E), thus inhibiting its translocation in the nucleus and the transcription of atrogenes.

### 2.4 | 25 VD and 1,25 VD have differential effects on the autophagic flux

Autophagy plays a central role in muscle homeostasis by regulating protein and organelle turnover and, for this reason, any perturbation of the autophagic flux may result in tissue loss. We, therefore, evaluated if 25 VD and 1,25 VD affected C2C12 autophagy by assessing the expression of autophagy-related genes Bnip3, Gabarapl1 and Cathepsin L.

Notably, 25 VD did not significantly perturb the expression of these autophagy-related genes, while 1,25 VD treatment increased the expression of Bnip3 and Gabarapl1, while

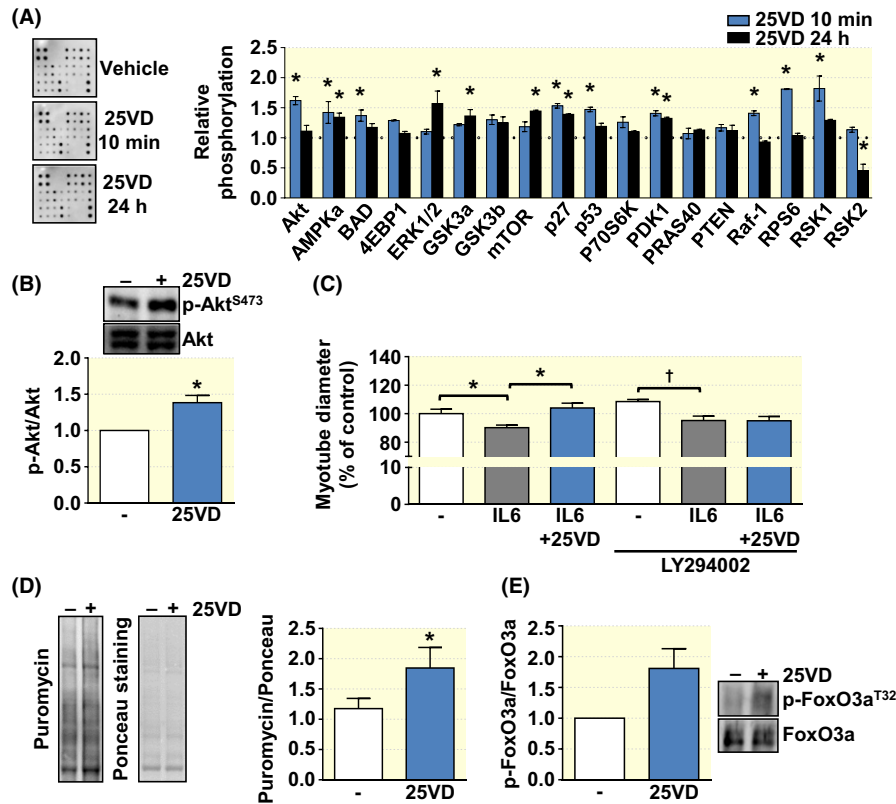


**FIGURE 3** 25 VD stimulates anti-atrophic pathways, protein synthesis, and its protective activity depends on Akt signalling. (A) Relative phosphorylation of proteins of the Akt pathway induced by 10 min or 24 h treatment in DM with 100 nmol/L 25 VD through protein array analysis. Reference line represents vehicle-treated cells. \**P* < 0.05 vs. control. (B) Treatment for 5 min with 100 nmol/L 25 VD enhances Akt<sup>S473</sup> phosphorylation. Representative western blot (top) and densitometry (bottom) of three independent experiments. (C) Protein synthesis upon 24 h treatment with 100 nmol/L 25 VD was assessed by SUnSET assay. Incorporation of puromycin into newly synthesized proteins was visualized by Western blotting and normalized on total proteins detected by Ponceau staining (left). Densitometry of three independent experiments is shown on the right part of the panel. (D) Treatment with 10 μmol/L LY294002, an inhibitor of PI3K/Akt pathway, abolishes 25 VD protective effect against 20 ng/mL IL-6-induced atrophy. Myotube diameters were measured as described before. (E) Treatment for 5 min with 100 nmol/L 25 VD enhances FoxO3a phosphorylation. Representative western blot (top) and densitometry (bottom) of three independent experiments. All treatment was performed in serum-free medium. Data are presented as means ± SEM of three independent experiments. \**P* < 0.05; †*P* < 0.01

substantially reducing Cathepsin L expression (Figure 4A), suggesting an upsurge of the autophagic flux yet its block in the final fusion of autophagosomes with lysosomes.

To assess the occurrence of this autophagic flux block, we measured the autophagosomal marker LC3, the lysosomal marker LAMP2, and their colocalization in C2C12 myotubes in the presence or absence of chloroquine, a treatment known to block the autophagic flux. Surprisingly, 25 VD induced a strong accumulation of LC3 staining only in chloroquine-treated cells, indicating an enhanced autophagic flux, while in 1,25 VD-treated cells LC3-positivity was already high and not further increased by chloroquine, suggesting a block of the autophagic flux (Figure 4B and C). Coherently, chloroquine treatment enhanced the formation of autophagolysosomes, seen as LC3-LAMP2 colocalization, only in 25 VD-treated cells (Figure 4B and D).

Given the opposite effects of 25 VD and 1,25 VD on autophagy and in promoting protein synthesis and degradation,

respectively, we explored the potential involvement of Atf4, a transcription factor at the crossroad between anabolic and catabolic processes, as it might induce the activation of autophagy-mTORC1-amino acid uptake and protein synthesis axis.<sup>25</sup> We assessed Atf4 expression at different time points after treatment with the two VD metabolites and observed that 25 VD did not induce any noteworthy change in Atf4 mRNA, while 1,25 VD caused a significant and persisting decrease of Atf4 expression (Figure 4E), suggesting a possible mechanism of autophagy impairment.

## 2.5 | VD-24-hydroxylase involvement in the differential effects of VD metabolites

In vivo, the kidney is the main organ that produces 1,25 VD; however, the mitochondrial enzyme 1 $\alpha$ -hydroxylase (encoded by the gene *Cyp27b1*) that mediates the production of 1,25 VD from 25 VD is expressed by a wide array



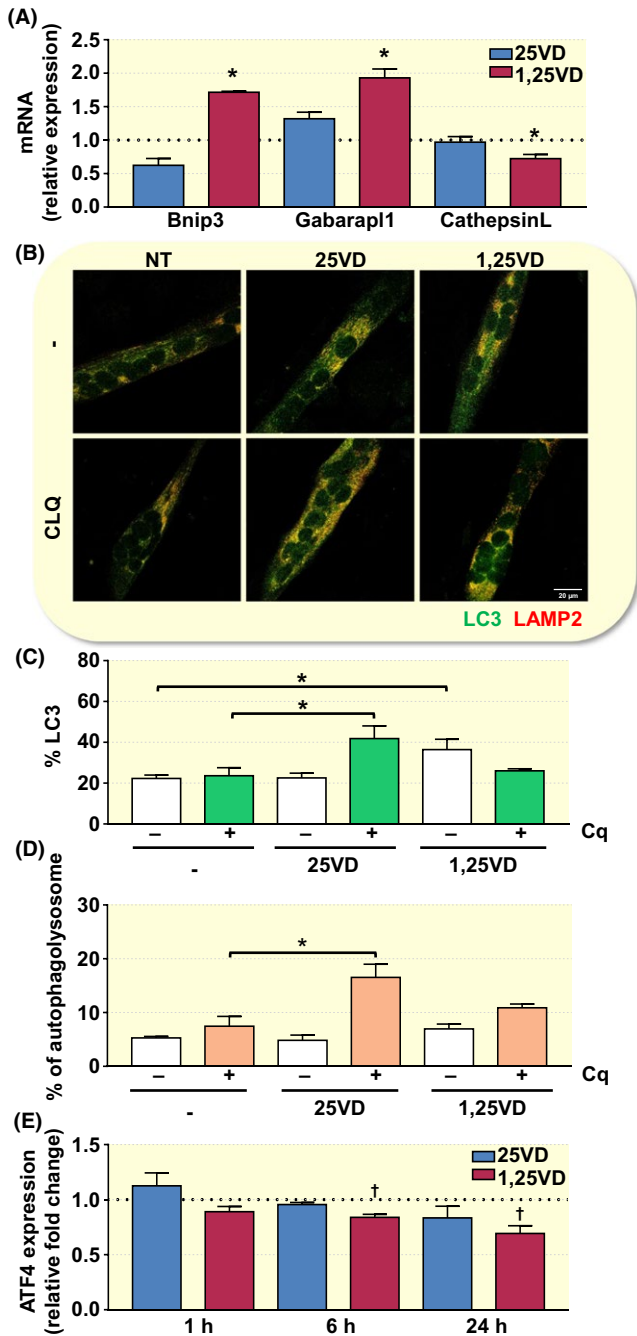


**FIGURE 4** 25 VD and 1,25 VD have differential effects on the autophagic flux. (A) 24 h after treatment with 100 nmol/L of 25 VD or 1,25 VD, expression of autophagic genes was assessed by real-time RT-PCR. Reference line represents control (vehicle-treated cells). \* $P < 0.05$  vs. control. (B) Representative images of LC3-LAMP2 immunofluorescence. C2C12 myotubes were treated for 24 h with 100 nmol/L of 25 VD and 1,25 VD in the presence or absence of 10 μmol/L of chloroquine (Cq). (C) Percentage of LC3 stained area above total myotube area and (D) percentage of LC3 area colocalized with LAMP2 above total myotube area. \* $P < 0.05$ . (E) *Atf4* expression was evaluated by real-time RT-PCR after 1, 6 and 24 h treatment with 100 nmol/L of both 25 VD and 1,25 VD. Reference line represents control (vehicle-treated cells). † $P < 0.01$  vs. control

of tissues and cells, including C2C12 myoblasts and myotubes, supposedly to allow the biological activity of 25 VD upon intracellular conversion to 1,25 VD.<sup>18</sup> Although in our in vitro system exogenous administrations of 25 VD and 1,25 VD to C2C12 myotubes have divergent effects, apparently, 25 VD needs to be intracellularly converted to 1,25 VD to exert its anti-atrophic activity, as silencing of 1 $\alpha$ -hydroxylase abrogated the anti-atrophic effect of 25 VD (Figure 5A). However, this result is totally in conflict with the pro-atrophic effect of 1,25-VD (Figure 1A). We, therefore, hypothesized that *Cyp27b1* silencing could affect the expression of VD-24-hydroxylase, the enzyme converting VD metabolites in 24-hydroxylated products targeted for excretion. The altered expression of *Cyp24a1* would thus modulate the levels of 24-hydroxylated metabolites that, in the context of skeletal muscle, might induce atrophy. Indeed, *Cyp27b1* silencing strongly induced the expression of *Cyp24a1* (Figure 5B), and treatment with 24,25-dihydroxy-VD (24,25 VD) induces atrophy in C2C12 myotubes (Figure 5C). Accordingly with our hypothesis, simultaneous silencing of both *Cyp27b1* and *Cyp24a1* restored the protective activity of 25 VD in myotubes treated with atrophic stimuli (Figure 5D). We further hypothesized that the divergent effects of 25 VD and 1,25 VD on C2C12 myotubes could be due to a differential induction of *Cyp24a1*. As a matter of fact, both 25 VD and 1,25 VD induced the expression of *Cyp24a1* but at different extents (Figure 5E). Treatment with 1,25 VD might result in its conversion to a pro-atrophic 1,24,25 VD metabolite. Coherently, silencing of *Cyp24a1* attenuated the atrophic activity of 1,25 VD (Figure 5F), suggesting that intracellular 24-hydroxylation of 1,25 VD mediates its atrophic activity. On the contrary, the slighter induction of *Cyp24a1* by 25 VD could induce a limited amount of 24,25 VD endowed with protective activity. Indeed, 24,25 VD elicits in C2C12 opposite outcomes depending on the concentration used, ranging from hypertrophic to atrophic effects (Figure 5G).

### 3 | DISCUSSION

Although 25 VD has been considered for a long time an inactive reservoir of 1,25 VD, a growing body of evidence indicates that it has its own biological activities in different tissues, including skeletal muscle.<sup>23,26-29</sup> The presence of *Cyp27b1* in skeletal muscle cells<sup>18</sup> would suggest, as a mechanism of action of 25 VD, its intracellular conversion to 1,25 VD by 25 VD-1 $\alpha$ -hydroxylase, a process indeed occurring in T cell response to 25 VD.<sup>30</sup> However, here we showed that 25 VD and 1,25 VD have opposite effects on differentiated C2C12 myotubes, leading to the inconsistency of such hypothesis. In particular, we demonstrated that 1,25 VD induces a sharp reduction of C2C12 myotube diameters, in agreement

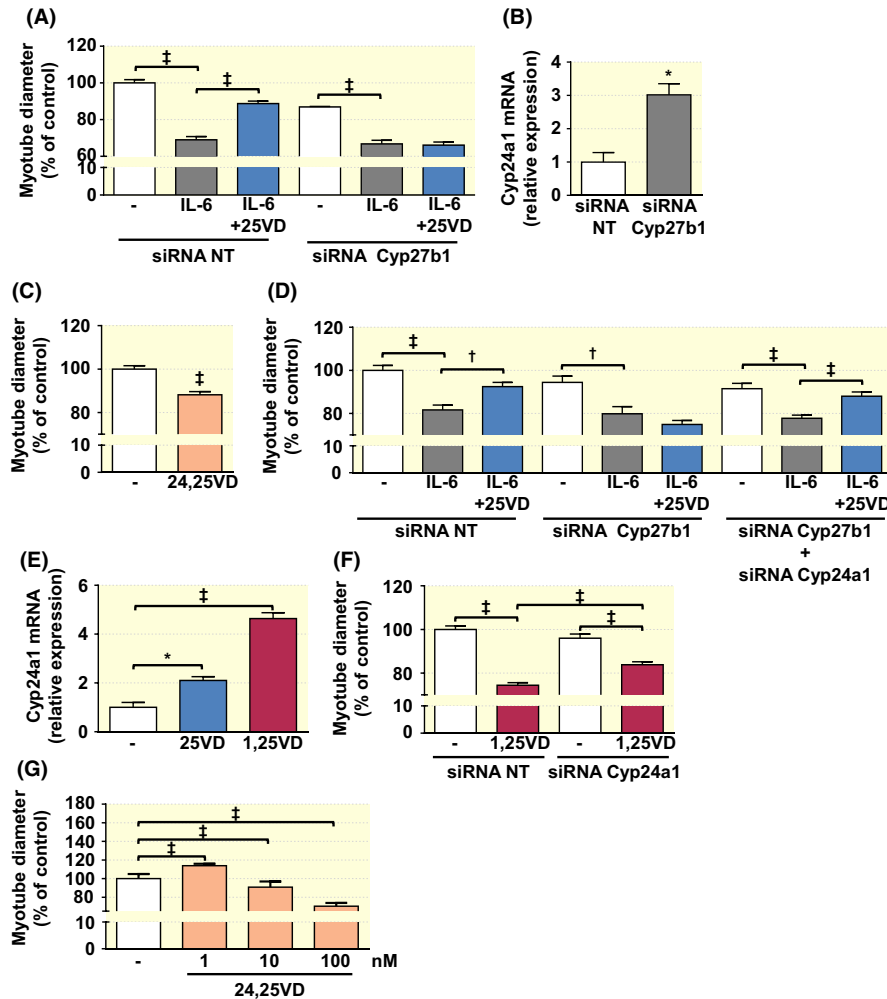


**FIGURE 5** Regulation of VD-24-hydroxylase and its role in muscle homeostasis. (A) C2C12 myotubes were transfected with *Cyp27b1* siRNA and, 24h later, were treated with IL-6 (20 ng/mL) with or without 100 nmol/L 25 VD. Myotube diameters were measured after further 24 h. ‡ $P < 0.001$ . (B) *Cyp24a1* expression was evaluated after 48h of *Cyp27b1* silencing. \* $P < 0.05$ . (C) Myotube diameters were measured after 24 h of 100 nmol/L 24,25 VD treatment. ‡ $P < 0.001$ . (D) C2C12 myotubes were transfected with *Cyp27b1* siRNA alone or in combination with *Cyp24a1* siRNA. 24h after silencing, C2C12 myotubes were treated with IL-6 (20 ng/mL) with or without 100 nmol/L 25 VD and myotube diameters measured after further 24 h. † $P < 0.01$ ; ‡ $P < 0.001$ . (E) *Cyp24a1* expression in C2C12 myotubes after 24 h treatment with 100 nmol/L 25 VD, 1,25 VD, 24,25 VD. \* $P < 0.05$ ; ‡ $P < 0.001$ . (F) C2C12 myotubes were treated with 100 nmol/L 1,25 VD after 24 h of *Cyp24a1* silencing. ‡ $P < 0.001$ . (G) Myotube diameters were measured after 24 h of treatment with increasing concentration of 24,25 VD. ‡ $P < 0.001$ . All treatments were in serum-free medium. Data are presented as means  $\pm$  SEM of three independent experiments

with previously published data.<sup>17</sup> Consistently, 1,25 VD treatment increased the expression of FoxO3a and the induction of Atrogin-1 and MuRF1 atrogenes, a well-characterized atrophic mechanism in skeletal muscle. The finding that VD receptor (VDR) directly associates with FoxO proteins and enhances FoxO binding to target gene promoters<sup>31</sup> suggests a further mechanism enhancing 1,25 VD-promoted atrophic effect. Besides being a key regulator of protein breakdown through the ubiquitin-proteasome, FoxO3 also modulates the autophagy-lysosomal proteolytic pathway.<sup>24</sup> Basal autophagy is necessary for cellular homeostasis, but its dysregulation, either its exacerbated activation or its block, may result in atrophy. Treatment of C2C12 myotubes with 1,25 VD decreased Cathepsin L expression (Figure 4A), a protein

required for the fusion of autophagosomes with lysosomes, thus leading to the accumulation of autophagosomes incapable of fusing with the lysosomes (Figure 4C) and the eventual blockage of the autophagic flux. 1,25 VD-induced reduction of ATF4, a transcription factor that, in stressful conditions induces autophagy,<sup>32</sup> could contribute to this impairment. The concomitant enhanced expression of *Bnip3* and *Gabarrpl1* genes (Figure 4A) suggests a compensatory intensification of the early autophagosome formation aimed at maintaining a functional autophagic flux. On the contrary, the increased autophagic flux upon 25 VD treatment (Figure 4D), could occur through a pathway mediated by AMPK (Figure 3A). Although excessive autophagy may lead to tissue wasting, this 25 VD-induced autophagy enhancement could be

beneficial, likely by increasing the availability of amino acids that, in turn, could contribute, together with Akt, to mTORC1 activation and protein synthesis.

25 VD, on the other hand, showed a protective effect against cytokine-induced atrophy and a mild hypertrophic effect when administered alone on C2C12 myotubes. Since muscle mass may be seen as the overall balance of anabolic and catabolic pathways, we suppose that the Akt pathway-mediated hypertrophic effect of 25 VD counterbalances cytokine-induced atrophy. Phosphorylation of FoxO3a (Figure 3E) suggests that also the inhibition of atrogene expression could be involved in 25 VD anti-atrophic activity, although in the system we used we could not appreciate cytokine-induced atrogene induction.

The differential induction of VDR by 1,25 VD and 25 VD and the weaker affinity of the latter for VDR itself<sup>19,23,33</sup> may explain the dissimilar effects of these VD metabolites on C2C12 myotubes as a divergent VDR-mediated enhancement of FoxO.<sup>31</sup> Nevertheless, in this work, we demonstrated the involvement of VD-24-hydroxylase induction and the transformation of VD metabolites in pro-atrophic 24-hydroxylated products. Despite the fact that previous studies demonstrate that VD metabolites regulate *Cyp24a1* expression,<sup>19,23</sup> the effect of 24-hydroxylated metabolites on skeletal myotubes have not been investigated, yet. Our data show that 24,25 VD has a hormetic effect on myotubes, seen as a hypertrophic effect at low doses and atrophic effect at higher doses (Figure 5G). On account of the strongest induction of *Cyp24a1* by 1,25 VD compared to 25 VD (Figure 5E), we hypothesize a central role of VD-24-hydroxylase in causing the differential effects of 1,25 VD and 25 VD on skeletal muscle. As it happens, *Cyp24a1* silencing attenuated the 1,25 VD atrophic effect on C2C12 myotubes (Figure 5F). We can speculate that, in C2C12 myotubes, 1,25 VD-triggered expression of VD-24-hydroxylase converts 1,25 VD in 1,24,25 VD, and that this metabolite, similarly to 24,25 VD, has an atrophic effect on C2C12 myotubes, though we could not test this hypothesis due to the lack of commercially available formulations of this metabolite. The involvement of VD-24-hydroxylase also explains the incongruous results emerging from the silencing of *Cyp27b1* used to assess the intracellular conversion of 25 VD in 1,25 VD, as *Cyp27b1* silencing leads to a significant increase of *Cyp24a1* mRNA expression (Figure 5B). Indeed, the idea that an anti-atrophic compound needed to be transformed in a pro-atrophic one to elicit its effect was disproved by *Cyp27b1* silencing-induced increase of *Cyp24a1* mRNA expression and by the fact that co-silencing of *Cyp27b1* and *Cyp24a1* restores 25 VD protective action against atrophic stimuli.

Low levels of VD are, together with fatigue and skeletal muscle loss, characteristics of cancer patients with cachexia.<sup>14</sup> VD status positively associates with muscle strength, physical performance, and a lower incidence of falls.<sup>34</sup> Therefore,

VD supplementation has been proposed as a possible preventive strategy in delaying muscle functional decline in several pathological conditions, including cancer cachexia. However, VD supplementation was ineffective in preventing cancer cachexia-associated muscle wasting in animals,<sup>17</sup> and a phase III clinical trial with cachectic patients was prematurely halted because of the detrimental effect of VD supplementation.<sup>16</sup> Because VD is a steroid, high dose regimens are usually proposed in clinical practice on the assumption of its storage in adipose tissue followed by a slow release.<sup>35,36</sup> However, high doses of VD do not mirror the physiological production of the hormone. Consistently, high VD intakes or treatments with very high doses as a bolus (every month or twice a year) have paradoxically been associated in several studies with adverse events in humans, including an increased incidence of falls and fracture, rates of prostatic and pancreatic cancers, and total mortality.<sup>35,37-39</sup> In agreement with the results of our and others work,<sup>23</sup> an up-regulation of *Cyp27b1*- and *Cyp24a1*-derived VD metabolites is therefore feasible upon high VD intakes.

Overall, this study shows how variously hydroxylated VD metabolites and the differential regulation of VD hydroxylases may trigger contrasting effects in C2C12 myotubes, thus explaining the lack of effectiveness of VD supplementation in vivo, both in animal models of cancer cachexia and in oncological patients. Our results shed light on other mechanisms involved in the failing or contradictory results of several clinical trials. In this regard, further studies will be necessary before considering VD supplementation for the maintenance of skeletal muscle mass in cancer patients.

## 4 | MATERIALS AND METHODS

### 4.1 | Reagents

25 VD and 1,25 VD were purchased from Merck (Burlington, Massachusetts, USA). 24,25 VD was from Sigma-Aldrich (Saint Louis, Missouri, USA). IL-6, TNF- $\alpha$ , and IFN $\gamma$  were from Peprotech (London, UK). Anti-tubulin antibody was from Sigma-Aldrich, anti-phospho-Akt<sup>S473</sup>, anti-Akt, anti-phospho-FoxO3a<sup>T32</sup>, anti-FoxO3a, and anti-LC3 antibodies were from Cell Signalling Technology (Danvers, Massachusetts, USA), anti-LAMP2 antibody was from Abcam (Cambridge, UK), and anti-puromycin antibody was from Merck. All other reagents, unless otherwise stated, were from Sigma-Aldrich.

### 4.2 | Cell cultures and myotube analysis

C2C12 myoblasts were grown at low density in DMEM (Gibco, Thermo Fisher Scientific, Waltham, Massachusetts, USA) supplemented with 10% foetal bovine serum (FBS, Gibco, Thermo Fisher Scientific), 100 U/mL penicillin, 100  $\mu$ g/mL

streptomycin, and 0.25 µg/mL antimycotic, referred to as growth medium (GM). To induce differentiation, cells were allowed to become confluent, and the medium was switched to differentiation medium (DM), consisting in DMEM supplemented with 2% horse serum, penicillin, streptomycin, and antimycotic as described above. Unless otherwise specified, myotubes were treated at day 4 of differentiation. Myotube diameters were measured as previously described.<sup>40</sup>

### 4.3 | Lewis lung carcinoma conditioned medium preparation

Lewis lung carcinoma cells (a kind gift from Prof. Paola Costelli, University of Turin) were grown in DMEM with 5% FBS, 100 U/mL penicillin, and 100 µg/mL streptomycin. For CM collection, cells were plated at a density of 50 000 cells/cm<sup>2</sup> and, after overnight attachment, the cells were washed three times with phosphate-buffered saline (PBS), followed by two washes with serum-free DMEM, and grown in serum-free DMEM containing 100 U/mL penicillin and 100 µg/mL streptomycin for 24 hours. The resulting CM was centrifuged at 500 g for 10 min, followed by additional centrifugation at 5000 g for 10 min. The CM was filtered using a 0.2 µm syringe filter and either used immediately or stored at -80°C. LLC CM was diluted at a 1:3 ratio with serum-free DMEM containing 100 U/mL penicillin and 100 µg/mL streptomycin for myotube treatment.

### 4.4 | Cyp27b1 and Cyp24a1 silencing

A quantity of 100 pmol of *Cyp27b1* siRNA, *Cyp24a1* siRNA (Ambion, Thermo Fisher Scientific), or siRNA negative control sequence (Ambion, Thermo Fisher Scientific) was transfected with Lipofectamine 3000 (Invitrogen, Thermo Fisher Scientific) in C2C12 at day 3 of differentiation. Myotubes underwent treatments 24 hours later. Transfection of myotubes with Block-iT (Invitrogen, Thermo Fisher Scientific) was used to assess transfection efficiency, which was always >90%.

### 4.5 | RNA extraction and analysis

Total RNA from myotubes was extracted by RNeasy (Sigma-Aldrich). The RNA was retro-transcribed with High-capacity cDNA Reverse Transcription Kit (Applied Biosystems, Thermo Fisher Scientific) and real-time PCR was performed with the StepOnePlus Real-time PCR System (Applied Biosystems, Thermo Fisher Scientific), using the following TaqMan probes (Thermo Fisher Scientific): Mm00499518\_m1 (*Fbxo32*, Atrogin-1/MAFbx), Mm01185221\_m1 (*Trim63*, MuRF1), Mm00515597\_m1 (*Ctstl*, Cathepsin L), Mm01275600\_g1 (*Bnip3*), Mm00457880\_m1 (*Gabarapl1*), Mm01197698\_m1 (*Gusb*), Mm00487244\_m1 (*Cyp24a1*), Mm00515325\_g1 (*Atf4*).

### 4.6 | Western Blotting

At the end of the indicated treatments, cells were washed in ice-cold PBS and solubilized with a lysis buffer containing 1% Triton X-100, 0.1% sodium deoxycholate, 0.1% sodium dodecyl sulfate, 1 mmol/L EDTA, 1 mmol/L EGTA, 50 mmol/L NaF, 160 mmol/L NaCl, 20mM Tris-HCl, pH 7.4, and supplemented with protease inhibitor cocktail. Lysates were stirred at 4°C for 15 min and centrifuged at 15 000 g for 15 minutes at 4°C. Protein concentration was determined by BCA protein assay kit (Thermo Fisher Scientific). Proteins (10-20 µg protein/lane) were separated by 10% SDS-PAGE and transferred to polyvinylidene difluoride filters (PVDF) (Hybond-P; GE Healthcare, Little Chalfont, Buckinghamshire, UK). Membranes were saturated with 4% bovine serum albumin (BSA), incubated with the primary antibodies overnight, washed with Tris-buffered saline-0.1% Tween, incubated with the appropriate secondary antibody (Invitrogen, Thermo Fisher Scientific), visualized with Western Lightning Chemiluminescence Reagent Plus (PerkinElmer Life and Analytical Sciences, Waltham, Massachusetts, USA), acquired with ChemiDoc Touch (Bio-Rad, Hercules, California, USA), and analysed with ImageLab (Bio-Rad). After anti-phospho-antibodies, membranes were stripped with Restore Plus Western blot stripping buffer (Thermo Fisher Scientific) and reblotted with the corresponding total protein antibodies.

### 4.7 | Immunofluorescence

For LAMP2 and LC3 detection, C2C12 myotubes were fixed in 4% paraformaldehyde for 10 minutes, washed with PBS, permeabilized with HEPES-TRITON X-100 0.5% for 5 minutes, and washed two times with PBS-0.2% BSA. For blocking the unspecific binding sites, cells were incubated in 2% BSA for 15 minutes at RT. LC3- and LAMP2-positive puncta were evaluated by incubation for 30 minutes with rabbit anti-LAMP2 (1:25) and mouse anti-LC3 (1:100), followed by the appropriate Alexa Fluor Dyes-conjugated secondary antibodies (546 anti-mouse, 488 anti-rabbit; Thermo Fisher Scientific). Nuclei were counterstained with TO-PRO-3 iodide (1:100, Thermo Fisher Scientific). Images were acquired with Leica confocal microscope TCS SP2 (Wetzlar, Germany) equipped with LCS Leica confocal software, using a 63X objective, NA 5 1.32, and fluorescence signals, normalized to the area of myotubes, for LC3, LAMP2, and their colocalization were quantified with ImageJ software.

### 4.8 | AKT pathway phosphorylation array

Mouse AKT pathway phosphorylation array C1 was purchased from RayBiotech, Inc (Norcross, Georgia, USA) and used according to manufacturer instructions.

## 4.9 | SUnSET protein synthesis assay

Differentiated myotubes were treated with 100 nmol/L 25 VD in DM for 24 hours, and, 30 minutes before cell lysis, 500 ng/mL puromycin was added to the medium. After western blotting with an anti-puromycin antibody, membranes were stained with Ponceau S red to visualize total proteins. Both western blots and stained membranes were acquired with ChemiDoc Touch (Bio-Rad, Hercules, California, USA), and analysed with ImageLab (Bio-Rad).

## 4.10 | Statistical analysis

Data are presented as the mean  $\pm$  SEM. The variation among groups was evaluated using ANOVA test. Statistical significance was assumed for  $P < 0.05$ . All statistical analyses were performed with GraphPad Prism 6 for OS Windows.

## ACKNOWLEDGEMENTS

The authors thank Paolo Porporato for scientific discussions and technical support. M.A.T. is beneficiary of a PhD fellowship from Compagnia di San Paolo. N.F. is recipient of a Fondazione CARIPLO grant (#2015\_0634). This research was partially funded by the AGING PROJECT-Department of Excellence University of Piemonte Orientale.

## CONFLICT OF INTEREST

The authors declare no conflict of interest.

## ORCID

Nicoletta Filigheddu  <https://orcid.org/0000-0002-3848-611X>

## REFERENCES

1. Dodson S, Baracos VE, Jatoi A, et al. Muscle wasting in cancer cachexia: clinical implications, diagnosis, and emerging treatment strategies. *Annu Rev Med*. 2011;62:265-279.
2. Vaughan VC, Martin P, Lewandowski PA. Cancer cachexia: impact, mechanisms and emerging treatments. *J Cachexia Sarcopenia Muscle*. 2013;4:95-109.
3. Fearon KC, Baracos VE. Cachexia in pancreatic cancer: new treatment options and measures of success. *HPB (Oxford)*. 2010;12:323-324.
4. Luo Y, Yoneda J, Ohmori H, et al. Cancer usurps skeletal muscle as an energy repository. *Cancer Res*. 2014;74:330-340.
5. Zhou X, Wang JL, Lu J, et al. Reversal of cancer cachexia and muscle wasting by ActRIIB antagonism leads to prolonged survival. *Cell*. 2010;142:531-543.
6. Jean G, Souberbielle JC, Chazot C. Vitamin D in chronic kidney disease and dialysis patients. *Nutrients*. 2017;9:328.
7. Mager DR, Carroll MW, Wine E, et al. Vitamin D status and risk for sarcopenia in youth with inflammatory bowel diseases. *Eur J Clin Nutr*. 2018;72:623-626.
8. Graumam RQ, Pinheiro MM, Nery LE, Castro C. Increased rate of osteoporosis, low lean mass, and fragility fractures in COPD patients: association with disease severity. *Osteoporos Int*. 2018;29:1457-1468.
9. Kang SY, Kang JH, Choi JC, Song SK, Oh JH. Low serum vitamin D levels in patients with myasthenia gravis. *J Clin Neurosci*. 2018;50:294-297.
10. Snijder MB, van Schoor NM, Pluijm SM, van Dam RM, Visser M, Lips P. Vitamin D status in relation to one-year risk of recurrent falling in older men and women. *J Clin Endocrinol Metab*. 2006;91:2980-2985.
11. Suzuki T, Kwon J, Kim H, et al. Low serum 25-hydroxyvitamin D levels associated with falls among Japanese community-dwelling elderly. *J Bone Miner Res*. 2008;23:1309-1317.
12. Iolascon G, Moretti A, de Sire A, Calafiore D, Gimigliano F. Effectiveness of calcifediol in improving muscle function in post-menopausal women: a prospective cohort study. *Adv Ther*. 2017;34:744-752.
13. Cangussu LM, Nahas-Neto J, Orsatti CL, Bueloni-Dias FN, Nahas EA. Effect of vitamin D supplementation alone on muscle function in postmenopausal women: a randomized, double-blind, placebo-controlled clinical trial. *Osteoporos Int*. 2015;26:2413-2421.
14. Dev R, Del Fabbro E, Schwartz GG, et al. Preliminary report: vitamin D deficiency in advanced cancer patients with symptoms of fatigue or anorexia. *Oncologist*. 2011;16:1637-1641.
15. Van Veldhuizen PJ, Taylor SA, Williamson S, Drees BM. Treatment of vitamin D deficiency in patients with metastatic prostate cancer may improve bone pain and muscle strength. *J Urol*. 2000;163:187-190.
16. Scher HI, Jia X, Chi K, et al. Randomized, open-label phase III trial of docetaxel plus high-dose calcitriol versus docetaxel plus prednisone for patients with castration-resistant prostate cancer. *J Clin Oncol*. 2011;29:2191-2198.
17. Camperi A, Pin F, Costamagna D, et al. Vitamin D and VDR in cancer cachexia and muscle regeneration. *Oncotarget*. 2017;8:21778-21793.
18. Srikuea R, Zhang X, Park-Sarge OK, Esser KA. VDR and CYP27B1 are expressed in C2C12 cells and regenerating skeletal muscle: potential role in suppression of myoblast proliferation. *Am J Physiol Cell Physiol*. 2012;303:C396-405.
19. Girgis CM, Clifton-Bligh RJ, Mokbel N, Cheng K, Gunton JE. Vitamin D signalling regulates proliferation, differentiation, and myotube size in C2C12 skeletal muscle cells. *Endocrinology*. 2014;155:347-357.
20. Buitrago CG, Arango NS, Boland RL.  $1\alpha,25(\text{OH})_2\text{D}_3$ -dependent modulation of Akt in proliferating and differentiating C2C12 skeletal muscle cells. *J Cell Biochem*. 2012;113:1170-1181.
21. Braga M, Simmons Z, Norris KC, Ferrini MG, Artaza JN. Vitamin D induces myogenic differentiation in skeletal muscle derived stem cells. *Endocr Connect*. 2017;6:139-150.
22. Porporato PE, Filigheddu N, Reano S, et al. Acylated and unacylated ghrelin impair skeletal muscle atrophy in mice. *J Clin Invest*. 2013;123:611-622.
23. van derMeijden K, Bravenboer N, Dirks NF, et al. Effects of  $1,25(\text{OH})_2\text{D}_3$  and  $25(\text{OH})\text{D}_3$  on C2C12 Myoblast Proliferation,

- Differentiation, and Myotube Hypertrophy. *J Cell Physiol.* 2016;231:2517-2528.
24. Zhao J, Brault JJ, Schild A, et al. FoxO3 coordinately activates protein degradation by the autophagic/lysosomal and proteasomal pathways in atrophying muscle cells. *Cell Metab.* 2007;6:472-483.
  25. Wortel I, van der Meer LT, Kilberg MS, van Leeuwen FN. Surviving stress: modulation of ATF4-mediated stress responses in normal and malignant cells. *Trends Endocrinol Metab.* 2017;28:794-806.
  26. Torremadé N, Bozic M, Goltzman D, Fernandez E, Valdivielso JM. Effects of the administration of 25(OH) vitamin D3 in an experimental model of chronic kidney disease in animals null for 1 alpha-hydroxylase. *PLoS One.* 2017;12:e0170654.
  27. Hassan-Smith ZK, Jenkinson C, Smith DJ, et al. (2017) 25-hydroxyvitamin D3 and 1,25-dihydroxyvitamin D3 exert distinct effects on human skeletal muscle function and gene expression. *PLoS One.* 2017;12:e0170665.
  28. Chun RF, Lauridsen AL, Suon L, et al. Vitamin D-binding protein directs monocyte responses to 25-hydroxy- and 1,25-dihydroxyvitamin D. *J Clin Endocrinol Metab.* 2010;95:3368-3376.
  29. Jeffery LE, Wood AM, Qureshi OS, et al. Availability of 25-hydroxyvitamin D(3) to APCs controls the balance between regulatory and inflammatory T cell responses. *J Immunol.* 2012;189:5155-5164.
  30. Kongsbak M, von Essen MR, Levring TB, et al. Vitamin D-binding protein controls T cell responses to vitamin D. *BMC Immunol.* 2014;15:35.
  31. An BS, Tavera-Mendoza LE, Dimitrov V, et al. Stimulation of Sirt1-regulated FoxO protein function by the ligand-bound vitamin D receptor. *Mol Cell Biol.* 2010;30:4890-4900.
  32. B'chir W, Maurin A-C, Carraro V, et al. The eIF2 $\alpha$ /ATF4 pathway is essential for stress-induced autophagy gene expression. *Nucleic Acids Res.* 2013;41:7683-7699.
  33. Ritter CS, Armbrrecht HJ, Slatopolsky E, Brown AJ. 25-Hydroxyvitamin D(3) suppresses PTH synthesis and secretion by bovine parathyroid cells. *Kidney Int.* 2006;70:654-659.
  34. Ceglia L, Harris SS. Vitamin D and its role in skeletal muscle. *Calcif Tissue Int.* 2013;92:151-162.
  35. Ross AC, Manson JE, Abrams SA, et al. The 2011 report on dietary reference intakes for calcium and vitamin D from the Institute of Medicine: what clinicians need to know. *J Clin Endocrinol Metab.* 2011;96:53-58.
  36. Holick MF, Binkley NC, Bischoff-Ferrari HA, et al. Evaluation, treatment, and prevention of vitamin D deficiency: an Endocrine Society clinical practice guideline. *J Clin Endocrinol Metab.* 2011;96:1911-1930.
  37. Gillespie LD, Robertson MC, Gillespie WJ, et al. Interventions for preventing falls in older people living in the community. *Cochrane Database Syst Rev.* 2009;2:CD007146.
  38. The Scientific Advisory Committee on Nutrition (SACN) recommendations on vitamin D. Vitamin D and health. (2016). Available at <https://www.gov.uk/government/publications/sacn-vitamin-d-and-health-report>. Accessed 26 April 2018.
  39. Bischoff-Ferrari HA, Dawson-Hughes B, Orav EJ, et al. Monthly high-dose vitamin D treatment for the prevention of functional decline: a randomized clinical trial. *JAMA Intern Med.* 2016;176:175-183.
  40. Wyart E, Reano S, Hsu MY, et al. Metabolic alterations in a slow-paced model of pancreatic cancer-induced wasting. *Oxid Med Cell Longev.* 2018;2018:6419805.

**How to cite this article:** Sustova H, De Feudis M, Reano S, et al. Opposing effects of 25-hydroxy- and 1 $\alpha$ ,25-dihydroxy-vitamin D<sub>3</sub> on pro-cachectic cytokine-and cancer conditioned medium-induced atrophy in C2C12 myotubes. *Acta Physiol.* 2019;e13269. <https://doi.org/10.1111/apha.13269>

**Introduction to the paper “Cholecalciferol (vitamin D3) has a direct protective activity against interleukin 6-induced atrophy in C2C12 myotubes”**

Alves Teixeira M, De Feudis M, Reano S, Raiteri T, Scircoli A, Ruga S, Salvadori L, Prodám F, Marzullo P, Molinari C, Corà D, Filigheddu N.

*Aging- under review*

After having demonstrated that 25 VD and 1,25 VD have opposite effects on C2C12 myotubes, likely *via* differential modulation of 24-hydroxylase, and that 24,25 VD itself has either atrophic or hypertrophic effects, depending on its concentration (Sustova et al., 2019), thus reinforcing the idea that all VD metabolites, and not only 1,25VD, might be biologically active (Raisz et al., 1980; Eisman et al., 2014), we wondered if also cholecalciferol (VD3), the non-hydroxylated upstream metabolite, could have a biological effect on muscle cells.

In the *in vitro* muscle model of C2C12 myotubes induced to undergo atrophy with IL-6 treatment, we demonstrated the protective activity of VD3. The lack of expression, in C2C12 myotubes, of the hydroxylase transforming VD3 suggests that VD3 protective effect on skeletal muscle are direct. Similarly to 25VD, VD3 could prevent atrophy through enhancing the autophagic flux, while it does not significantly affect protein synthesis. Moreover, we demonstrated that VDR is required for VD3 biological activity, hinting that VDR could bind, besides 1,25VD and 25VD, also their non-hydroxylated precursor. Finally, we showed that VD3 was unable to protect from dexamethasone-induced atrophy, suggesting a limited anti-atrophic potential of cholecalciferol, depending on the underlying cause of muscle wasting. Overall, our results widen the horizons of the extra-skeletal effects of vitamin D, as well as the potential therapeutic benefits and limits of vitamin D supplementation.



## **Cholecalciferol (vitamin D3) has a direct protective activity against interleukin 6-induced atrophy in C2C12 myotubes**

Maraiza Alves Teixeira<sup>1,2</sup>, Marilisa De Feudis<sup>1</sup>, Simone Reano<sup>1</sup>, Tommaso Raiteri<sup>1</sup>, Andrea Scircoli<sup>1</sup>, Sara Ruga<sup>1</sup>, Laura Salvadori<sup>1,2</sup>, Flavia Prodam<sup>3</sup>, Paolo Marzullo<sup>1</sup>, Claudio Molinari<sup>1</sup>, Davide Corà<sup>1</sup>, Nicoletta Filigheddu<sup>1,2</sup>

<sup>1</sup>Department of Translational Medicine, University of Piemonte Orientale, Novara, Italy

<sup>2</sup>Istituto Interuniversitario di Miologia (IIM)

<sup>3</sup>Department of Health Sciences, University of Piemonte Orientale, Novara, Italy

Corresponding author: Nicoletta Filigheddu, Department of Translational Medicine, University of Piemonte Orientale, Via Solaroli 17, 28100 Novara, Italy. Phone: (+39) 0321660529; Fax: (+39) 0321620421 email: [nicoletta.filigheddu@med.uniupo.it](mailto:nicoletta.filigheddu@med.uniupo.it)

[maraiza.teixeira@med.uniupo.it](mailto:maraiza.teixeira@med.uniupo.it); [marilisa.defeudis@med.uniupo.it](mailto:marilisa.defeudis@med.uniupo.it); [simone.reano@med.uniupo.it](mailto:simone.reano@med.uniupo.it); [tomraiteri@gmail.com](mailto:tomraiteri@gmail.com); [andre.scircoli@gmail.com](mailto:andre.scircoli@gmail.com); [sara.ruga@uniupo.it](mailto:sara.ruga@uniupo.it); [laura.salvadori@uniupo.it](mailto:laura.salvadori@uniupo.it); [flavia.prodam@med.uniupo.it](mailto:flavia.prodam@med.uniupo.it); [paolo.marzullo@med.uniupo.it](mailto:paolo.marzullo@med.uniupo.it); [claudio.molinari@med.uniupo.it](mailto:claudio.molinari@med.uniupo.it); [davide.cora@med.uniupo.it](mailto:davide.cora@med.uniupo.it)

**Keywords:** sarcopenia; cachexia; autophagy; vitamin D hydroxylases; VDR

## **ABSTRACT**

We previously determined that different vitamin D metabolites can have opposite effects on C2C12 myotubes, depending on the sites of hydroxylation or doses. This study aimed to clarify whether also cholecalciferol (VD3), the non-hydroxylated upstream metabolite, has a direct effect on muscle cells. Assessing the effects of VD3 treatment on mouse C2C12 skeletal muscle myotubes undergoing atrophy induced by IL6, we demonstrated that VD3 has a protective action, preserving C2C12 myotubes size, likely through enhancing the autophagic flux. The lack, in C2C12 myotubes, of the hydroxylase transforming VD3 in the anti-atrophic 25VD metabolite, suggests that VD3 may have a direct biological activity on the skeletal muscle. Furthermore, the protective action of VD3 depended on VDR, implying that also VD3 might bind and activate VDR.

In conclusion, also VD3, in addition to its best-known metabolites, may directly impact on skeletal muscle homeostasis.

## **INTRODUCTION**

Skeletal muscle wasting may occur in several physio-pathological conditions and represents one of the main overlapping features between the physiological age-related sarcopenia and cachexia, which often associates with an underlying disease, such as cancer, especially in the terminally ill patients.

In both cases, the occurrence of chronic systemic inflammation may directly contribute to the loss of skeletal muscle mass and functionality [1–5].

Another feature often associated with both muscle wasting-inducing conditions is an important reduction of vitamin D<sub>3</sub>, seen as decreased 25(OH)D<sub>3</sub> (25-hydroxycholecalciferol, hereafter 25VD) circulating levels [6,7].

In humans, vitamin D<sub>3</sub> synthesis begins with skin exposure to ultraviolet B radiation and the consequent photochemical conversion of the precursor, 7-dehydrocholesterol (pro-vitamin D<sub>3</sub>), in pre-vitamin D<sub>3</sub>. Through thermal isomerization, pre-vitamin D<sub>3</sub> is converted to vitamin D<sub>3</sub> (cholecalciferol, hereafter VD3), which is hydroxylated in the liver by the 25-hydroxylases (25-

OHases encoded by CYP27A1 and CYP2R1 genes); the resultant 25VD is further converted in 1,25(OH)<sub>2</sub>D<sub>3</sub> (1,25-dihydroxy vitamin D<sub>3</sub> or calcitriol, hereafter 1,25VD) in the kidney by 1 $\alpha$ -hydroxylase (1 $\alpha$ -OHase, encoded by the CYP27B1 gene). Lastly, the 24-hydroxylase encoded by the gene CYP24A1 catalyzes the conversion of both 25VD and 1,25VD into 24-hydroxylated products targeted for inactivation and excretion.

1,25VD exerts its biological activities through the binding to vitamin D receptor (VDR), inducing the heterodimerization of VDR with the retinoic acid receptor RXR, the recruitment of various coregulators, and the binding of this complex to specific regions on DNA. Though the bone is the best-known target of vitamin D, VDR is almost ubiquitously expressed through the cells and tissues of the body, suggesting that vitamin D has wide pleiotropic activities. Likewise, the widespread extra-renal expression of the CYP27B1 hydroxylase suggests that 25VD could be locally converted to 1,25VD, thus providing a mechanism explaining the ever-growing observations of 25VD-elicited biological activities [8,9]. Nevertheless, we have demonstrated that, in C2C12 myotubes, 25VD has a biological anti-atrophic activity that does not depend on its intracellular conversion to 1,25VD. Unexpectedly, in this *in vitro* model of skeletal muscle, 25VD and 1,25VD have antithetical effects, likely *via* differential modulation of 24-hydroxylase [10]. Furthermore, we showed that, on C2C12 myotubes, 24,25(OH)<sub>2</sub>D<sub>3</sub> (24,25VD) itself could have divergent effects, either atrophic or hypertrophic, depending on its concentration. These observations are in accordance with and strengthen the idea that all vitamin D<sub>3</sub> metabolites, and not only 1,25VD, might be biologically active [11,12]. Proceeding with this view, here we explored the hypothesis that VD<sub>3</sub> as well could have a direct biological activity on skeletal muscle cells.

## RESULTS

### **VD3 treatment protects C2C12 myotubes from IL-6 induced atrophy**

To assess whether VD3 could have protective activity in the skeletal muscle, we mimicked *in vitro* the condition of inflammation-prompted muscle wasting by treating murine C2C12-derived myotubes with the pro-atrophic cytokine interleukin-6 (IL-6) [10]. C2C12 myotubes incubated for 24 hours with 20 ng/ml IL-6 underwent a consistent atrophy, appraised as a reduction of 20% in myotube thickness (Figure 1A). Co-treatment with VD3 prevented the reduction of myotube diameter in a dose-dependent manner, starting from 1 nM concentrations. At concentrations of 10 and 100 nM, VD3 completely blocked the atrophic effect of IL-6 (Figure 1A). The supplementation of VD3 alone had no evident effects on C2C12 myotube size (Figure 1B).

### **VD3 stimulates the autophagic flux in C2C12 myotubes**

Skeletal muscle homeostasis depends on the balance between anabolic and catabolic processes. Coherently with the lack of effect on myotube diameters (Figure 1B), VD3 did not stimulate protein synthesis, although we observed a mild, not significant increase in puromycin incorporation in SUnSET assay (Figure 2A). We, therefore, investigated whether VD3 could affect autophagy, another mechanism that can regulate muscle homeostasis by regulating protein and organelle turnover [13,14]. To assess the effect of VD3 on the autophagic flux, we measured the colocalization of the autophagosomal marker LC3 with the lysosomal marker LAMP2 in C2C12 myotubes in the presence or absence of chloroquine, a blocker of the autophagic flux. We observed that VD3 induced a drastic accumulation of LC3-LAMP2 co-staining only in cells co-treated with chloroquine, denoting an increased formation of autophagolysosomes, indicative of an enhancement of the autophagic flux (Figure 2B).

### **VD3 anti-atrophic activity is VDR-dependent but does not depend on intracellular conversion to 25VD**

The complexity of vitamin D biological activity is further complicated by the ability of distinct vitamin D metabolites to modulate the expression of the hydroxylases involved in vitamin D metabolism and of VDR [15]. To explore if the hitherto observed effects of VD3 on C2C12 myotubes could depend on its transformation on other metabolites with already proven biological activity, we assessed the expression of the main players of vitamin D metabolism upon VD3 treatment. In particular, as we have previously demonstrated that 25 VD has a powerful anti-atrophic activity in C2C12 myotubes treated with pro-cachectic cytokines, including IL-6 [10], we explored the hypothesis that the observed anti-atrophic effect of VD3 could be due to its intracellular conversion to 25 VD in C2C12 myotubes. *In vivo*, VD3 is hydroxylated in the liver by 25-hydroxylases (in mouse, mainly by Cyp2r1; Ohyama & Shinki, 2016; Thacher & Levine, 2017) to yield 25 VD. Using murine liver as a positive control, we found that the Cyp2r1 was not expressed in C2C12 myotubes, neither basally nor upon stimulation with VD3 or IL6 (data not shown), providing evidence for a direct biological action of VD3 on C2C12 myotubes.

In addition, we found that, similarly to 25VD and 1,25VD [18], VD3 did not affect the expression of *Cyp27b1* (Figure 3A). However, differently from 25VD and 1,25VD metabolites [10,18], VD3 did not modulate the expression of 24-hydroxylase *Cyp24a1* (Figure 3B), nor that of *Vdr* (Figure 3C). Also, VD3 had no effect on the expression of *Pdia3*, the gene encoding for the 1,25D3-MARRS (Membrane Associated, Rapid Response Steroid binding), an alternative vitamin D receptor regarded as the one mediating the membrane-initiated signaling of 1,25VD3 (Figure 3D).

### **VD3 anti-atrophic activity is VDR-dependent**

Although VD3 does not modulate the expression of *Vdr* (Figure 3C), the silencing of *Vdr* completely abrogated the protective activity of VD3 against IL6-induced atrophy (Figure 4A), indicating that VDR mediates VD3 anti-atrophic activity in C2C12 myotubes. On the contrary, 1,25D3-MARRS

receptor is not involved in VD3 anti-atrophic action, as the silencing of *Pdia3* did not affect the activity of VD3 (Figure 4B).

### **VD3 does not protect C2C12 myotubes from dexamethasone-induced atrophy**

To investigate if VD3 could have a broad anti-atrophic activity, we assessed its effect by co-treating C2C12 myotubes undergoing atrophy upon treatment with dexamethasone, a synthetic glucocorticoid that induces muscle protein degradation *via* the activation of the ubiquitin-proteasome system (UPS) [19]. Myotubes were treated with 5  $\mu$ M dexamethasone for 24 h in the presence or absence of 100 nM VD3. Treatment with dexamethasone reduced myotube diameters by 10% and induced the muscle-specific ubiquitin ligase Atrogin-1 (MAFbx) expression. VD3 was not able to impair this atrophy (Figure 5A and B), indicating that VD3 ability to counteract muscle atrophy is limited.

## **DISCUSSION**

The impact of vitamin D on muscle morphology and functionality has been largely investigated, and vitamin D deficiency has been implicated in pathological conditions such as frailty and sarcopenia in the elders and cachexia in cancer patients [6,20]. Even though the deficiency of vitamin D clearly correlates with muscle condition impairment, the effectiveness of vitamin D supplementation depends on the context of use. In fact, a relevant number of epidemiological studies have suggested the potential role of vitamin D intake in order to maintain or improve muscle strength and function in older people [21]. On the other hand, the efficacy of VD supplementation in cancer cachexia remains non-conclusive [20].

In our previous attempt to better understand these different biological responses in the skeletal muscle to vitamin D supplementation, we realized that, *in vitro*, different vitamin D metabolites have distinctive activities. In particular, we conjectured that a different extent of 24-hydroxylase modulation by 25VD and 1,25VD results in divergent effects on C2C12 myotubes, being 25VD

protective against cytokine-induced atrophy and 1,25VD atrophic *per se*. Furthermore, 24,25VD itself can either protect or induce atrophy, depending on its concentration [10].

Here, we showed that also the un-hydroxylated VD3 could prevent IL-6-induced atrophy in C2C12 myotubes (Figure 1). Notably, the absence in these cells, either in unstimulated condition or upon atrophic stimuli, of *Cyp2r1*, the principal vitamin D 25-hydroxylase in mice [16,17], rules out an intracellular conversion of VD3 in 25VD, whose anti-atrophic activity has already been demonstrated [10] and implies a direct activity of VD3 in C2C12 myotubes. In addition, the loss of anti-atrophic activity upon silencing of *Vdr* (Figure 4A) suggests that VDR could also bind VD3, in addition to 1,25VD and 25VD [22], although specific binding studies should be performed to confirm this hypothesis and to determine the binding affinity.

Our data indicate that the anti-atrophic activity of VD3 is not generic but depends on the stimulus inducing atrophy. Indeed, VD3 was unable to protect from dexamethasone-induced atrophy and to prevent the induction of the muscle-specific ubiquitin ligases Atrogin-1 (Figure 4). As the ability of IL-6 to induce Atrogin-1 remain debated, with several works reporting contrasting finding [23], we can speculate that VD3 can protect from stimuli that do not involve, as the primary mechanism, the induction of atrogenes (muscle-specific ubiquitin ligases) and activation of the proteasome system. Another reason for the lack of protection against dexamethasone-induced atrophy might lie in the heterodimerization of the glucocorticoid receptor (GR) with RXR, the main partner for VDR heterodimerization upon ligand binding. GR-RXR dimerization occurs in the case of dexamethasone-induced death of murine T-cells and thymocytes [24]. In the light of the involvement of VDR in the anti-atrophic activity of VD3 (Figure 4A), we can speculate that dexamethasone signaling could induce the dimerization of GR with RXR, thus preventing the formation of VDR-RXR complex and the anti-atrophic activity of VD3. Furthermore, the strong GR activation induced by dexamethasone could trap coregulators like steroid receptor coactivator-1 (SRC-1), modifying the mutual binding to glucocorticoid- and vitamin D-responsive elements (GREs and VDREs, respectively) on DNA and, consequently, the activation/inhibition of specific genes [25–27].

On the other hand, IL-6-induced muscle atrophy depends on the activation of STAT3 [28] that, in turn, leads to the inhibition of autophagosome formation and autophagy [29,30]. Autophagy is essential in maintaining muscle homeostasis through the elimination of defective proteins and the recycling of amino acids [31], and its inhibition may result in muscle weakness and atrophy [14]. Coherently, VD3 could overcome the IL-6-mediated inhibition of autophagy through boosting the autophagic flux (Figure 2B).

Collectively, our findings suggest that VD3 supplementation *in vivo* -where it is physiologically converted in 25VD, 1,25VD, and 24-hydroxylated products- can result in a combination of effects due to the simultaneous action of different vitamin D metabolites, each of which with its own pro- or anti-atrophic activity [10]. Moreover, although C2C12 myotubes do not express *Cyp2r1*, this 25-hydroxylase is present in the whole muscle [32,33], thus possibly transforming VD3 in 25VD. Although VD3 did not modulate the expression of the other hydroxylases involved in vitamin D metabolism (Figure 3), some of those may be modulated by other [10,18] and by systemic inflammation [34] in a tissue-specific manner, further raveling the scenario and providing a putative explanation for the contrasting outcomes of VD3 supplementation in different conditions. In conclusion, our findings suggest the need to assess, before VD3 supplementation *in vivo*, the levels of as many as possible vitamin D metabolites as a readout of the activity of different hydroxylases, thus avoiding the increase of the pro-atrophic metabolites. Also, the design of VD3-derived not-hydroxylable molecules that maintain the anti-atrophic property of VD3 preventing the sequential hydroxylations that could result in pro-atrophic molecules might represent a prominent strategy to overcome the limitations of VD3 supplementation in some pathological conditions.



## FIGURES

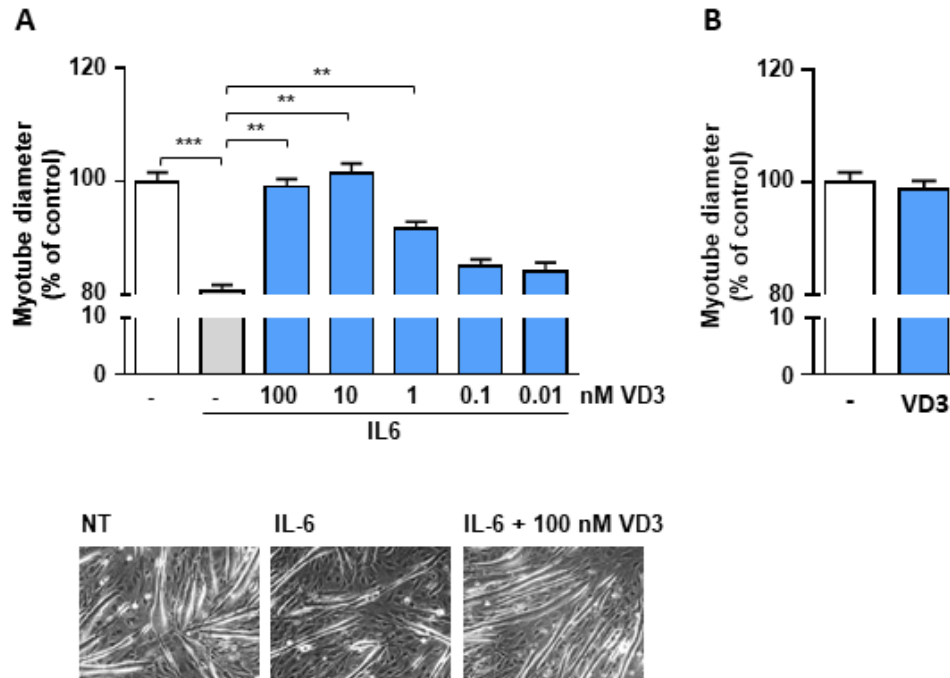


Figure 1. **VD3 protects C2C12 myotubes from IL-6-induced atrophy.** (A) Myotube diameters were measured after 24h treatment in serum-free medium with 20 ng/ml IL-6 alone or in combination with decreasing concentrations (100 – 0.01 nM) of VD3. At the bottom of the panel, representative phase-contrast images of differentiated myotubes after 24h of treatment with IL-6 in the absence or presence of 100nM VD3. (B) Myotube diameters were measured after 24h treatment in serum-free medium with 100nM VD3. Data are presented as the mean  $\pm$  SEM. \*\*\* $P < 0.001$ .

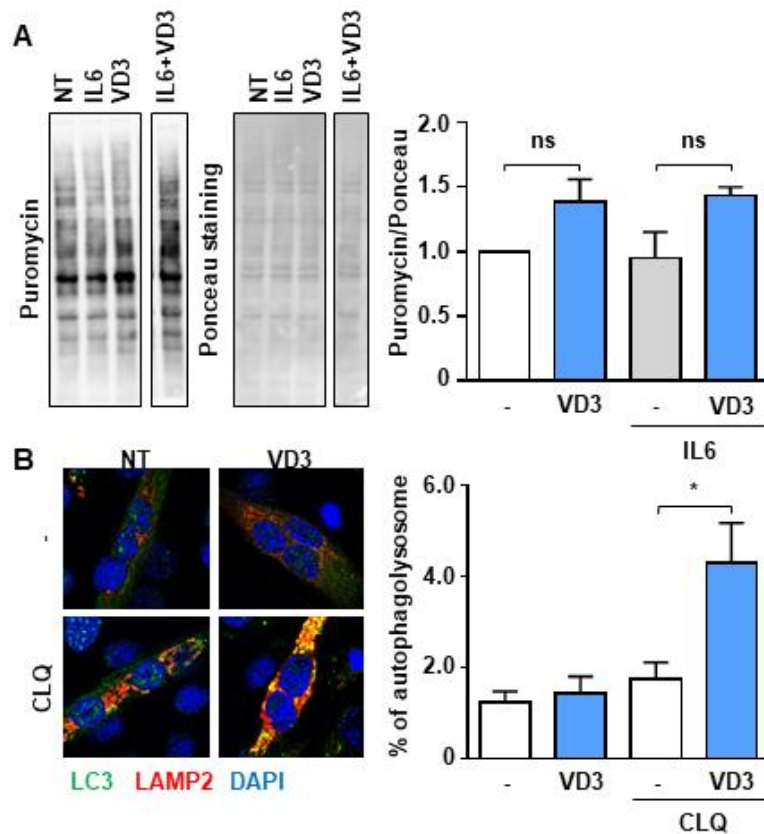


Figure 2. **VD3 does not stimulate protein synthesis but intensify the autophagic flux.** (A) Protein synthesis upon 24h treatment with 20 ng/ml IL-6 in the presence or absence of 100nM VD3 was evaluated by SUnSET assay. Incorporation of puromycin into newly synthesized proteins was visualized by Western blotting and normalized on total proteins detected by Ponceau staining (representative images on the left of the panel). Densitometry of three experiments is shown on the right part of the panel. (B) C2C12 myotubes in DM were treated for 24h with 100nmol/L VD3 in the presence and absence of 10µmol/L of chloroquine (CLQ). LC3 (autophagosome marker) and LAMP2 (lysosomal marker) were detected by immunofluorescence. Autophagic flux was assessed by quantifying the colocalization of LC3-LAMP2 in the presence vs. absence of CLQ. On the left of the panel, representative images; on the right, percentage of LC3 area colocalized with LAMP2 above total myotube area. \* $P < 0.05$ .

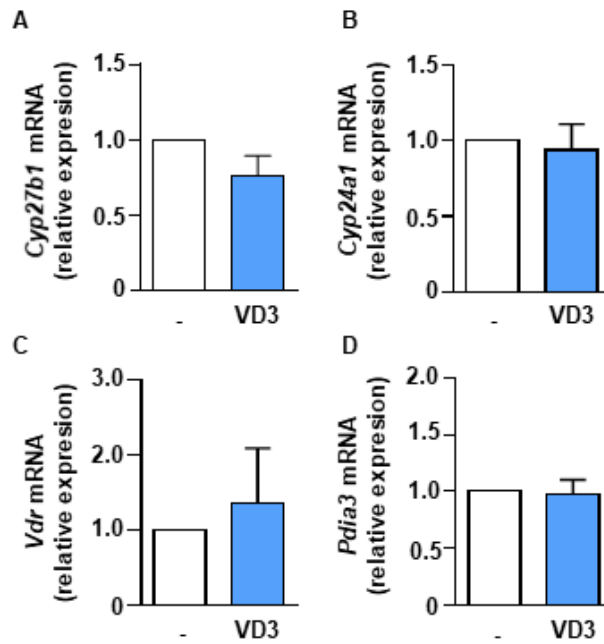


Figure 3. **VD3 did not alter the expression of hydroxylases and receptors involved in vitamin D metabolism and activity.** C2C12 myotubes were treated in serum-free medium with VD3 for 24h, and mRNA levels of (A) *Cyp27b1*, (B) *Cyp24a1*, (C) *Vdr*, and (D) *Pdia3* were assayed by real-time PCR, using *Gusb* as the housekeeping gene. In Data are presented as the mean  $\pm$  SEM of three independent experiments. \* $P < 0.05$ .

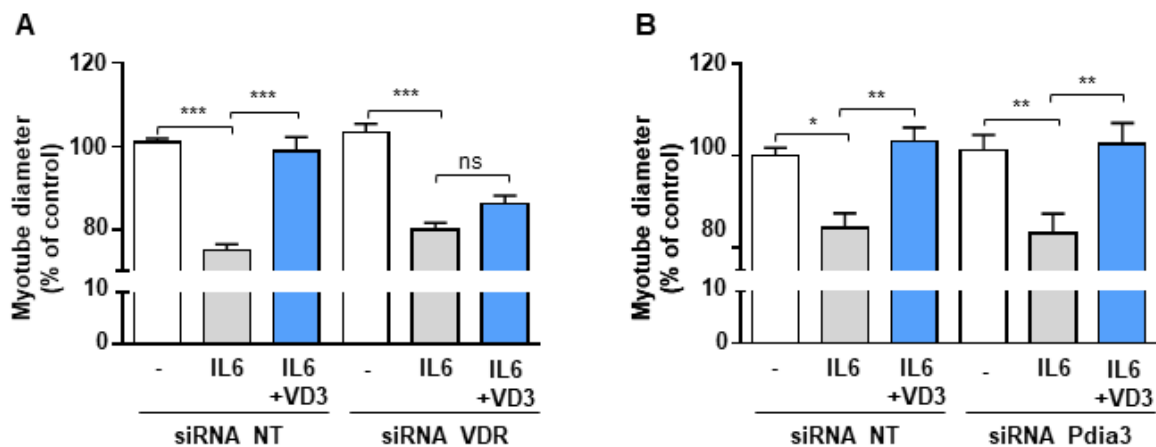


Figure 4. **VDR, but not 1,25D3-MARRS (*Pdia3*), mediates VD3 anti-atrophic activity.** C2C12 myotubes were transfected with (A) *Vdr* or (B) *Pdia3* specific siRNAs. 24h after silencing, C2C12 myotubes were treated with 20ng/mL IL-6 in the absence or presence of 100 nM VD3 and myotube diameters measured after further 24h. Data are presented as the mean  $\pm$  SEM. \* $P < 0.05$ ; \*\* $P < 0.01$ ; \*\*\* $P < 0.001$ .

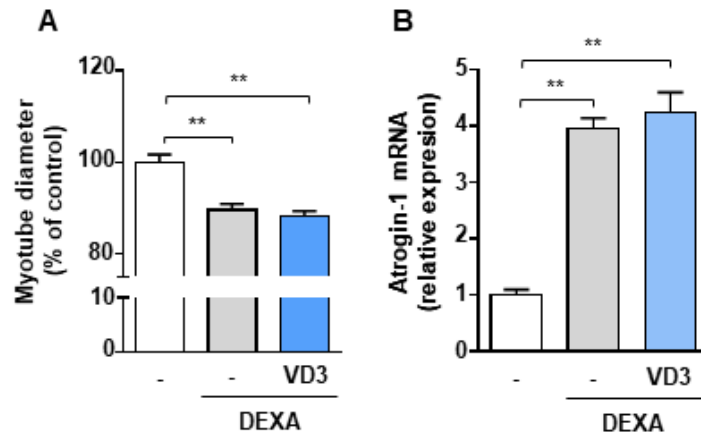


Figure 5. **VD3 does not protect myotubes against atrophy induced by dexamethasone.** (A) Myotube diameters were measured after 24h treatment with 5  $\mu$ M dexamethasone (DEXA) alone or in combination with 100 nM VD3. (B) Expression of Atrogin-1 (*Fbxo32*) was assessed by real-time RT-PCR. Data are presented as the mean  $\pm$  SEM. \*\*  $P < 0.01$ .

## MATERIALS AND METHODS

### Reagents

VD3 was purchased from Cayman Chemicals (Ann Arbor, Michigan, USA) and dissolved in ethanol. IL-6 was from Peprotech (London, UK). Water-soluble dexamethasone (DEXA) was from Merck Life Science (Milan, Italy). The anti-LC3 antibody was from Proteintech (Rosemont, Illinois, USA), the anti-LAMP2 antibody was from Abcam (Cambridge, UK), and the anti-puromycin antibody was from Merck Life Science. All other reagents, unless otherwise stated, were from Merck Life Science.

### Cell cultures and myotube analysis

C2C12 myoblasts were grown at low density in DMEM (Gibco, Thermo Fisher Scientific, Waltham, Massachusetts, USA) supplemented with 10% fetal bovine serum (FBS, Gibco, Thermo Fisher Scientific), 100 U/mL penicillin, 100  $\mu$ g/mL streptomycin, and 0.25  $\mu$ g/mL antimycotic. To induce

differentiation, cells were allowed to become confluent, and the medium was switched to differentiation medium (DM), consisting in DMEM supplemented with 2% horse serum (GE Healthcare Bio-Sciences, Uppsala, Sweden), penicillin, streptomycin, and antimycotic as described above. Unless otherwise specified, myotubes were treated after 4 days of differentiation in serum-free medium. Control cells were treated with ethanol. Myotube diameters were measured as previously described [35].

### **Western Blotting**

At the end of the indicated treatments, cells were washed in ice-cold PBS and solubilized with a lysis buffer containing 1% Triton X-100, 0.1% sodium deoxycholate, 0.1% sodium dodecyl sulfate, 1 mmol/L EDTA, 1 mmol/L EGTA, 50 mmol/L NaF, 160 mmol/L NaCl, 20mM Tris-HCl, pH 7.4, and supplemented with protease inhibitor cocktail. Lysates were stirred at 4°C for 15 min and centrifuged at 15 000 g for 15 minutes at 4°C. Protein concentration was determined by BCA protein assay kit (Thermo Fisher Scientific). Proteins (10-20 µg protein/lane) were separated by 10% SDS-PAGE and transferred to polyvinylidene difluoride filters (PVDF) (Hybond-P; GE Healthcare, Little Chalfont, Buckinghamshire, UK). Membranes were saturated with 4% bovine serum albumin (BSA), incubated with the primary antibodies overnight, washed with Tris buffered saline-0.1% Tween, incubated with the appropriate secondary antibody (Invitrogen, Thermo Fisher Scientific), visualized with Western Lightning Chemiluminescence Reagent Plus (PerkinElmer Life and Analytical Sciences, Waltham, Massachusetts, USA), acquired with ChemiDoc Touch (BioRad, Hercules, California, USA), and analyzed with ImageLab (Bio-Rad).

### **SUnSET protein synthesis assay**

Protein synthesis was evaluated by SUnSET assay [36]. Differentiated myotubes were treated with 100 nM VD3 in serum-free medium for 24 hours, and, 30 minutes before cell lysis, 500 ng/mL puromycin was added to the medium. After western blotting with an anti-puromycin antibody,

membranes were stained with Ponceau S red to visualize total proteins. Both western blots and stained membranes were acquired with ChemiDoc Touch (Bio-Rad, Hercules, California, USA), and analysed with ImageLab (Bio-Rad).

### **Immunofluorescence**

For LAMP2 and LC3 detection, C2C12 myotubes were fixed in 4% paraformaldehyde for 10 minutes, washed with PBS, permeabilized with HEPES-TRITON X-100 0.5% for 5 minutes, and washed two times with PBS-0.2% BSA. For blocking the unspecific binding sites, cells were incubated in 4% BSA for 1 h at RT. LC3- and LAMP2-positive puncta were evaluated by incubation for 1 h with rat anti-LAMP2 (1:100) and rabbit anti-LC3 (1:100), followed by the appropriate Alexa Fluor Dyes-conjugated secondary antibodies (546 anti-mouse 1:400, 488 anti-rabbit 1:400; Thermo Fisher Scientific). Nuclei were counterstained with DAPI (1:100, Thermo Fisher Scientific). Images were acquired with a Leica TCS SP8 confocal laser scanning microscope (Leica, Wetzlar, Germany) equipped with LCS Leica confocal software, using a 63X objective, NA 5 1.32, and fluorescence signals, normalized to the area of myotubes, for LC3, LAMP2, and their colocalization were quantified with ImageJ software.

### **RNA extraction and analysis**

Total RNA from myotubes was extracted by RNAzol (SigmaAldrich). The RNA was retro-transcribed with High-capacity cDNA Reverse Transcription Kit (Applied Biosystems, Thermo Fisher Scientific) and real-time PCR was performed with the StepOnePlus Real-time PCR System (Applied Biosystems, Thermo Fisher Scientific), using the following TaqMan probes (Thermo Fisher Scientific): Mm00499518\_m1 (*Fbxo32*, Atrogin-1/MAFbx), Mm00487244\_m1 (*Cyp24a1*), Mm01165918\_g1 (*Cyp27b1*), Mm00437297\_m1 (*Vdr*), Mm00433130\_m1 (*Pdia3*), Mm01159413\_m1 (*Cyp2r1*), Mm01197698\_m1 (*Gusb*).

## **VDR and PDIA3 silencing**

A concentration of 10 nM of *Vdr* siRNA, *Pdia3* siRNA (Integrated DNA Technologies), or siRNA negative control sequence (Integrated DNA Technologies) was transfected with Lipofectamine 3000 (Invitrogen, Thermo Fisher Scientific) in C2C12 at day 3 of differentiation. Myotubes underwent treatments with IL6 and VD3 24 hours later. Transfection of myotubes with Block-iT (Invitrogen, Thermo Fisher Scientific) was used to assess transfection efficiency, which was always >90%.

## **Statistical analysis**

Data are presented as the mean  $\pm$  SEM. Outliers in the measurements were identified by mean of the interquartile range (IQR), as either below  $Q1 - 1.5 \text{ IQR}$  or above  $Q3 + 1.5 \text{ IQR}$ , and excluded from the analysis. The variation among groups was evaluated using ANOVA test followed by Tukey's Multiple comparisons test unless otherwise stated. Statistical significance was assumed for  $P < 0.05$ . All statistical analyses were performed with GraphPad Prism 6.

## **ABBREVIATIONS**

1,25D3-MARRS:	Membrane Associated, Rapid Response Steroid binding
1,25VD:	1,25-dihydroxy vitamin D <sub>3</sub> , 1,25(OH) <sub>2</sub> D <sub>3</sub> , calcitriol
1 $\alpha$ -OHase:	1 $\alpha$ -hydroxylase
24,25VD:	24,25-dihydroxy vitamin D <sub>3</sub> , 24,25(OH) <sub>2</sub> D <sub>3</sub> ,
25-OHases:	25-hydroxylases
25VD:	25-hydroxycholecalciferol, 25(OH)D <sub>3</sub>
BCA:	Bicinchoninic acid
BSA:	bovine serum albumin
DAPI:	4',6-diamidino-2-phenylindole
DEXA:	dexamethasone

DM:	differentiation medium
DMEM:	Dulbecco's Modified Eagle Medium
EDTA:	Ethylenediaminetetraacetic acid
EGTA:	Ethylene glycol-bis(2-aminoethylether)-N,N,N',N'-tetraacetic acid
GR:	Glucocorticoid Receptor
GREs:	Glucocorticoid-Responsive Elements
HEPES:	4-(2-HydroxyEthyl)-1-PiperazineEthanesulfonic Acid
IL-6:	Interleukin 6
IQR:	interquartile range
LAMP2:	Lysosomal-Associated Membrane Protein 2
LC3:	Light Chain 3
MAFbx:	Muscle Atrophy F-box
PBS:	Phosphate Buffered Saline
PVDF:	polyvinylidene difluoride filters
RT:	room temperature
RXR:	retinoic acid receptor
SDS-PAGE:	Sodium Dodecyl Sulfate Polyacrylamide Gel Electrophoresis
SEM:	Standard error of the mean
SRC-1:	Steroid Receptor Coactivator-1
STAT3:	Signal transducer and activator of transcription 3
SUnSET:	SURface SEnsing of Translation
Tris:	2-Amino-2-(hydroxymethyl)-1,3-propanediol
UPS:	Ubiquitin-Proteasome System
VD:	Vitamin D
VD3:	Cholecalciferol, Vitamin D <sub>3</sub> , D <sub>3</sub> , VD <sub>3</sub>
VDR:	Vitamin D receptor



VDREs: Vitamin D-Responsive Elements

## **AUTHOR CONTRIBUTIONS**

NF: study conception and design; manuscript writing. FP, PM, CM: study conception and design.

MAT, MDF, SR, TR, AS, SR, LS: conduction of experiments and data collection. FP, DC, SR, NF: data analysis and interpretation.

## **CONFLICTS OF INTERESTS**

The authors declare no conflict of interest.

## **FUNDING**

This study was funded by the Università del Piemonte Orientale, FAR-2019, and by the Italian Ministry of University and Research program "Departments of Excellence 2018-2022", AGING Project – Department of Translational Medicine, Università del Piemonte Orientale.

MAT is beneficiary of a PhD fellowship from Compagnia di San Paolo.

## **REFERENCES**

1. Rea IM, Gibson DS, McGilligan V, McNerlan SE, Alexander HD, Ross OA. Age and Age-Related Diseases: Role of Inflammation Triggers and Cytokines. *Front Immunol*. Frontiers Media S.A.; 2018; 9: 586. Available from: <http://journal.frontiersin.org/article/10.3389/fimmu.2018.00586/full>
2. Marceca GP, Londhe P, Calore F. Management of Cancer Cachexia: Attempting to Develop New Pharmacological Agents for New Effective Therapeutic Options. *Front Oncol*. 2020; 10. Available from: <https://www.frontiersin.org/article/10.3389/fonc.2020.00298/full>

3. Biswas AK, Acharyya S. Understanding cachexia in the context of metastatic progression. *Nat Rev Cancer*. Springer US; 2020; 20: 274–84. Available from: <http://dx.doi.org/10.1038/s41568-020-0251-4>
4. Peixoto da Silva S, Santos JMO, Costa e Silva MP, Gil da Costa RM, Medeiros R. Cancer cachexia and its pathophysiology: links with sarcopenia, anorexia and asthenia. *J Cachexia Sarcopenia Muscle*. 2020; : jcsm.12528. Available from: <https://onlinelibrary.wiley.com/doi/abs/10.1002/jcsm.12528>
5. da Fonseca GWP, Farkas J, Dora E, von Haehling S, Lainscak M. Cancer cachexia and related metabolic dysfunction. *Int J Mol Sci*. 2020; 21: 1–19.
6. Caristia, Filigheddu, Barone-Adesi, Sarro, Testa, Magnani, Aimaretti, Faggiano, Marzullo. Vitamin D as a Biomarker of Ill Health among the Over-50s: A Systematic Review of Cohort Studies. *Nutrients*. MDPI AG; 2019; 11: 2384. Available from: <https://www.mdpi.com/2072-6643/11/10/2384>
7. Dev R, Del Fabbro E, Schwartz GG, Hui D, Palla SL, Gutierrez N, Bruera E. Preliminary Report: Vitamin D Deficiency in Advanced Cancer Patients with Symptoms of Fatigue or Anorexia. *Oncologist*. 2011; 16: 1637–41. Available from: <https://onlinelibrary.wiley.com/doi/abs/10.1634/theoncologist.2011-0151>
8. Zehnder D, Bland R, Williams MC, McNinch RW, Howie AJ, Stewart PM, Hewison M. Extrarenal Expression of 25-Hydroxyvitamin D 3 -1 $\alpha$ -Hydroxylase 1. *J Clin Endocrinol Metab*. The Endocrine Society; 2001; 86: 888–94. Available from: <https://academic.oup.com/jcem/article-lookup/doi/10.1210/jcem.86.2.7220>
9. Morris HA, Anderson PH. Autocrine and paracrine actions of vitamin d. *Clin Biochem Rev*. 2010; .
10. Sustova H, De Feudis M, Reano S, Alves Teixeira M, Valle I, Zaggia I, Agosti E, Prodám F, Filigheddu N. Opposing effects of 25-hydroxy- and 1 $\alpha$ ,25-dihydroxy-vitamin D<sub>3</sub> on pro-cachectic cytokine-and cancer conditioned medium-induced atrophy in C2C12 myotubes.

Acta Physiol. 2019; 226: 1–10.

11. Raisz LG, Kream BE, Smith MD, Simmons HA. Comparison of the effects of vitamin D metabolites on collagen synthesis and resorption of fetal rat bone in organ culture. *Calcif Tissue Int.* 1980; 32: 135–8. Available from: <http://link.springer.com/10.1007/BF02408532>
12. Eisman JA, Bouillon R. Vitamin D: direct effects of vitamin D metabolites on bone: lessons from genetically modified mice. *Bonekey Rep.* Nature Publishing Group; 2014; 3: 1–6. Available from: <http://dx.doi.org/10.1038/bonekey.2013.233>
13. Behrends C, Sowa ME, Gygi SP, Harper JW. Network organization of the human autophagy system. *Nature.* 2010; 466: 68–76. Available from: <http://www.nature.com/articles/nature09204>
14. Margeta M. Autophagy Defects in Skeletal Myopathies. *Annu Rev Pathol Mech Dis.* 2020; 15: 261–85. Available from: <https://www.annualreviews.org/doi/10.1146/annurev-pathmechdis-012419-032618>
15. Jones G, Prosser DE, Kaufmann M. Cytochrome P450-mediated metabolism of vitamin D. *J Lipid Res.* 2014; 55: 13–31. Available from: <http://www.jlr.org/lookup/doi/10.1194/jlr.R031534>
16. Thacher TD, Levine MA. CYP2R1 mutations causing vitamin D-deficiency rickets. *J Steroid Biochem Mol Biol.* 2017; 173: 333–6. Available from: <https://linkinghub.elsevier.com/retrieve/pii/S0960076016302138>
17. Ohyama Y, Shinki T. Cholecalciferol. In: Takei Y, Ando H, Tsutsui K, editors. *Handbook of Hormones.* Elsevier; 2016. p. 551–3. Available from: <https://linkinghub.elsevier.com/retrieve/pii/B9780128010280002373>
18. van der Meijden K, Bravenboer N, Dirks NF, Heijboer AC, den Heijer M, de Wit GMJ, Offringa C, Lips P, Jaspers RT. Effects of 1,25(OH)<sub>2</sub>D<sub>3</sub> and 25(OH)D<sub>3</sub> on C2C12 Myoblast Proliferation, Differentiation, and Myotube Hypertrophy. *J Cell Physiol.* Wiley-Liss Inc.; 2016; 231: 2517–28. Available from: <http://doi.wiley.com/10.1002/jcp.25388>

19. Bodine SC. Identification of Ubiquitin Ligases Required for Skeletal Muscle Atrophy. *Science* (80- ). 2001; 294: 1704–8. Available from:  
<https://www.sciencemag.org/lookup/doi/10.1126/science.1065874>
20. Garcia M, Seelaender M, Sotiropoulos A, Coletti D, Lancha AH. Vitamin D, muscle recovery, sarcopenia, cachexia, and muscle atrophy. *Nutrition*. Elsevier Inc.; 2019; 60: 66–9. Available from: <https://linkinghub.elsevier.com/retrieve/pii/S089990071830697X>
21. Remelli F, Vitali A, Zurlo A, Volpato S. Vitamin D Deficiency and Sarcopenia in Older Persons. *Nutrients*. MDPI AG; 2019; 11: 2861. Available from:  
<https://www.mdpi.com/2072-6643/11/12/2861>
22. Lips P. Relative Value of 25(OH)D and 1,25(OH)2D Measurements. *J Bone Miner Res*. 2007; 22: 1668–71. Available from: <http://doi.wiley.com/10.1359/jbmr.070716>
23. Muñoz-Cánoves P, Scheele C, Pedersen BK, Serrano AL. Interleukin-6 myokine signaling in skeletal muscle: a double-edged sword? *FEBS J*. 2013; 280: 4131–48. Available from:  
<http://doi.wiley.com/10.1111/febs.12338>
24. Tóth K, Sarang Z, Scholtz B, Brázda P, Ghyselinck N, Chambon P, Fésüs L, Szondy Z. Retinoids enhance glucocorticoid-induced apoptosis of T cells by facilitating glucocorticoid receptor-mediated transcription. *Cell Death Differ*. 2011; 18: 783–92. Available from:  
<http://www.nature.com/articles/cdd2010136>
25. Ratman D, Vanden Berghe W, Dejager L, Libert C, Tavernier J, Beck IM, De Bosscher K. How glucocorticoid receptors modulate the activity of other transcription factors: A scope beyond tethering. *Mol Cell Endocrinol*. 2013; 380: 41–54. Available from:  
<https://linkinghub.elsevier.com/retrieve/pii/S0303720712005382>
26. Helsen C, Claessens F. Looking at nuclear receptors from a new angle. *Mol Cell Endocrinol*. Elsevier Ireland Ltd; 2014; 382: 97–106. Available from:  
<https://linkinghub.elsevier.com/retrieve/pii/S0303720713003717>
27. Bouillon R, Carmeliet G, Verlinden L, van Etten E, Verstuyf A, Luderer HF, Lieben L,

- Mathieu C, Demay M. Vitamin D and Human Health: Lessons from Vitamin D Receptor Null Mice. *Endocr Rev.* Oxford Academic; 2008; 29: 726–76. Available from: <https://academic.oup.com/edrv/article-lookup/doi/10.1210/er.2008-0004>
28. Bonetto A, Aydogdu T, Jin X, Zhang Z, Zhan R, Puzis L, Koniaris LG, Zimmers TA. JAK/STAT3 pathway inhibition blocks skeletal muscle wasting downstream of IL-6 and in experimental cancer cachexia. *Am J Physiol - Endocrinol Metab.* 2012; 303: 410–21.
29. Yamada E, Bastie CC, Koga H, Wang Y, Cuervo AM, Pessin JE. Mouse Skeletal Muscle Fiber-Type-Specific Macroautophagy and Muscle Wasting Are Regulated by a Fyn/STAT3/Vps34 Signaling Pathway. *Cell Rep.* Elsevier; 2012; 1: 557–69.
30. Qin B, Zhou Z, He J, Yan C, Ding S. IL-6 Inhibits Starvation-induced Autophagy via the STAT3/Bcl-2 Signaling Pathway. *Sci Rep.* Nature Publishing Group; 2015; 5: 1–10.
31. Levine B, Kroemer G. Autophagy in the Pathogenesis of Disease. *Cell.* 2008; 132: 27–42. Available from: <https://linkinghub.elsevier.com/retrieve/pii/S0092867407016856>
32. Jain SK, Parsanathan R, Achari AE, Kanikarla-Marie P, Bocchini JA. Glutathione Stimulates Vitamin D Regulatory and Glucose-Metabolism Genes, Lowers Oxidative Stress and Inflammation, and Increases 25-Hydroxy-Vitamin D Levels in Blood: A Novel Approach to Treat 25-Hydroxyvitamin D Deficiency. *Antioxid Redox Signal.* 2018; 29: 1792–807. Available from: <https://www.liebertpub.com/doi/10.1089/ars.2017.7462>
33. Bièche I, Narjoz C, Asselah T, Vacher S, Marcellin P, Lidereau R, Beaune P, de Waziers I. Reverse transcriptase-PCR quantification of mRNA levels from cytochrome (CYP)1, CYP2 and CYP3 families in 22 different human tissues. *Pharmacogenet Genomics.* 2007; 17: 731–42. Available from: <http://journals.lww.com/01213011-200709000-00006>
34. Hummel DM, Fetahu IS, Gröschel C, Manhardt T, Kállay E. Role of proinflammatory cytokines on expression of vitamin D metabolism and target genes in colon cancer cells. *J Steroid Biochem Mol Biol.* 2014; 144: 91–5. Available from: <https://linkinghub.elsevier.com/retrieve/pii/S096007601300191X>

35. Wyart E, Reano S, Hsu MY, Longo DL, Li M, Hirsch E, Filigheddu N, Ghigo A, Riganti C, Porporato PE. Metabolic Alterations in a Slow-Paced Model of Pancreatic Cancer-Induced Wasting. *Oxid Med Cell Longev*. 2018; 2018: 1–10. Available from: <https://www.hindawi.com/journals/omcl/2018/6419805/>
36. Schmidt EK, Clavarino G, Ceppi M, Pierre P. SUnSET, a nonradioactive method to monitor protein synthesis. *Nat Methods*. Nature Publishing Group; 2009; 6: 275–7.

## **Vitamin D and muscle homeostasis - Unpublished data**

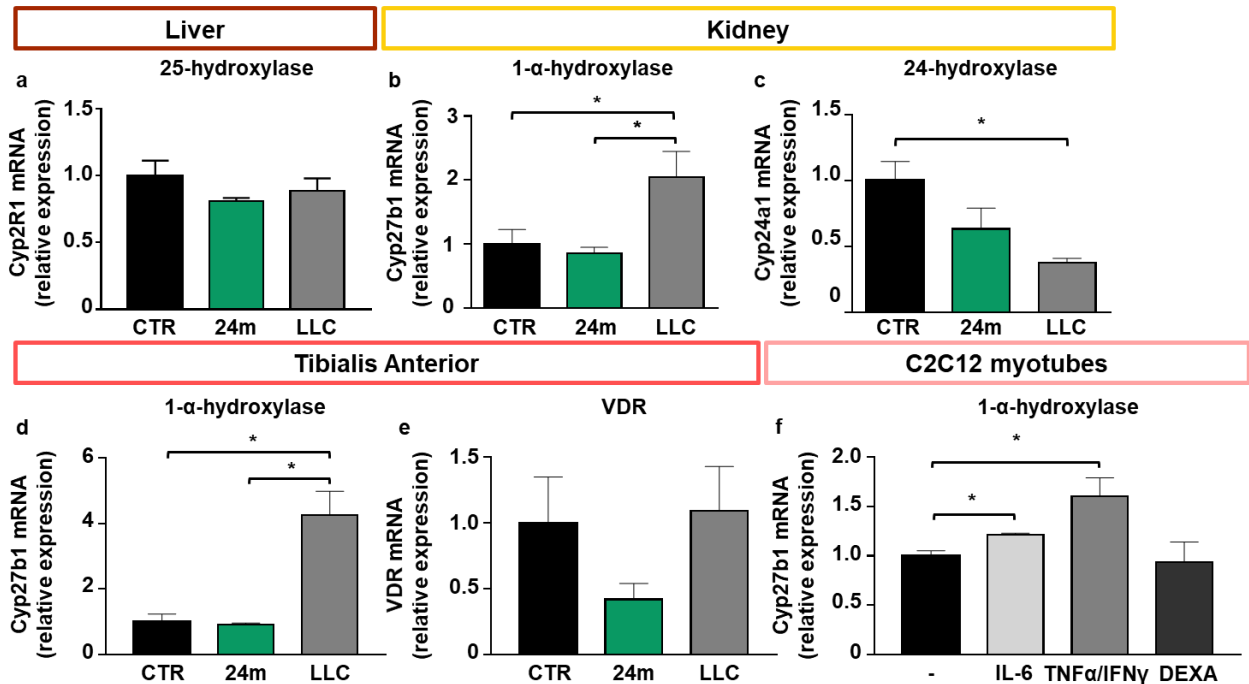
Low VD circulating levels characterize both elderly sarcopenic subjects and cachectic oncologic patients (Janssen et al., 2002; Mosekilde, 2005; Dev et al, 2011), and VD status positively correlates with muscle strength as well (Beudart et al., 2014; Iolascon et al. 2017). However, VD supplementation leads to different outcomes depending on the context of use, resulting a good strategy to counteract aged-related muscle wasting but not cancer cachexia-associated muscle atrophy (Remelli et al., 2019; Garcia et al., 2019). We demonstrated that un-hydroxylated VD<sub>3</sub> and 25 VD protect C2C12 myotubes from cytokine-induced atrophy, while 1,25 induces atrophy. Moreover, 24,25 VD exerts either protective or atrophic effect depending on concentration. The observation that opposite effect of VD metabolites on C2C12 could be due to different modulation of 24-hydroxylase by 25 VD and 1,25, prompted to hypothesizes that VD hydroxylase system modulation *in vivo* may profoundly affect VD supplementation outcome.

Preliminary results obtained from the analysis of VD hydroxylases in several anatomic districts of cachectic and sarcopenic mice encourage this hypothesis.

In accordance with the evidence that 25-hydroxylase is constitutive expressed in liver and subjected to just a little feedback regulation (Omdahl et al., 2002; Girgis et al., 2013), there are no significant differences in the hepatic expression of the aforementioned enzyme between the experimental analyzed groups (Fig. a).

Interestingly, in kidney, the main organ responsible for the conversion of 25 VD in 1,25 VD, the expression on 1- $\alpha$ -hydroxylase is dramatically higher in tumor-bearing animals then in control and sarcopenic mice (Fig. b). Furthermore, the expression of 24-hydroxylase is deregulated as well, resulting significantly lower in cachectic mice compared to control (Fig. c). In Tibialis Anterior, 1- $\alpha$ -hydroxylase expression pattern perfectly mirror what has been observed in kidney (Fig. d), indicating that different pathophysiologic condition might be characterized by a different status of VD hydroxylases.

As a further confirmation, *in vitro* 1- $\alpha$ -hydroxylase expression increases just upon stimuli mimicking cancer cachexia (Fig. f).



**VD hydroxylases are dysregulated in cachectic but not in old mice.** VD hydroxylase and VDR expression was evaluated in three experimental group: control mice (CTR), 24-month-old mice (24m) and tumor bearing mice injected with LLC. (a) Cyp2R1 expression in liver. In kidney, Cyp27b1 (b) and Cyp24a1 (c) expression was assessed. Cyp27b1 expression levels in muscle were checked both *ex vivo* in Tibialis anterior (d) and *in vitro* in C2c12 myotubes (f). (e) VDR expression was evaluated in Tibialis anterior. \*P<0.05.

Our preliminary data might suggest that in elderly the not altered hydroxylase expression pattern allows a physiologic VD metabolism, inducing VD circulating level rescue and determining a positive outcome of treatment. While the lack of effectiveness of VD supplementation to counteract cancer cachexia-associated muscle wasting could be due to a dysregulated VD metabolism, that in turn may lead even to an increased concentration of pro-atrophic metabolites.



In this regard, evaluating VD metabolites concentration both in cancer cachexia and sarcopenia animal models after VD administration, could help clarifying if supplemented VD is processed differentially based on context, proposing new insights for clinical practice. Moreover, our findings might represent a starting point to design new drugs with restricted hydroxylability to overcome the limitations of VD3 supplementation in some pathological conditions.

## Ghrelin

Ghrelin is a circulating 28-aa hormone, mainly produced by X/A-like cells in the oxyntic glands of the gastric mucosa, discovered as an endogenous ligand of the growth hormone secretagogue receptor 1a (GHSR1a), a seven-transmembrane G-protein-coupled receptor (GPCR) (Kojima et al., 1999; Howard et al., 1996)

The human ghrelin gene, GHRL, is localized on chromosome 3p25-26 (Kojima and Kangawa, 2005) and encodes for preproghrelin, consisting of 117 amino acids and post-transcriptionally processed into pro-ghrelin (Labarthe et al., 2014). Prohormone convertase (PC) 1/3 is the endoprotease responsible for the intracellular conversion of proghrelin to ghrelin (Zhu et al., 2006).

Ghrelin exists in two major different forms: acylated (AG) and unacylated (UnAG). During protein maturation, a portion of the ghrelin pool undergoes a post-translational octanoacylation on serine 3 residue of the mature hormone. This unique post-translational modification is catalyzed by the enzyme ghrelin *O*-acyl-transferase (GOAT) within the endoplasmic reticulum of ghrelin cells (Gutierrez et al., 2008; Yang et al., 2008) and it is necessary for the GHSR1a binding (Kojima et al., 1999) (Fig. 7). AG, through GHSR1a, induces a strong release of growth hormone (GH), stimulates food intake, modulate glucose metabolism, increases body weight and adiposity (Kojima et al., 1999; Kohno et al., 2003; Reimer et al., 2003, Broglio et al., 2001; Dezaki et al., 2004). UnAG, which is more abundant in plasma than AG, does not bind to GHSR1a, does not induce GH release and has no direct effects on food intake, but it shares with AG several biological activities independently of GHSR1a, reliant to a yet unidentified receptor (Porporato et al. 2013). Both AG and UnAG prevent cell death in cardiomyocytes and endothelial cells (Baldanzi et al., 2002), promote fusion and differentiation of C2C12 myoblasts (Filigheddu et al., 2007), induce proliferation and inhibit apoptosis in  $\beta$ -pancreatic cells (Granata et al., 2007). In addition, UnAG enhances muscle satellite cell activity, activates autophagy and mitophagy, and stimulates insulin sensitivity, thus promoting muscle regeneration or preventing skeletal mass loss in different disease models, including hindlimb ischemia, high-fat diet-induced diabetes, and chronic kidney disease (Togliatto etl a., Gortan

Cappellari et al., 2016; Gortan Cappellari et al., 2017; Reano et al., 2017). As GHSR1a receptor is not expressed on cardiomyocytes, skeletal myoblasts and pancreatic, the effects of Ghrelin on these cell populations is GHSR1a-independent, proving the existence of an alternative receptor, perhaps a GPCR with a G $\alpha$ s subunit (Granata et al., 2007; Porporato et al., 2013).

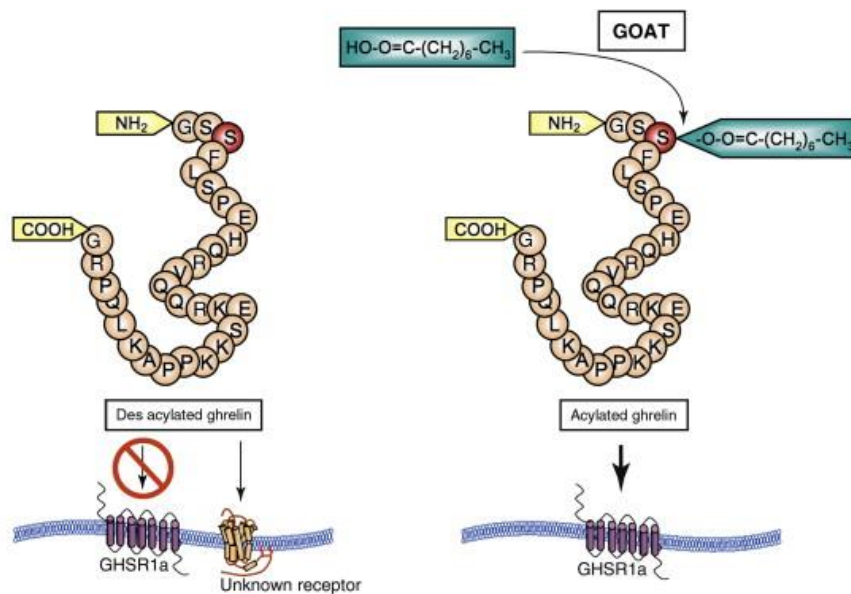


**Figure 7. Ghrelin acylation by GOAT is necessary for GHSR1a binding.** Ghrelin circulates in plasma in two forms: acylated and unacylated ghrelin. GOAT-dependent post translational acylation on serine 3 residue of ghrelin is crucial to confer biological activity via GHSR1a. UnAG ghrelin does not bind GHSR1a, but shares with AG several biological activities independently of GHSR1a, reliant to a yet unidentified receptor (Andrews, 2010).

## Ghrelin and skeletal muscle

The lack of expression of GHSR1a receptor on skeletal muscle means that ghrelin peptides affect directly skeletal muscle through the yet unidentified receptor. In particular, it has been demonstrated that UnAG impairs catabolic activities induced by the combined treatment with TNF- $\alpha$  and IFN- $\gamma$  in cultured C2C12 myotubes (Sheriff S etl al. 2012), and both AG and UnAG protect from dexamethasone-induced atrophy (Porporato et al. 2013).

Moreover, ghrelin influence regulation of skeletal muscle mass by stimulation of insulin-like growth factor 1 (IGF-1) production (Chen et al., 2015). However, independently of GH/IGF- axis activation and GHSR1a binding, AG as well as UnAG display a direct antiatrophic activity on skeletal muscles in vivo. Indeed, in vivo studies have shown that both ghrelin peptides protect skeletal muscle from wasting induced by burning, fasting, and denervation (Sheriff S etl al. 2012; Porporato et al. 2013; Wu et al., 2018).

Cachexia and sarcopenia are two different multifactorial processes phenotypically characterized by muscle loss. The evidence of ghrelin dysregulation in both muscle-wasting associated conditions and the well-established protective effect of ghrelin peptides from muscle atrophy, encouraged further studies about the involvement of ghrelin system both in cachexia and sarcopenia.

## **Ghrelin in cachexia**

Plasma ghrelin levels raise during fasting or low body mass index (BMI)-associated conditions, such as cachexia (Akamizu et al., 2010; Haqq et al., 2003).

Ghrelin peptide levels are increased in most patients affected by cancer cachexia compared with patients without cancer or cancer patients without cachexia (Shimizu et al., 2003; Garcia et al., 2005; Mondello et al., 2014). However, despite the increased ghrelin levels, cancer cachectic patients did not show increased appetite. During cachexia progression, ghrelin levels could be enhanced as a compensatory mechanism in response to weight loss, negative energy balance, reduced appetite, and inflammation (Chopin et al., 2012; Garcia et al. 2005, Baatar et al. 2011), suggesting that cachexia might lead to a ghrelin resistance status. Nevertheless, this latter condition did not limit ghrelin use in therapy, as it has been demonstrated that treatments with high dose of ghrelin or with molecules able to potentiate ghrelin signaling ameliorate anorexia symptoms overcoming ghrelin resistance (Terawaki et al., 2017; Argilés, 2013). Ghrelin controls mediators involved in the cachectic process (Argilés 2013), indeed it is a multi-functional hormone affecting positively a variety of organs

impaired during cancer cachexia. Moreover, even if ghrelin activates GH/IGF1 pathway, null or inverse association with risk or progression of most cancers has been shown *in vivo* (Sever et al., 2016). As a consequence, ghrelin has been considered a worthwhile treatment to counteract cancer cachexia-associated muscle wasting (Terawaki et al., 2017; Argilés, 2013), and for this reason AG analogues have been designed and tested, leading to good outcomes (Graf and Garcia, 2017; Currow et al., 2017).

### **Ghrelin in sarcopenia**

Endocrine system and metabolic deregulation, which occurs during aging, could contribute to the onset of sarcopenia. Elderly subjects display a decline of circulating ghrelin levels (Nass et al., 2014) and ghrelin system results dysregulated during aging, as ghrelin-dependent release of growth hormone is attenuated. The decline in ghrelin activity can be due to lowered production, decreased expression of GHSR1a or alteration in signal transduction (Yin and Zhang, 2016). Otherwise, in animal models circulating ghrelin significantly increase with age, probably as a compensatory mechanism to the impaired receptor functions observed in aged animals (Kappeler et al., 2004; Akimoto et al., 2012; Sun et al., 2007). Ghrelin system impairment plays a role in aging-related metabolic alteration, since it is involved in food intake reduction (Akimoto et al., 2012) impaired thermogenesis (Lin et al., 2011; Lin et al., 2014), alteration of glucose, lipid and immune system homeostasis (Reed et al., 2008; Nesic et al., 2013; Dixit et al., 2007; Dixit et al., 2009; Youm et al., 2009). Moreover, the hypoghrelinemic status in humans might also participate to sarcopenia development by facilitating the progression of muscle wasting and limiting skeletal muscle regeneration. Indeed, ghrelin stimulates myoblast fusion and differentiation, exerts a direct anti-atrophic activity, and promotes skeletal muscle regeneration (Filigheddu et al., 2007; Porporato et al., 2013; Reano et al., 2017). Overall, these evidence strongly suggest that ghrelin may be a therapeutic strategy to counteract sarcopenia.

**Introduction to the paper “Both ghrelin deletion and unacylated ghrelin overexpression preserve muscles in aging mice”**

Agosti E, De Feudis M, Angelino E, Belli R, Alves Teixeira M, Zaggia I, Tamiso E, Raiteri T, Scircoli A, Ronzoni FL, Muscaritoli M, Graziani A, Prodam F, Sampaolesi M, Costelli P, Ferraro E, Reano S, Filigheddu N.

*Aging – under review*

Low ghrelin circulating levels have been observed in elderly subjects, and this condition could participate in the establishment of sarcopenia by facilitating the progression of muscle atrophy and limiting skeletal muscle regeneration capability.

Administration of AG analogues has been explored in several conditions characterized by muscle wasting, including cancer cachexia and aging (Garcia J et al., 2015; Currow et al., 2017; White et al., 2009; Adunsky et al., 2011). However, in sarcopenia, conversely to the beneficial effects observed in cancer cachexia, the administration of AG display scarce effect on skeletal muscle accompanied by an increase in adiposity that might worsen age-related insulin resistance and metabolic dysfunction. Since AG could have adverse metabolic effects potentially worsening sarcopenic status in the elderly, we explored the potentiality of UnAG in protecting from age-associated muscle wasting in animal models. We showed that not only lifelong overexpression of UnAG in mice, but also the deletion of ghrelin gene attenuated the age-associated muscle atrophy and functionality decline, as well as systemic inflammation. Overall, our findings prompted the design of UnAG mimetics which could be more useful than AG analogs for the treatment of sarcopenia.

## **Both ghrelin deletion and unacylated ghrelin overexpression preserve muscles in aging mice**

Emanuela Agosti<sup>1,2</sup>, Marilisa De Feudis<sup>1</sup>, Elia Angelino<sup>3</sup>, Roberta Belli<sup>4</sup>, Maraiza Alves Teixeira<sup>1</sup>, Ivan Zaggia<sup>1</sup>, Edoardo Tamiso<sup>1</sup>, Tommaso Raiteri<sup>1</sup>, Andrea Scircoli<sup>1</sup>, Flavio L. Ronzoni<sup>5,6</sup>, Maurizio Muscaritoli<sup>4</sup>, Andrea Graziani<sup>3</sup>, Flavia Prodam<sup>2</sup>, Maurilio Sampaolesi<sup>5,7,8,11</sup>, Paola Costelli<sup>9,11</sup>, Elisabetta Ferraro<sup>10</sup>, Simone Reano<sup>1\*</sup>, Nicoletta Filigheddu<sup>1,11\*</sup>

<sup>1</sup>Department of Translational Medicine, University of Piemonte Orientale, Novara, Italy.

<sup>2</sup>Department of Health Sciences, University of Piemonte Orientale, Novara, Italy.

<sup>3</sup>Division of Oncology, San Raffaele Scientific Institute and Vita-Salute San Raffaele University, Milano, Italy.

<sup>4</sup>Department of Translational and Precision Medicine, Sapienza University, Rome, Italy.

<sup>5</sup>Department of Public Health, Experimental and Forensic Medicine, Institute of Human Anatomy, University of Pavia, Pavia, Italy

<sup>6</sup>Department of Biomedical Sciences, Humanitas University, Rozzano, Italy.

<sup>7</sup>Center for Health Technologies (CHT), University of Pavia, Pavia, Italy

<sup>8</sup>Stem Cell Institute, KU Leuven, Leuven, Belgium

<sup>9</sup>Department of Clinical and Biological Sciences, University of Torino, Turin, Italy.

<sup>10</sup>Division of Orthopaedics and Traumatology, Hospital “Maggiore della Carità”, Novara, Italy.

<sup>11</sup>Istituto Interuniversitario di Miologia (IIM)

\*These authors contributed equally to this work



Corresponding author: Nicoletta Filigheddu, Department of Translational Medicine, University of Piemonte Orientale, Via Solaroli 17, 28100 Novara, Italy. Phone: (+39) 0321660529; Fax: (+39) 0321620421 email: [nicoletta.filigheddu@med.uniupo.it](mailto:nicoletta.filigheddu@med.uniupo.it)

Elisabetta Ferraro current address: Department of Biology, University of Pisa, Pisa, Italy

Elia Angelino and Andrea Graziani current address: Molecular Biotechnology Center, Department of Molecular Biotechnology & Health Sciences, University of Torino, Turin, Italy

[emanuela.agosti@med.uniupo.it](mailto:emanuela.agosti@med.uniupo.it); [marilisa.defeudis@med.uniupo.it](mailto:marilisa.defeudis@med.uniupo.it); [angelino.elia@hsr.it](mailto:angelino.elia@hsr.it);  
[robiuz.89@gmail.com](mailto:robiuz.89@gmail.com); [maraliza.teixeira@med.uniupo.it](mailto:maraliza.teixeira@med.uniupo.it); [ivanzaggia@gmail.com](mailto:ivanzaggia@gmail.com);  
[e.tamiso96@gmail.com](mailto:e.tamiso96@gmail.com); [tomraiteri@gmail.com](mailto:tomraiteri@gmail.com); [andre.scircoli@gmail.com](mailto:andre.scircoli@gmail.com);  
[flavio.ronzoni@unipv.it](mailto:flavio.ronzoni@unipv.it); [maurizio.muscaritoli@uniroma1.it](mailto:maurizio.muscaritoli@uniroma1.it); [andrea.graziani@unito.it](mailto:andrea.graziani@unito.it);  
[flavia.prodam@med.uniupo.it](mailto:flavia.prodam@med.uniupo.it); [maurilio.sampaolesi@unipv.it](mailto:maurilio.sampaolesi@unipv.it); [paola.costelli@unito.it](mailto:paola.costelli@unito.it);  
[elisabetta.ferraro@unipi.it](mailto:elisabetta.ferraro@unipi.it); [simone.reano@med.uniupo.it](mailto:simone.reano@med.uniupo.it)

**Keywords:** growth hormone secretagogue receptor; skeletal muscle atrophy; sarcopenia; inflammaging; sarcobesity

## **Abstract**

Sarcopenia, the decline in muscle mass and functionality during aging, might arise from age-associated endocrine dysfunction. Ghrelin is a hormone circulating in both acylated (AG) and unacylated (UnAG) forms with anti-atrophic activity on skeletal muscle. Here, we show that not only lifelong overexpression of UnAG (Tg) in mice, but also the deletion of ghrelin gene (*Ghrl* KO) attenuated the age-associated muscle atrophy and functionality decline, as well as systemic inflammation. Yet, the aging of Tg and *Ghrl* KO mice occurs with different dynamics: while old Tg mice seem to preserve the characteristics of young animals, *Ghrl* KO mice features deteriorate with aging. However, young *Ghrl* KO mice show more favorable traits compared to WT animals that result, on the whole, in better performances in aged *Ghrl* KO animals. Since *Ghrl* KO mice share several features of mice devoid of AG-specific receptor Ghsr-1a, we speculate that, in *Ghrl* KO mice, the major determinant factor of their overall better conditions is the lack of AG-mediated activation of Ghsr-1a. Altogether, these data confirmed and expanded some of the previously reported findings and advocate for the design of UnAG analogs rather than AG ones to treat sarcopenia.

## **Introduction**

Sarcopenia, the decline in muscle mass and functionality during aging, often results in poor balance, higher risk of falls, fractures, immobilization, loss of independence, and increased morbidity and mortality, thus representing a major health issue in elder individuals [1–3].

Muscle wasting follows the general decline in trophic hormones or in their ability of eliciting their standard cellular response (“resistance”) and the establishment of a chronic mild inflammatory status characteristic of aging [4].

Ghrelin is a gastric hormone peptide circulating in both acylated (AG) and unacylated (UnAG) forms. AG is the endogenous ligand of the growth hormone secretagogue receptor (GHSR-1a), and it is involved in metabolic regulation and energetic balance through induction of appetite, food intake, and adiposity [5,6]. UnAG does not induce GH release and has no direct effects on food intake, but

it shares with AG several biological activities both in vitro and in vivo independently of the expression of AG receptor. Indeed, in vivo, both AG and UnAG protect *Ghsr* KO mice from fasting- and denervation-induced skeletal muscle atrophy, thus proving the existence of a yet unidentified receptor that mediates the common AG and UnAG biological activities [7]. Consistently, both AG and UnAG have direct biological activities in vitro on skeletal muscle, including promotion of myoblast differentiation [8], protection from atrophy [7], and stimulation of mitochondrial respiration capacity [9]. In addition, UnAG boosts muscle satellite cell activity, activates autophagy and mitophagy, and stimulates insulin sensitivity, thus promoting muscle regeneration or preventing skeletal mass loss in different disease models, including hindlimb ischemia, high-fat diet-induced diabetes, and chronic kidney disease [10–14].

Similarly to other hormones, in humans, ghrelin levels decrease with aging [15], and the hypoghrelinemic state in the elderly could participate in the establishment of sarcopenia by facilitating the progression of muscle atrophy and limiting skeletal muscle regeneration capability. In mice, on the contrary, it was reported an increase in circulating levels of AG during aging [16], a phenomenon that has been proposed to represent a compensatory mechanism to a decline in receptor or post-receptor functions [17].

The role of ghrelin during aging has been recently investigated through the analysis of ghrelin knockout mice, and, surprisingly, it has emerged that ghrelin deletion prevents age-associated development of obesity and attenuates the decline in muscle strength and endurance seen with aging [18]. Nevertheless, the treatment of old WT mice with AG partially restored muscle performance while increasing food intake and body weight, especially fat mass [18]. Since an increase in obesity, a side effect of AG, in elderly subjects could worsen sarcopenia [19], inducing insulin resistance and diabetes [20], and mediating age-associated adipose tissue inflammation [21], here we explored the potentiality of UnAG in protecting from age-associated muscle wasting avoiding the potential adverse metabolic effects of AG. In addition, we expanded the previously reported characterization of ghrelin knockout mice during aging, especially focusing on the differences between young and aged muscles.

## Results

### **Body weight, body composition, and food intake in young and old WT, Tg, and *Ghrl* KO mice.**

To address whether ghrelin levels during aging affect sarcopenia development, we examined young (3-month-old) and old (24-month-old) *Myh6/Ghrl* transgenic mice characterized by high levels of circulating UnAG, up to 100 times more than WT animals (Tg; [7,13]), their WT littermates, and ghrelin knockout (*Ghrl* KO; [22]) mice, lacking all the gene-derived peptides.

Beside the already demonstrated age-related increase of AG [16], in WT mice, we also observed a rise in the circulating levels of UnAG (Supplementary Fig. 1), a phenomenon that could represent a compensatory mechanism to age-induced ghrelin resistance.

We observed a general increase in BMI and food intake for both WT and Tg mice during aging, while *Ghrl* KO mice exhibited a higher BMI and food intake already at 3 months of age without a further increase during aging (Fig. 1A and B). Despite the increase of BMI, at 24 months of age, a drop of both epididymal fat and skeletal muscles were observed (Fig. 1C and D, and Supplementary Fig. 2), indicating a general loss of fat mass and sarcopenic status in all genotypes and suggesting that other factors contribute to the observed increase in BMI of WT and Tg animals.

### **Muscle and cognitive performance in young and old WT, Tg, and *Ghrl* KO mice.**

To assess the effect of altered ghrelin levels during aging on muscle functionality, we measured the performances of young and old WT, Tg, and *Ghrl* KO mice using the hanging wire test. This test allows determining muscle function and coordination by counting the times a mouse falls or reaches one of the sides of the wire and the tension that the animal develops for maintaining itself on the wire, against gravity, by measuring the longest suspension time. Surprisingly, *Ghrl* KO mice outclassed both WT and Tg mice, at both ages in the “falls and reach” score (Fig. 2A). On the other hand, Tg mice performances were barely distinguishable from those of their WT littermates, both in young and old animals. However, the latency times between two successive falls, recorded in the same functional test, showed that Tg mice were able to maintain a good muscle condition during aging and confirmed

the better performance of *Ghrl* KO mice at both ages (Fig. 2B). In general, both WT and *Ghrl* KO mice showed a decrease in muscle performance during aging, while, apparently, Tg mice performances were preserved.

Since the score on the hanging wire test could be affected by cognitive performance and stress susceptibility, we assessed if cognitive capability and anxiety/depression of mice were different among the strains. At 3 months of age, *Ghrl* KO mice undergoing the object recognition test obtained a higher discrimination index than WT and Tg (Fig. 2C). However, at 24 months of age, while no significant changes were observed in the discrimination index of WT and Tg mice, that of *Ghrl* KO mice dropped to a level similar to those of WT mice. The tail suspension test, with the time spent immobile representing a measure of anguish, showed no differences in the immobility time of young mice (Fig. 2D). During aging, both WT and Tg mice showed a mild increase in the immobility time compared to young mice, suggesting the development of depression-like behavior. On the contrary, *Ghrl* KO mice showed substantial preservation of this parameter during aging.

### **Skeletal muscle atrophy during aging in WT, Tg, and *Ghrl* KO mice**

Despite the lack of significant differences in the weight of muscles among the three genotypes and the general decrease in muscle mass in aged mice (Fig. 1D and Supplementary Fig. 2), a closer examination of muscles revealed differences in the expression of Atrogin-1 (*Fbxo32*), a marker and a mediator of muscle atrophy, during aging [23]. The age-dependent increase of Atrogin-1 mRNA expressions was remarkable in gastrocnemii of WT and Tg mice and was milder in *Ghrl* KO mice (Fig. 3A), although it should be considered that Atrogin-1 mRNA levels were basally lower in young *Ghrl* KO mice compared to the other genotypes. This was also true in *tibialis anterior* (TA) muscles, where Atrogin-1 was significantly increased during aging only in *Ghrl* KO mice, reaching the values of young WT and Tg animals. Conversely, the increase of Atrogin-1 during aging was not significant in WT and absent in Tg animals. Nevertheless, analyzing the fiber cross-sectional area distributions of gastrocnemius (GAS) muscles from young adult and old WT mice, it was evident a clear shift

toward smaller areas in the latter (supplementary Fig. 3). Since the muscles of young Tg and KO mice, in unstimulated conditions, do not differ from those of WT animals [13,22], the shift towards larger areas in old Tg and *Ghrl* KO muscles compared to WT (Fig. 3B), indicate that both high levels of circulating UnAG and the lack of ghrelin peptides protect against muscle mass loss during aging.

### **Muscle fiber types and metabolism in old WT, Tg, and *Ghrl* KO mice**

Muscles are more susceptible/resistant to atrophy also depending on their fiber type composition, being glycolytic fibers more prone to undergo mass loss compared to the oxidative ones [24]; therefore, we assessed if high levels of UnAG or the lack of ghrelin peptides could affect muscle metabolism. Succinate-dehydrogenase (SDH) staining revealed that oxidative ability, *i.e.*, the activity of complex II of the electron transport chain, decreases with aging both in WT and *Ghrl* KO mice, whereas it was maintained in Tg (Fig. 4A-B), suggesting that UnAG stimulates an oxidative metabolism, counteracting the age-associated shift from oxidative to glycolytic metabolism.

Since aging muscles display mitochondrial dysfunction [25], we assessed the expression levels of mitochondria and oxidative metabolism markers such as mitochondrial transcription factor A (TFAM), ATP-synthase  $\beta$ -subunit ( $\beta$ -ATPase), SDH subunit-A (SDHA) and peroxisome proliferator-activated receptor gamma (PPAR $\gamma$ ). In line with the results reported in Fig. 4A-B, we observed an up-regulation of SDHA in old Tg mice compared to WT (Fig. 4C-D). In addition, old Tg mice showed an increase in PPAR $\gamma$  with a more oxidative metabolism induced by UnAG. On the other hand,  $\beta$ -ATPase and PPAR $\gamma$ -coactivator-1-alpha (PGC1 $\alpha$ ), a master regulator of mitochondrial biogenesis, did not show different expression levels among the three genotypes. Yet, *Ghrl* KO mice showed an up-regulation of TFAM, another marker of mitochondrial biogenesis.

### **Inflammation markers in old WT, Tg, and *Ghrl* KO mice**

With age, the spleen undergoes enlargement and disorganization of its architecture that can lead to age-related decline of immune function and chronic inflammation, that, in turn, could contribute to

the decrease in muscle mass and functionality [26–28]. All three genotypes showed a significant increase of spleen weight with age, although to a lesser extent in *Ghrl* KO mice (Fig. 5A). Adipose tissue as well contributes to the establishment of age-associated systemic inflammation, as it becomes dysfunctional with age, increasing the production of pro-inflammatory cytokines while decreasing the anti-inflammatory ones [29]. TNF $\alpha$  mRNA levels in epididymal fat equally increased during aging in all the genotypes, but to a lesser extent in Tg and *Ghrl* KO mice (Fig. 5B), confirming the low-grade systemic inflammation in these mice. The impact of ghrelin peptide levels on age-related systemic inflammation was explored through an antibody-spotted array directed against several circulating markers of inflammation (Fig. 5C and Supplementary Fig. 4). As expected, old WT mice showed a general increase of pro-inflammatory markers and a concomitant decrease of the anti-inflammatory ones compared to young mice (reference line in Fig. 5C). The levels of some of these markers, such as SDF1 $\alpha$ , eotaxin-1 (CCL11), I-309 (CCL1), leptin, M-CSF, and IL-12p70, were lower in both old Tg and *Ghrl* KO mice compared to old WT. Conversely, the anti-inflammatory soluble TNF-R1 was increased in both Tg and *Ghrl* KO mice. Old Tg mice distinguished themselves from WT and *Ghrl* KO for the high levels of BLC (CXCL13), while characteristics of *Ghrl* KO mice were a lower level of IL-13 and higher levels of IL-12.

### **Changes in brown adipose tissue in old WT, Tg, and *Ghrl* KO mice**

Brown adipose tissue (BAT) controls energy expenditure and metabolism through uncoupling protein (UCP)1-mediated heat production, thus increasing energy expenditure, reducing adiposity, and lowering insulin resistance. Therefore, it has been proposed that age-associated decrease in BAT depots and functionality contributes to the metabolic deregulation characteristic of aging [30], which may lead to thermogenic impairment and age-associated obesity [16]. We observed a decrease in BAT depots in all the strains studied (Fig. 6A). However, UCP-1 expression, an indicator of BAT function, was maintained in old Tg mice, and even increased in *Ghrl* KO mice (Fig. 6B), thus likely maintaining proper metabolism homeostasis.

## Discussion

The decline in muscle mass, functionality, and physical performance distinctive of aging can be ascribed, at least in part, to age-associated endocrine and metabolic dysfunction. Among the dysregulated hormones, in humans, it has been observed reduced circulating levels of ghrelin and decreased expression on the cell surface of its receptor GHSR-1a [17] that may contribute to sarcopenia by facilitating the progression of muscle atrophy and limiting skeletal muscle regeneration capability. In mice, on the contrary, it was reported an increase in circulating levels of AG during aging and no changes in UnAG [16]. However, together with the age-related increase of AG, we also observed a rise in the circulating levels of UnAG (Supplementary Fig. 1), a phenomenon that could represent a compensatory mechanism to a decline in receptor or post-receptor functions [17]. The age-related increase in AG and UnAG levels may be part of an adaptive response to a negative energy balance and suggests that these peptides could be involved in the aging process for the many activities that characterize each or both forms of ghrelin peptide, including the protection from muscle wasting (AG and UnAG; [7]). Muscle atrophy is indeed one of the main degenerative processes involved in sarcopenia and, for the above-mentioned anti-atrophic activity of AG and UnAG, it was reasonable to expect that high circulating levels of UnAG, as in the Tg mice used in this study, would result in less sarcopenia by protecting from muscle wasting. This was actually the case, being Tg muscles partially resistant to the loss of muscle mass and functionality during aging (Fig. 2B, and Fig. 3).

On the contrary, the finding that old *Ghrl* KO mice were atrophy-resistant, featuring both lower levels of Atrogin-1 and larger myofiber areas than WT mice (Fig. 3), was less expected, as we have formerly demonstrated that, upon a traumatic event, muscle regeneration in *Ghrl* KO mice is reduced, due to an impaired satellite cell self-renewal activity [22]. Also, old *Ghrl* KO mice are more susceptible to fasting-induced muscle atrophy likely because of an altered mitochondrial function [9]. Nevertheless, most of our findings on aged *Ghrl* KO mice are in accordance with the previous demonstration that ghrelin gene deletion results in the prevention of the age-associated decline in muscle strength and endurance [18]. In particular, *Ghrl* KO muscles showed enhanced physical performance compared to



the WT (Fig. 2B). Yet, we also obtained some different results compared with the previously published ones. For a start, we observed a loss of muscle weight with aging in both WT and *Ghrl* KO mice (Fig. 1D and Supplementary Fig. 2). However, the weighing of freshly isolated muscles is a rough evaluation of muscle mass, and, indeed, a more accurate assessment of muscles uncovered relevant differences between WT and *Ghrl* KO mice. The lack of ghrelin affected muscle cross-sectional areas, with old *Ghrl* KO muscles displaying a reduced number of the smallest myofibers in CSA distribution compared to WT and expressing less Atrogin-1, which was lower in young *Ghrl* KO than in WT as well (Fig. 3). More importantly, the discrepancies between our data and some of the previously published ones, *e.g.*, BMI/body weight and food intake of *Ghrl* KO mice (Fig. 1 compared to the data shown in [18]) depend on the different age ranges used, *i.e.*, 3-month-old for young animals instead of 6- to 9-month-old young adults. Indeed, the differences observed in BMI in young mice disappear at the age of 6 months (Supplementary Fig. 5).

The changes in muscle mass occurring during aging may arise from the age-related dysregulation of the immune system that leads to progressive systemic inflammation, with a general increase in circulating pro-inflammatory cytokines, which can affect muscle homeostasis. Actually, old WT mice exhibited higher spleen dimension and increased levels of TNF- $\alpha$  expression in epididymal adipose tissue and of plasmatic pro-inflammatory markers compared to young animals, confirming the existence of low-grade systemic inflammation (Fig. 5 A-C). Based on the vast amount of the anti-inflammatory activities of ghrelin peptides [31], a worsening of the inflammatory status in *Ghrl* KO mice was plausible. However, *Ghrl* KO mice displayed reduced systemic inflammation and less inflamed adipose tissue (Fig. 5B and C), a phenotype strongly reminiscent of that of *Ghsr* KO mice [32], in which the ablation of AG receptor promotes a shift in macrophages toward the anti-inflammatory M2 status and reduced macrophage infiltration and pro-inflammatory cytokine expression in white and brown adipose tissues.

Also, the pro-inflammatory effects of Ghrelin on macrophages profoundly limits lipid mobilization and energy expenditure in adipose tissue [21], processes that are highly perturbed during aging [33].

In particular, it was proposed that AG could participate in the age-related impairment of thermogenesis –thus contributing to the onset of age-related obesity and insulin resistance– through its receptor Ghsr-1a, whose expression in fat increases with aging [32]. Despite the general age-dependent reduction in brown fat, the higher levels of UCP-1 in *Ghrl* KO mice suggest an enhanced thermogenic activity. Therefore, it is conceivable that ghrelin ablation might shift the metabolic state of old mice from obesogenic to thermogenic. However, a specific assessment of energy expenditure would be needed to prove this hypothesis. Altogether, these observations strongly suggest that, in *Ghrl* KO mice, one of the major determinant factors of their overall better conditions is the lack of AG-mediated activation of Ghsr-1a. Conversely, the lack of UnAG in these mice becomes critical under stressful conditions, such as starvation or acute muscle injury, impacting on the physiological homeostasis [9,22].

Of note, the feeding behavior of *Ghrl* KO mice was different from what previously reported [18,34], as we observed higher food consumption not only during aging in WT but, more curiously, also in young *Ghrl* KO mice (Fig. 1B). The BMI seems to reflect the food intake, with young *Ghrl* KO mice showing a higher BMI compared to WT (Fig. 1A). However, the loss in muscle and epididymal fat mass indicates that other tissues contribute to the increase in BMI. Indeed, we observed a remarkable increase in spleen (Fig. 5A) and liver weight (data not shown) with aging that could account for the BMI values.

Besides the effects on skeletal muscle, aging also associates often with a gradual cognitive impairment and depression that deeply worst elder people quality of life [35]. The role of AG in regulating sleep and memory [36] and its anti-depressant activity when administered to stressed mice [37] suggest that the impairment of ghrelin signaling during aging could affect cognitive function as well. In assessing the behavioral contribution to the physical performance tests, we skimmed the surface of this issue and surprisingly found that the lack of ghrelin peptides improved the memory capacity of young mice, although this effect was not maintained in old mice (Fig. 2C). Conversely, the lack of the ghrelin gene protected against the onset of the aging-dependent depression-like

behaviors (Fig. 2D). Altogether, the pattern of cognitive function could have partially affected the measure of endurance in the hanging wire test (Fig. 2B), as the cleverness could drive the mice to quickly reach the ends of the wire (Fig. 2C), while the anxiety/depression (Fig. 2D) may induce the mice to abandon the attempt. Therefore, old WT mice could have performed worse than their young counterpart also because of the establishment of age-induced anxiety/depression. On the contrary, *Ghrl* KO mice could have had a starting advantage due to higher cognitive performance in youth. Although this parameter declined with age, it reached the level of young WT animals, and the lack of anxiety/depression during aging could have resulted in overall better performances both in young and old *Ghrl* KO mice than their WT peers.

Exogenous administration of AG to overcome a presumed peripheral ghrelin resistance has been explored in several contexts characterized by loss of skeletal muscle mass, including cancer cachexia [38,39] and aging [18]. However, while in cancer cachexia the administration of AG has a beneficial activity on skeletal muscle also by contrasting anorexia and the rapid loss of adipose tissue, in sarcopenia the effects on skeletal muscle are limited and accompanied by an increase in adiposity that might worsen age-related insulin resistance and metabolic dysfunction. The pro-adipogenic feature of AG relies on its acylation and resulting binding to Ghsr-1a [6,40]. Since UnAG does not activate this receptor and does not increase fat mass, while protecting the skeletal muscle from several atrophic stimuli [41], we investigated the potentiality of this hormone in preventing sarcopenia by monitoring the aging of *Myh6/Ghrl* Tg mice characterized by normal levels of AG but increased levels of UnAG [7,13]. Despite both Tg and WT animals display similar tendencies in how BMI, epididymal fat, and skeletal muscle weight change with aging (Fig. 1 and Supplementary Fig. 2), higher circulating levels of UnAG seem to globally maintain in the long run the structure, performance, and metabolism typical of young muscles (Fig. 2 A-B, Fig. 3, and Fig. 4). In particular, old Tg muscles display higher levels of mitochondrial protein than WT littermates (Fig. 4D) that likely accounts for the maintenance of the oxidative metabolism (Fig. 4A and B) and the overall protection from sarcopenia. This is consistent with the ability of UnAG to impair muscle catabolism by mitigating mitochondrial damage

[14]. The preserved muscle mass and functionality may be the result of the direct anti-atrophic activity of UnAG [7,8], as well as of the reduced age-associated chronic inflammation (Fig. 5B). Although old Tg spleen weight did not differ from that of WT (Fig. 5A), old Tg animals were characterized by lower levels of inflammatory markers (Fig. 5B), such as SDF-1 $\alpha$ , I-309, leptin, M-CSF, IL-12p70, and higher levels of soluble TNF-R1 that can act as scavenger for the circulating inflammatory TNF- $\alpha$  [42]. On the other hand, age-associated IL-12 and IL-13 levels were quite similar to those observed in WT animals, possibly reflecting the presence of AG in Tg mice.

Differently from *Ghrl* KO mice, the lower systemic inflammation does not associate with increased UCP-1 expression (Fig. 6B). However, we imagine that the maintenance during aging of brown fat (Fig. 6A), could result in a similar thermogenic, obesity-resistant phenotype.

In conclusion, we showed that both high circulating levels of UnAG and the lack of ghrelin gene prevent the decline of muscle function associated with aging, although with different dynamics. Indeed, old Tg mice seem to preserve the characteristics of young animals, while *Ghrl* KO mice features deteriorate with aging. However, young *Ghrl* KO mice in general show more favorable traits compared to WT animals that result, on the whole, in better performances in aged *Ghrl* KO animals. The only exception is the SDH activity (Fig. 4B) that declines with age in both WT and *Ghrl* KO mice, but, differently from the other parameters assessed in this work, young *Ghrl* KO mice do not have the initial advantage of higher SDH activity in youth. On the contrary, similarly to other parameters, Tg mice maintain a constant SDH activity, putatively due to higher levels of mitochondrial proteins (Fig. 4D). Therefore, we can hypothesize that the maintenance of the oxidative metabolism could, at least in part, explain the protection from sarcopenia in Tg mice, while, in *Ghrl* KO mice, the lack of Ghsr-1a-mediated inflammation could play a major role. The fact that *Ghrl* KO mice are protected from sarcopenia might still appear in contradiction with our previous work demonstrating that both AG and UnAG have anti-atrophic activities [7]. However, it should be noted that the anti-atrophic effects of AG UnAG were assessed in *Ghsr* KO mice, *i.e.*, in circumstances in which AG was not signaling via Ghsr-1a, but through a yet unidentified receptor.

The astonishingly similarity between old *Ghrl* KO mice and old *Ghsr* KO mice indeed strongly suggests a detrimental role for GHSR-1a in the onset of sarcopenia. We reckon that, in mice, the physiological increase of UnAG with aging is not enough to counteract the negative effects of the increased AG levels, and that, in humans, the adverse effects of impaired ghrelin signaling in aging are mainly due to the decline in UnAG rather than AG. Altogether, these results should encourage the design of analogs to UnAG rather than AG to therapeutically treat this condition in humans.

## Figures

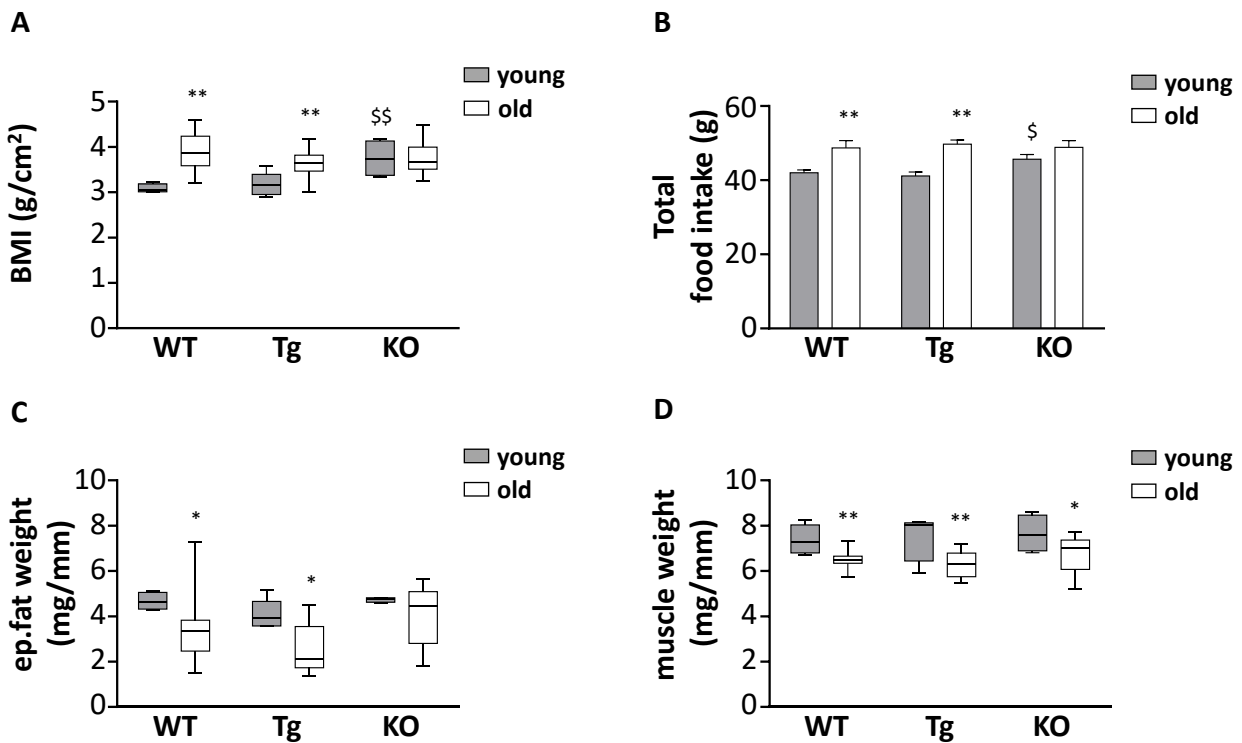


Figure 1. **Body mass composition and food intake in young and old WT, Tg, and *Ghrl* KO mice.** (A) Body mass composition measured as body mass index (BMI) in 3-month old (young) and 24-month old (old) mice. Young mice: WT= 4, Tg= 5, *Ghrl* KO = 4; old mice: WT= 13, Tg= 14, *Ghrl*<sup>-/-</sup>= 11. (B) Total food intake consumed by mice in 12 days with *ad libitum* access to standard chow diet. Young mice: WT= 5, Tg= 5, *Ghrl* KO = 5); old mice: WT= 7, Tg= 7, *Ghrl* KO = 7. (C) Epididymal fat mass normalized to anus-nose length and (D) gastrocnemius weight normalized to the tibial length. Young mice: WT= 4, Tg= 5, *Ghrl* KO = 4; old mice: WT= 13, Tg= 14, *Ghrl* KO = 11. Data in bar graph are presented as mean  $\pm$  SEM. For each box plot, the lower and up boundaries denote the 25th and the 75th percentile of each data set, respectively, the horizontal line represents the median, and the whiskers represent the min and max of values. \* $p < 0.05$  and \*\* $p < 0.01$  old vs. young; \$\$ $p < 0.01$  *Ghrl* KO vs. WT.

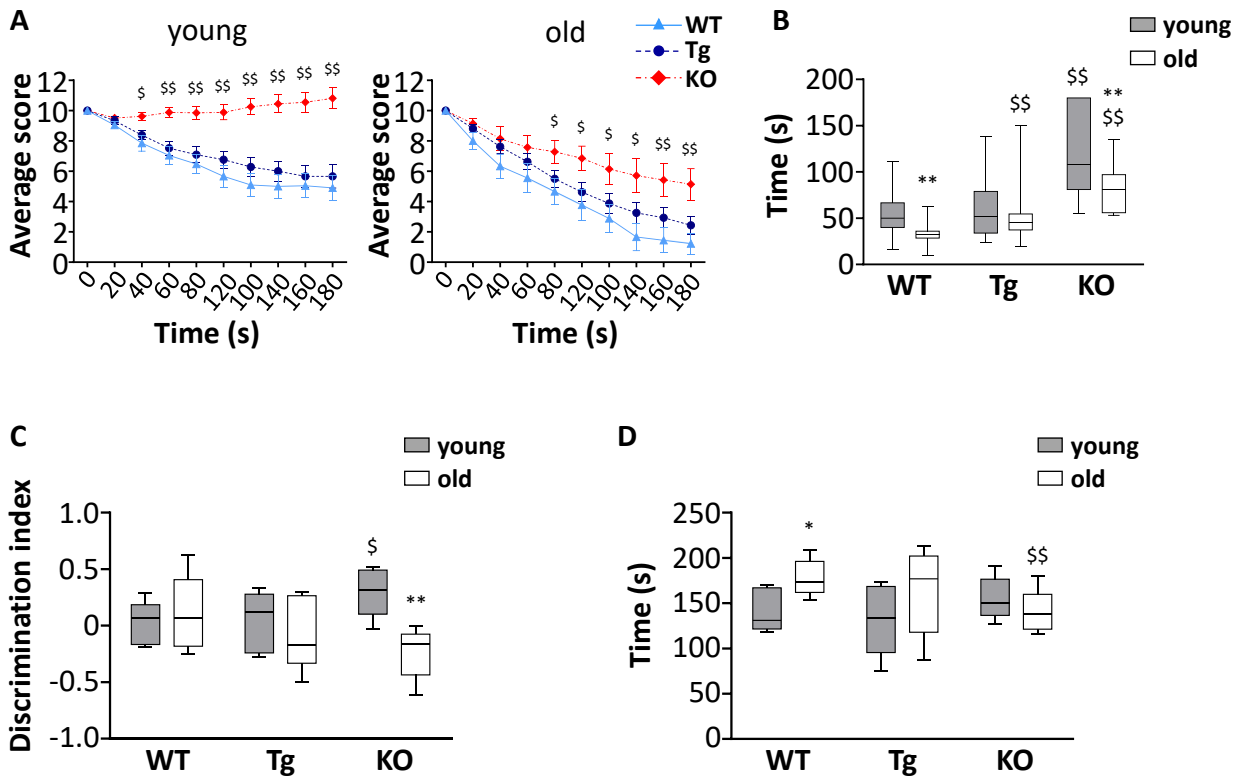


Figure 2. **Muscle functionality and behavior in young and old WT, Tg, and *Ghrl* KO mice.** (A) Average score trend in hanging wire test of in 3-month old (young) and 24-month old (old) WT, Tg, and *Ghrl* KO mice and (B) average latency-to-fall in the same test. Young mice: WT= 21, Tg= 21, *Ghrl* KO= 27; old mice: WT= 9, Tg= 16, *Ghrl* KO= 7. \* $p < 0.05$  and \*\* $p < 0.01$  vs WT. (C) Memory was evaluated through the object recognition test and expressed as a discrimination index between a familiar and a novel object (seconds on novel – seconds on familiar)/(seconds on novel + seconds on familiar). (D) Anxiety was assessed as the time spent immobile after a minute of tail suspension. Young mice: WT= 5, Tg= 5, *Ghrl* KO= 5; old mice: WT= 6, Tg= 7, *Ghrl* KO= 6. For each box plot, the lower and up boundaries denote the 25th and the 75th percentile of each data set, respectively, the horizontal line represents the median, and the whiskers represent the min and max of values. \* $p < 0.05$  and \*\* $p < 0.01$  old vs. young;  $^{\$}p < 0.05$  and  $^{\$\$}p < 0.01$  *Ghrl* KO and Tg vs. WT.

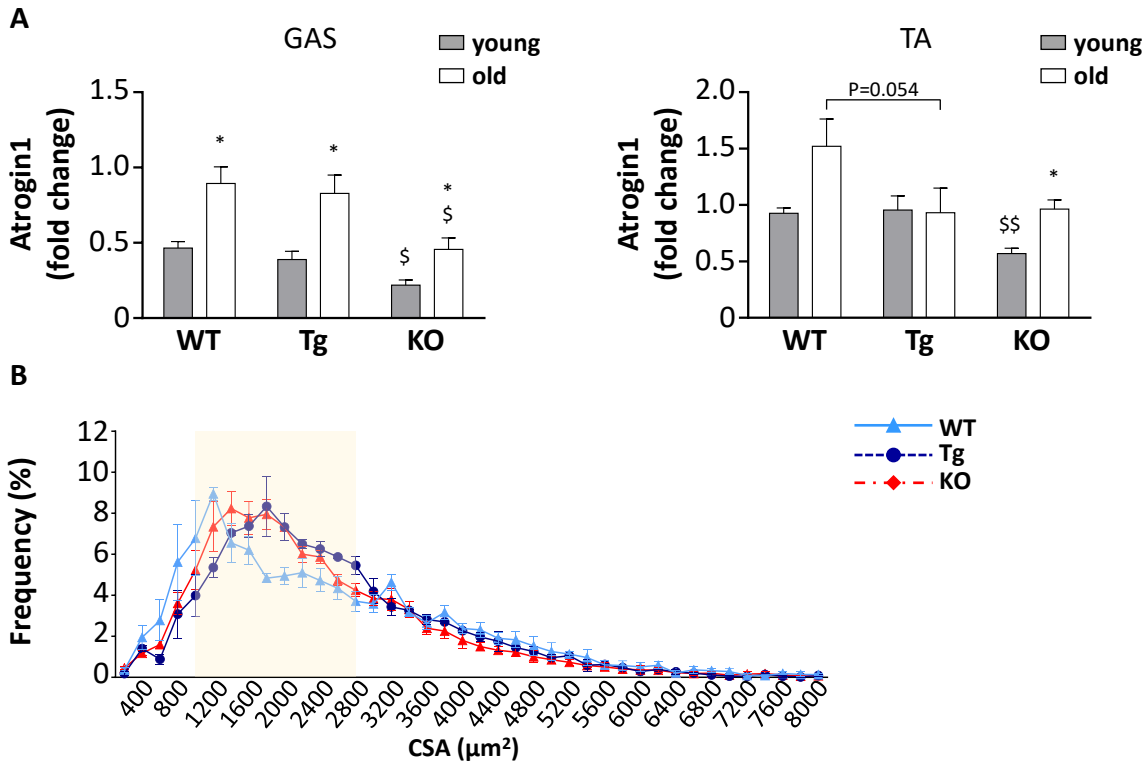


Figure 3. **Ghrelin peptides effects on sarcopenia-dependent atrophy.** (A) Atrogin-1 (*Fbxo32*) expression in gastrocnemius (GAS) and *tibialis anterior* (TA) of 3-month old (young) and 24-month old (old) mice determined by real-time RT-PCR. In TA, young mice: WT= 4, Tg= 3, *Ghrl* KO= 4; old mice: WT= 8, Tg= 9, *Ghrl* KO= 8. In GAS, young mice: WT= 4, Tg= 4, *Ghrl* KO= 4; old mice: WT= 4, Tg= 3, *Ghrl* KO= 4. (B) Cross-sectional area (CSA) frequency distribution of myofibers in GAS of old WT, Tg, and *Ghrl* KO mice. WT= 4, Tg= 3, *Ghrl* KO= 5. The shadowed area of the graph represents the section of statistically significant differences among curves. Data are presented as mean  $\pm$  SEM. \* $p < 0.05$  and \*\* $p < 0.01$  old vs. young; \$ $p < 0.05$  and \$\$ $p < 0.01$ , *Ghrl* KO and Tg vs. WT.



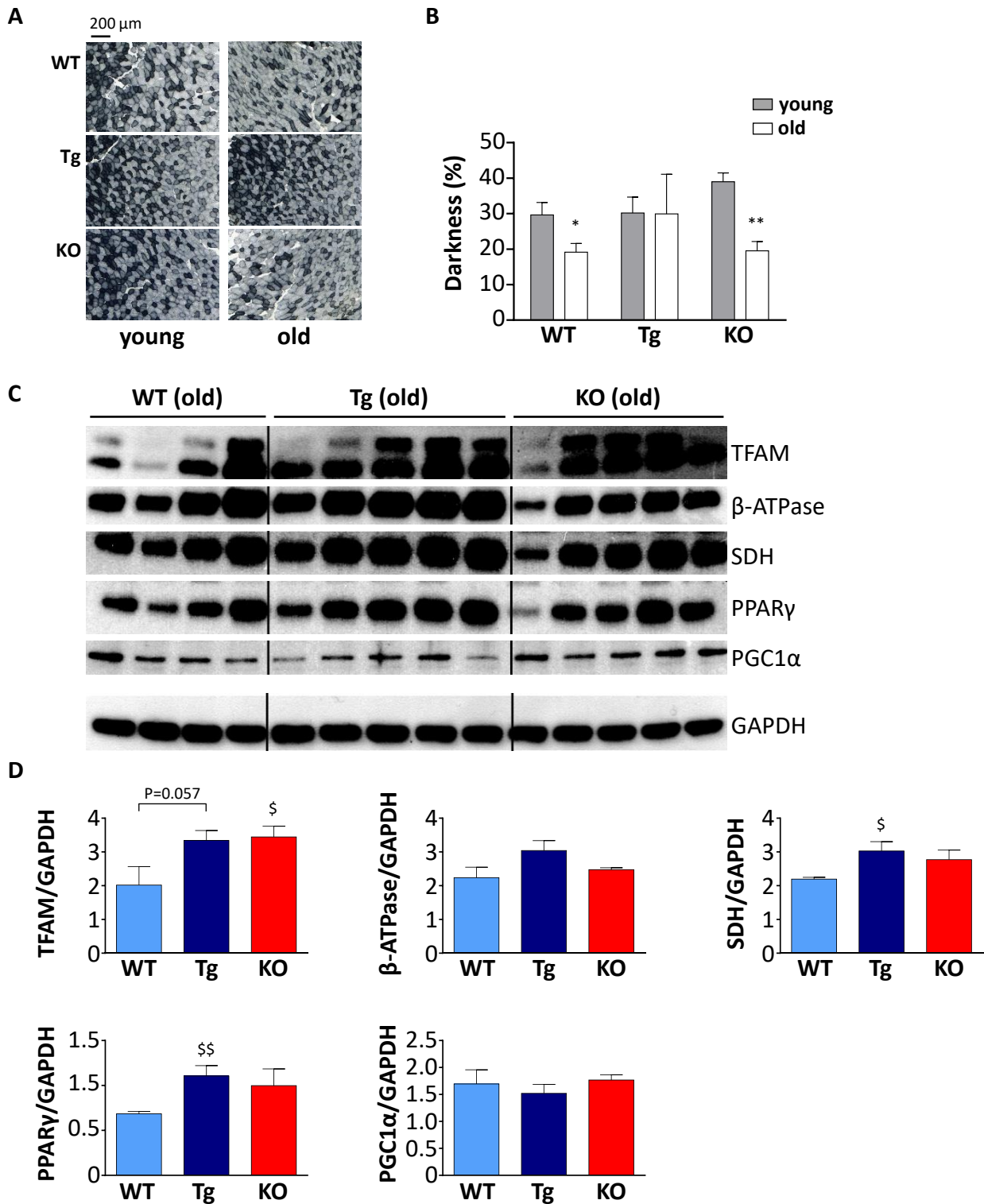


Figure 4. Metabolic shift in TA muscles of WT, Tg, and *Ghrl* KO mice. (A) Representative images of succinate dehydrogenase (SDH) staining (scale bars: 200  $\mu$ m) representing the oxidative capacity of TA muscles of 3-month old (young) and 24-month old (old) mice. (B) Quantification of SDH-positive fibers in TA muscle presented as the percentage of SDH-positive area above the total muscle surface. Young mice: WT= 5, Tg= 4, *Ghrl* KO= 5; old mice: WT= 4, Tg=

3, *Ghrl* KO= 5. (C) Representative Western blots images and (D) protein densitometry quantification for mitochondrial transcription factor A (TFAM), ATP-synthase  $\beta$ -subunit ( $\beta$ -ATPase), succinate-dehydrogenase complex subunit-A (SDHA), peroxisome proliferator-activated receptor gamma (PPAR $\gamma$ ), and PPAR $\gamma$ -coactivator-1- $\alpha$  (PGC1 $\alpha$ ) protein levels. Protein levels were probed in gastrocnemii of old mice, WT= 4, Tg= 5, *Ghrl* KO= 5. Data are presented as mean  $\pm$  SEM. \* $p$ <0.05 and \*\* $p$ <0.01, old vs. young;  $^{\$}$  $p$ <0.05 and  $^{\$\$}$  $p$ <0.01, *Ghrl* KO and Tg vs. WT.

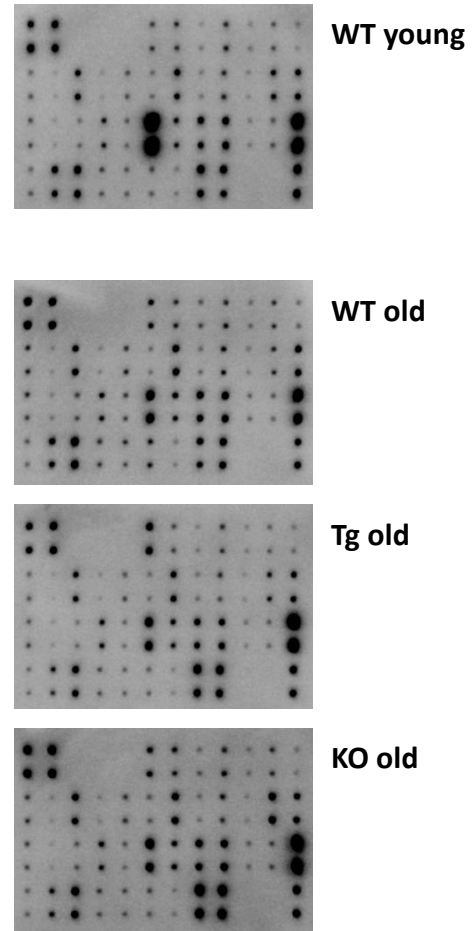
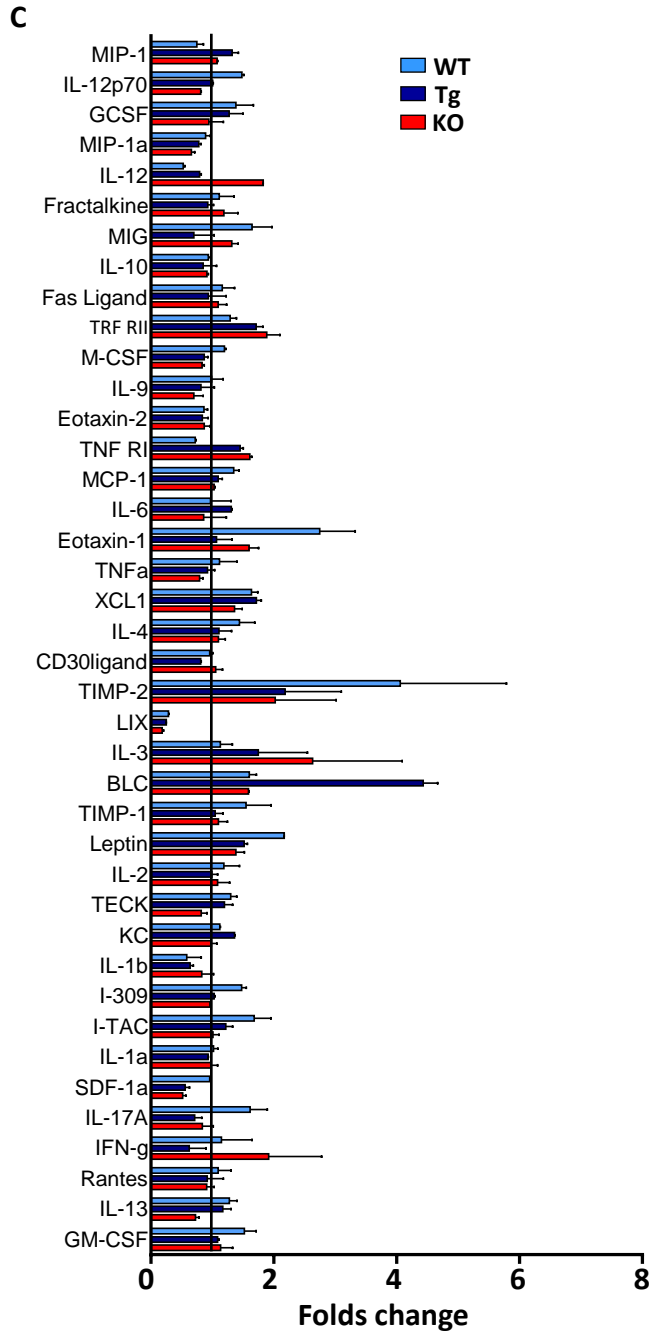
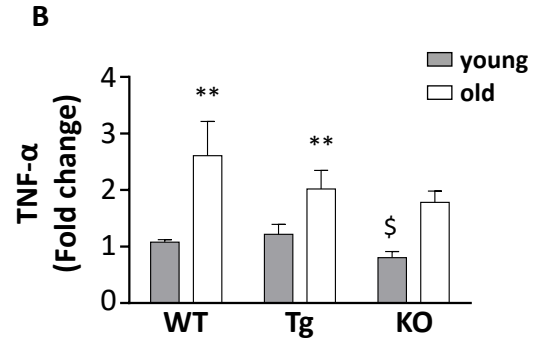
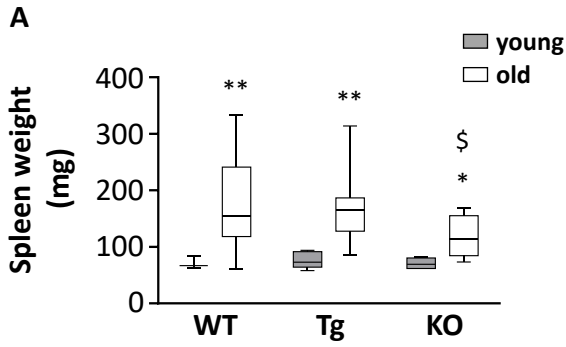


Figure 5. **Systemic inflammation in old WT, Tg, and Ghrl KO mice.** (A) Spleen weight in 3-month old (young) and 24-month old (old) mice. Young mice: WT= 4, Tg= 5, *Ghrl* KO= 4; old mice: WT= 13, Tg= 14, *Ghrl* KO= 11. (B) TNF- $\alpha$  (*Tnf*) expression in epididymal fat of 3-month old (young) and 24-month old (old) WT, Tg, and *Ghrl* KO mice, determined by real-time RT-PCR. Young mice: WT= 3, Tg= 4, *Ghrl* KO = 4; old mice: WT= 5, Tg= 7, *Ghrl* KO = 5. (C) Serum biomarkers involved in systemic inflammation normalized on the levels in young WT mice (reference line). Young mice WT=4; old mice: WT= 4, Tg= 4, *Ghrl* KO = 4 pulled into two groups. For each box plot, the lower and up boundaries denote the 25th and the 75th percentile of each data set, respectively, the horizontal line represents the median, and the whiskers represent the min and max of values. Data in bar graph are presented as mean  $\pm$  SEM (B) and mean  $\pm$  SD (C). Data are presented as mean  $\pm$  SEM. \* $p$ <0.05 and \*\* $p$ <0.01, old vs. young;  $\text{\$}$  $p$ <0.05 *Ghrl* KO and Tg vs. WT.

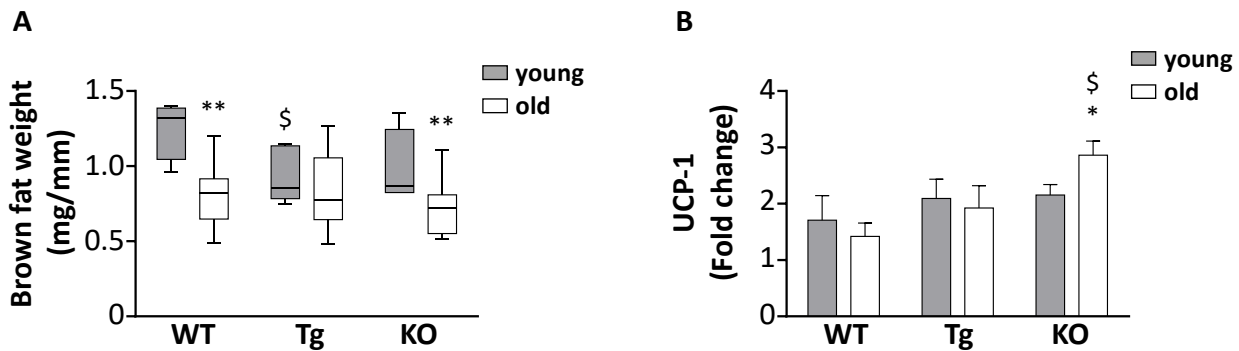
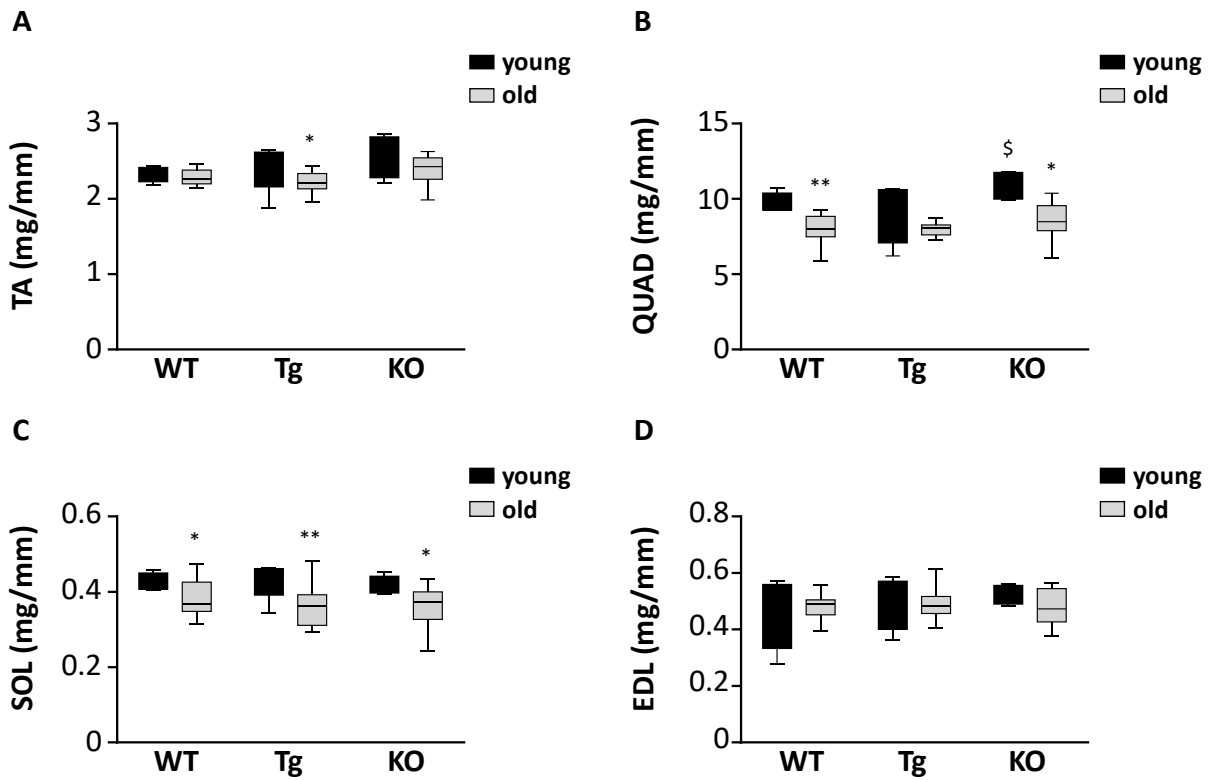


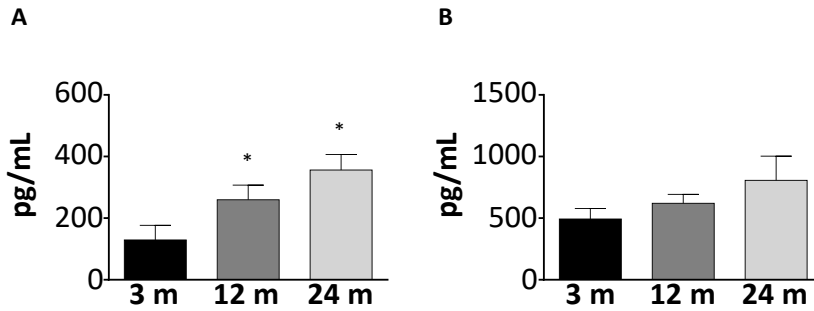
Figure 6. **Changes in brown adipose tissue in old ghrelin WT, Tg, and Ghrl KO mice.** (A) Brown fat mass normalized to anus-nose length. Young mice: WT= 4, Tg= 5, *Ghrl* KO = 4; old mice: WT= 13, Tg= 14, *Ghrl* KO = 11. (B) Uncoupling protein-1 (*Ucp-1*) expression in brown fat of young and old WT, Tg, and *Ghrl* KO mice determined by real-time RT-PCR. Young mice: WT= 4, Tg= 4, *Ghrl* KO= 4; old mice: WT= 3, Tg= 4, *Ghrl* KO= 3. Data in bar graph are presented as mean  $\pm$  SEM. For each box plot, the lower and up boundaries denote the 25th and the 75th percentile of each data set, respectively, the horizontal line represents the median, and the whiskers represent the min and max of values. \* $p$ <0.05 and \*\* $p$ <0.01 old vs. young;  $\text{\$}$  $p$ <0.05 *Ghrl* KO and Tg vs. WT.



Supplementary figure 1. **Muscle weight in young and old WT, Tg, and KO mice.** Tibialis anterior (TA) (A), quadriceps (QUAD) (B), soleus (SOL) (C), extensor digitorum longus (EDL) (D) weight normalized to tibial length. Young mice: WT= 4, Tg= 5, KO = 4; old mice: WT= 13, Tg= 14, KO = 11. Data are presented as mean  $\pm$  SEM. \* $p < 0.05$  and \*\* $p < 0.01$  old vs. young. \$ $p < 0.05$  KO and Tg vs WT.

	A	B	C	D	E	F	G	H	I	J	K	L
1	POS	POS	NEG	NEG	BLANK	BLC (CXCL13)	CD30 Ligand (TNFSF8)	Eotaxin-1 (CCL11)	Eotaxin-2 (CCL24)	Fas Ligand (TNFSF56)	Fractalkine (TNFSF8)	GCSF (CCL11)
2												
3	GM-CSF	IFN-gamma	IL-1 alpha (IL-1 F1)	IL-1 beta (IL-1 F2)	IL-2	IL-3	IL-4	IL-6	IL-9	IL-10	IL-12 p70	IL-12 p40/p71
4												
5	IL-13	IL-17A	I-TAC (CXCL1)	KC (CXCL1)	Leptin	LIX	XCL1	MCP-1 (CCL2)	M-CSF	MIG (CXCL9)	MIP-1 alpha (CCL3)	MIP-1 gamma
6												
7	RANTES (CCL5)	SDF-1 alpha (CXCL12 a)	I-309 (TCA-3/CCL1)	TECK (CCL25)	TIMP-1	TIMP-2	TNF alpha	TNF RI (TNFRS1A)	TNF RII (TNFRS1A)	BLANK	BLANK	POS
8												

Supplementary figure 2. **Array map of the Mouse Inflammation Antibody Array.** Each antibody is spotted in duplicate vertically.



Supplementary figure 3. **Increase of AG and UnAG plasmatic levels during aging in WT mice.** Plasmatic levels of AG (A) and UnAG (B) in 3-, 12-, and 24-month-old mice determined by EIA; 3-month-old mice: N = 5, 12-month-old mice N = 8, 24-month-old mice N = 6. \*p<0.05 and \*\* p<0.01 vs. 3-month-old mice.

## Materials and methods

**Animals.** Animal experiments were performed according to procedures approved by the Institutional Animal Care and Use Committee at the University of Piemonte Orientale. C57BL/6 male mice, matched for age and weight, were used for all experiments. C57BL/6 *Ghrl*<sup>-/-</sup> (*Ghrl* KO) and C57BL/6-*Myh6/Ghrl* transgenic (Tg) mice were generated as previously described [7,22,43]. WT mice were littermates of Tg animals. *Ghrl* KO strain was kept in homozygosity. Animals were housed in groups of 4/6 animals and fed ad libitum with unrestricted access to drinking water. For food intake analysis and behavioral tests, mice were single-caged for the acclimation plus experimental periods. The light/dark cycle in the room consisted of 12/12 h with artificial light. The numbers of mice ranged from 3 to 27 per experiment. BMI was calculated as animal weight/(nose-to-anus length)<sup>2</sup>. AG and UnAG plasmatic levels were measured by EIA kits (SPIbio Bertin Pharma). Mice were killed through cervical dislocation, and tissues used for the study immediately excised, weighted, and processed or stored for further analysis.

**Hanging wire test.** A wire-hanging test was employed to assess whole-body muscle strength and endurance. The test was performed as previously described [13]. Briefly, mice were subjected to 180 sec hanging test, during which “falling” and “reaching” scores were recorded. When a mouse fell or reached one of the sides of the wire, the “falling” score or “reaching” score was diminished or increased by 1, respectively. A Kaplan-Meier-like curve was created afterward. Moreover, the longest time between two falls was taken as the latency-to-fall value.

**Object recognition test.** Recognition memory was measured using various objects of different sizes and materials, as previously described [44]. Briefly, mice were separated in single cages 10 days before the test. The task started with a familiarization trial (day 1) in which two identical objects were presented to the animals, followed by the test trial (day 2), where one familiar object was substituted with a novel one. In detail, in day 1, mice were left with two identical objects (familiarization phase). Exploration was recorded for 10 min by an investigator blinded to the strain assessed. Sniffing, touching, and stretching the head toward the object at a distance  $\leq 2$  cm were scored as object investigation. In day 2 mice were again left in the same cage containing two objects: one identical to one of the objects presented during the familiarization phase (familiar object), and a new, different one (novel object), and the time spent exploring the two objects was recorded for 10 min. Memory was expressed as a discrimination index calculated as follows: (seconds on novel–seconds on familiar)/(seconds on novel + seconds on familiar). Animals with memory impairment spend lesser investigating time with the novel object, thus giving a lower discrimination index.

**Tail suspension test.** Mice anxiety/depression was measured as previously described [45]. Briefly, mice were individually suspended in the air by tape attached to a shelf (50 cm height) for 6 min. Trials were video-recorded, and a blinded experimenter scored the time during which mice remained immobile as a measure of depressive-like behavior. A small cylindrical tube was slipped over the mouse tail to prevent climbing motion and to escape.

**Histological analysis.** Muscles were excised, weighted, mounted in Killik embedding medium (Bio-optica), frozen in liquid-nitrogen-cooled isopentane, and stored at -80 °C. Transverse muscle sections (7 µm) were cryosectioned from the middle part of each muscle. Myofiber areas were determined by immunofluorescence with anti-laminin (1:200; Dako). Slices were fixed in 4% PFA for 20 min, washed, permeabilized with 0.2% Triton X-100 in 1% BSA for 15 min, and blocked with 4% BSA for 30 min. One hour of incubation with primary antibodies was followed by 45 min of secondary antibody (Alexa Fluor 488-anti-rabbit; Thermo Fisher Scientific) at RT. DAPI was incubated for 5 min at RT to visualize nuclei. SDH staining was performed to reveal the oxidative fibers within a muscle. Frozen transverse TA muscles were incubated in a working solution (SUCCINIC DEHYDROGENASE Stain Lyophilized, Bio-optica) for 45 minutes at 37°C. The sections were then rinsed in distilled water, fixed in 4% PFA for 10 minutes, placed in 15% ethanol for 10 minutes, and, finally, mounted with aqueous mounting medium. Images of whole muscle sections were acquired with the slide scanner Panoramic Midi 1.14 (3D Histech) and cross-sectional areas (CSA) of fibers or SDH staining quantified with ImageJ software (v1.49o).

**Gene expression analysis.** Total RNA from muscles was extracted by RNAzol (Sigma-Aldrich). RNA was retro-transcribed with High-Capacity cDNA Reverse Transcription Kit (Thermo Fisher Scientific), and real-time PCR was performed with the StepOnePlus Real-Time PCR System (Thermo Fisher Scientific) using the following TaqMan assays: Mm00499518\_m1 (*Fbxo32*, Atrogin-1/MAFbx), Mm01244861\_m1 (*Ucp1*), Mm00443258\_m1 (*Tnf*), and Mm00506384\_m1 (*Ppif*).

**Western Blotting.** Tissue samples from gastrocnemii were homogenized by using GentleMACS Dissociator (Miltenyi Biotec) and lysed in ice-cold RIPA Buffer (50 mM Tris/HCL, pH= 8.0; 1% Triton X-100; 150mM NaCl; 0.5% sodium deoxycholate; 0.1% SDS) supplemented with a protease inhibitor cocktail (Roche) and a phosphatase inhibitor cocktail (Sigma-Aldrich). A clear supernatant



was obtained by centrifugation of lysates at 13,000 g for 20 min at 4°C. Protein concentration in the supernatant was determined by Bradford protein assay (Bio-Rad). Aliquots of total cell lysates (20 mg) were then separated by SDS-PAGE by using Miniprotean precast gels (BioRad), and proteins were transferred to nitrocellulose membranes (BioRad).

Membranes were blocked 1h at RT with 5% non-fat milk in Tris-buffered saline with 0.05% Tween 20 and then probed by using the following antibodies directed against PGC1 $\alpha$  (AB3242; Millipore),  $\beta$  chain-ATP Synthase (MAB3494; Millipore), PPAR $\gamma$  (sc-7273; Santa Cruz Biotechnology), SDH (sc-377302; Santa Cruz Biotechnology), TFAM (sc-23588; Santa Cruz Biotechnology), GAPDH (G8795; Sigma-Aldrich).

The appropriate secondary horseradish peroxidase-conjugated antibodies from Jackson ImmunoResearch were used in 5% not-fat- milk (blocking solution) for 1 h at room temperature. Immunoreactive bands were visualized by Clarity Western ECL Substrate (Biorad). Equal loading of samples was confirmed by GAPDH (G8795; Sigma-Aldrich) normalized and quantified by densitometry by ImageJ Software.

**Mouse Inflammation Antibody Array.** Serum cytokines and biomarkers of systemic inflammation were detected using the Mouse Inflammation Antibody Array C1 (RayBiotech, Norcross, Georgia, USA) according to manufacturer instructions.

**Statistical analysis.** All data were expressed as mean  $\pm$  SEM or mean  $\pm$  SD, when appropriate, absolute values, or percentages. Outliers in the measurements were identified by mean of the interquartile range (IQR), as either below Q1 – 1.5 IQR or above Q3 + 1.5 IQR, and excluded from the analysis. The variation between groups was compared by using nonparametric Wilcoxon, Mann-Whitney U, or  $\chi^2$  tests, as appropriate. Statistical significance was assumed for  $p < 0.05$ . The statistical analysis was performed with IBM SPSS Statistics for Windows version 25.0. The \* symbol indicates a statistically significant difference between old and young animals, for any genotype group; the §

symbol identifies a statistically significant difference between WT animals and either Tg or *Ghrl* KO within the same age group.

### Abbreviations

AG	acylated ghrelin
BAT	brown adipose tissue
β-ATPase	ATP-synthase beta-subunit
BLC	B lymphocyte chemoattractant (CXCL13)
BMI	body mass index
BSA	bovine serum albumin
CCL11	C-C motif chemokine ligand 11 (eotaxin-1)
CCL1	C-C motif chemokine ligand 1 (I-309)
CSA	cross-sectional area
CXCL13	C-X-C motif chemokine ligand 13 (BLC)
DAPI	4',6-diamidino-2-phenylindole
EDL	extensor digitorum longus
Fbxo32	F-Box Protein 32 (Atrogin-1)
GAPDH	glyceraldehyde 3-phosphate dehydrogenase
GAS	gastrocnemius
GH	growth hormone
<i>Ghrl</i>	ghrelin (gene)
<i>Ghsr</i>	growth hormone secretagogue receptor (gene)
GHSR-1a	growth hormone secretagogue receptor type 1a
IL-13	interleukin-13
IL-12	interleukin-12

IL-12p70	interleukin-12 70 kDa light chain
KO	knock-out
M-CSF	macrophage colony-stimulating factor
<i>Myh6</i>	myosin heavy chain 6 (gene)
PGC1 $\alpha$	PPAR $\gamma$ -coactivator-1-alpha
PFA	paraformaldehyde
PPAR $\gamma$	peroxisome proliferator-activated receptor gamma
Ppif	peptidyl-prolyl cis-trans isomerase, mitochondrial
QUAD	quadriceps
SDF1 $\alpha$	stromal cell-derived factor-1-alpha
SDH	succinate dehydrogenase
SDHA	succinate dehydrogenase complex flavoprotein subunit A
SOL	soleus
TA	tibialis anterior
TFAM	mitochondrial transcription factor A
TNF $\alpha$	tumor necrosis factor alpha
TNF-R1	tumor necrosis factor receptor 1
Tg	transgenic
UCP1	Uncoupling Protein 1
UnAG	unacylated ghrelin
WT	wild type

### **Author contributions**

NF and SR: study conception and design; manuscript writing. MM, AG, MS, PC, EF: study conception and design. EAg, MDF, RB, EAn, MAT, IZ, ET, TR, AS, FLR: conduction of experiments and data collection. FP, EF, SR, NF: data analysis and interpretation.

## **Acknowledgments**

The authors are grateful to Catherine-Laure Tomasetto (Université de Strasbourg, France) for providing the *Ghrl* KO mice.

## **Conflicts of interests**

The authors declare no conflict of interest.

## **Funding**

This study was funded by a research grant from Fondazione Cariplo (Grant 2015\_0634 to NF, PC, and MS) and partially supported by funds from the AGING PROJECT-Department of Excellence – Department of Translational Medicine, and by University of Piemonte Orientale FAR 2019. EAn was supported by a FIRC-AIRC fellowship for Italy. MAT is beneficiary of a PhD fellowship from Compagnia di San Paolo.

## **References**

1. Wang H, Hai S, Cao L, Zhou J, Liu P, and Dong B-R. Estimation of prevalence of sarcopenia by using a new bioelectrical impedance analysis in Chinese community-dwelling elderly people. *BMC Geriatr.* 2016; 16: 216.
2. Landi F, Liperoti R, Russo A, Giovannini S, Tosato M, Capoluongo E, Bernabei R, and Onder G. Sarcopenia as a risk factor for falls in elderly individuals: Results from the ilSIRENTE study. *Clinical Nutrition.* 2012; 31: 652–658.
3. Bokshan SL, DePasse JM, and Daniels AH. Sarcopenia in orthopedic surgery. *Orthopedics.* 2016; 39: e295–e300.
4. Chung HY, Kim DH, Eun KL, Chung KW, Chung S, Lee B, Seo AY, Chung JH, Jung YS, Im E, Lee J, Kim ND, Choi YJ, et al. Redefining Chronic Inflammation in Aging and Age-Related Diseases: Proposal of the Senoinflammation Concept. *Aging and disease.* 2019; 10: 367–82.

5. Kojima M, Hosoda H, Date Y, Nakazato M, Matsuo H, and Kangawa K. Ghrelin is a growth-hormone-releasing acylated peptide from stomach. *Nature*. 1999; 402: 656–660.
6. Tschöp MH, Smiley DL, and Heiman ML. Ghrelin induces adiposity in rodents. *Nature*. 2000; 407: 908–913.
7. Porporato PE, Filigheddu N, Reano S, Ferrara M, Angelino E, Gnocchi VF, Prodám F, Ronchi G, Fagoonee S, Fornaro M, Chianale F, Baldanzi G, Surico N, et al. Acylated and unacylated ghrelin impair skeletal muscle atrophy in mice. *Journal of Clinical Investigation*. 2013; 123: 611–622.
8. Filigheddu N, Gnocchi VF, Coscia M, Cappelli M, Porporato PE, Taulli R, Traini S, Baldanzi G, Chianale F, Cutrupi S, Arnoletti E, Ghè C, Fubini A, et al. Ghrelin and Des-Acyl Ghrelin Promote Differentiation and Fusion of C2C12 Skeletal Muscle Cells. *Molecular Biology of the Cell*. 2007; 18: 986–994.
9. Wu C-S, Wei Q, Wang H, Kim DM, Balderas M, Wu G, Lawler J, Safe S, Guo S, Devaraj S, Chen Z, and Sun Y. Protective Effects of Ghrelin on Fasting-Induced Muscle Atrophy in Aging Mice. *J Gerontol A Biol Sci Med Sci* [Internet]. 2018 [cited 2020 Jan 8]; . Available from: <https://academic.oup.com/biomedgerontology/advance-article/doi/10.1093/gerona/gly256/5165582>
10. Ruozi G, Bortolotti F, Falcione A, Dal Ferro M, Ukovich L, MacEdo A, Zentilin L, Filigheddu N, Cappellari GG, Baldini G, Zweyer M, Barazzoni R, Graziani A, et al. AAV-mediated in vivo functional selection of tissue-protective factors against ischaemia. *Nature Communications*. 2015; 6.
11. Togliatto G, Trombetta A, Dentelli P, Cotogni P, Rosso A, Tschöp MH, Granata R, Ghigo E, and Brizzi MF. Unacylated ghrelin promotes skeletal muscle regeneration following hindlimb ischemia via SOD-2-mediated miR-221/222 expression. *Journal of the American Heart Association*. 2013; 2.

12. Gortan Cappellari G, Zanetti M, Semolic A, Vinci P, Ruozi G, Falcione A, Filigheddu N, Guarnieri G, Graziani A, Giacca M, and Barazzoni R. Unacylated Ghrelin Reduces Skeletal Muscle Reactive Oxygen Species Generation and Inflammation and Prevents High-Fat Diet–Induced Hyperglycemia and Whole-Body Insulin Resistance in Rodents. *Diabetes*. 2016; 65: 874–86.
13. Reano S, Angelino E, Ferrara M, Malacarne V, Sustova H, Sabry O, Agosti E, Clerici S, Ruozi G, Zentilin L, Prodam F, Geuna S, Giacca M, et al. Unacylated Ghrelin Enhances Satellite Cell Function and Relieves the Dystrophic Phenotype in Duchenne Muscular Dystrophy mdx Model. *STEM CELLS*. 2017; 35: 1733–1746.
14. Gortan Cappellari G, Semolic A, Ruozi G, Vinci P, Guarnieri G, Bortolotti F, Barbetta D, Zanetti M, Giacca M, and Barazzoni R. Unacylated ghrelin normalizes skeletal muscle oxidative stress and prevents muscle catabolism by enhancing tissue mitophagy in experimental chronic kidney disease. *The FASEB Journal*. 2017; 31: 5159–5171.
15. Nass R, Farhy LS, Liu J, Pezzoli SS, Johnson ML, Gaylinn BD, and Thorner MO. Age-Dependent Decline in Acyl-Ghrelin Concentrations and Reduced Association of Acyl-Ghrelin and Growth Hormone in Healthy Older Adults. *The Journal of Clinical Endocrinology & Metabolism*. 2014; 99: 602–608.
16. Lin L, Lee JH, Bongmba OYN, Ma X, Zhu X, Sheikh-Hamad D, and Sun Y. The suppression of ghrelin signaling mitigates age-associated thermogenic impairment. *Aging*. 2014; 6: 1019–1032.
17. Yin Y, and Zhang W. The Role of Ghrelin in Senescence: A Mini-Review. *GER*. 2016; 62: 155–62.
18. Guillory B, Chen J, Patel S, Luo J, Splenser A, Mody A, Ding M, Baghaie S, Anderson B, Iankova B, Halder T, Hernandez Y, and Garcia JM. Deletion of ghrelin prevents aging-associated obesity and muscle dysfunction without affecting longevity. *Aging Cell*. 2017; 16: 859–869.

19. Batsis JA, and Villareal DT. Sarcopenic obesity in older adults: aetiology, epidemiology and treatment strategies. *Nat Rev Endocrinol*. 2018; 14: 513–37.
20. Wiedmer P, Nogueiras R, Broglio F, D'Alessio D, and Tschöp MH. Ghrelin, obesity and diabetes. *Nat Rev Endocrinol*. 2007; 3: 705–12.
21. Lin L, Lee JH, Buras ED, Yu K, Wang R, Wayne Smith C, Wu H, Sheikh-Hamad D, and Sun Y. Ghrelin receptor regulates adipose tissue inflammation in aging. *Aging*. 2016; 8: 178–191.
22. Angelino E, Reano S, Bollo A, Ferrara M, De Feudis M, Sustova H, Agosti E, Clerici S, Prodam F, Tomasetto CL, Graziani A, and Filigheddu N. Ghrelin knockout mice display defective skeletal muscle regeneration and impaired satellite cell self-renewal. *Endocrine*. 2018; 62: 129–135.
23. Gumucio JP, and Mendias CL. Atrogin-1, MuRF-1, and sarcopenia. *Endocrine*. 2013; 43: 12–21.
24. Wang Y, and Pessin JE. Mechanisms for fiber-type specificity of skeletal muscle atrophy. *Current Opinion in Clinical Nutrition & Metabolic Care*. 2013; 16: 243–50.
25. Peterson CM, Johannsen DL, and Ravussin E. Skeletal Muscle Mitochondria and Aging: A Review. Brown-Borg, HM, editor. *Journal of Aging Research*. Hindawi Publishing Corporation; 2012; 2012: 194821.
26. Turner VM, and Mabbott NA. Influence of ageing on the microarchitecture of the spleen and lymph nodes. *Biogerontology*. 2017; 18: 723–38.
27. Rea IM, Gibson DS, McGilligan V, McNerlan SE, Alexander HD, and Ross OA. Age and Age-Related Diseases: Role of Inflammation Triggers and Cytokines. *Frontiers in Immunology*. 2018; 9: 586.
28. Aw D, Hilliard L, Nishikawa Y, Cadman ET, Lawrence RA, and Palmer DB. Disorganization of the splenic microanatomy in ageing mice. *Immunology*. 2016; 148: 92–101.
29. Mau T, and Yung R. Adipose tissue inflammation in aging. *Experimental Gerontology*. 2018; 105: 27–31.

30. Zoico E, Rubele S, De Caro A, Nori N, Mazzali G, Fantin F, Rossi A, and Zamboni M. Brown and Beige Adipose Tissue and Aging. *Frontiers in Endocrinology*. 2019; 10: 368.
31. Prodam F, and Filigheddu N. Ghrelin Gene Products in Acute and Chronic Inflammation. *Archivum Immunologiae et Therapiae Experimentalis*. 2014; 62: 369–84.
32. Lin L, Saha PK, Ma X, Henshaw IO, Shao L, Chang BHJ, Buras ED, Tong Q, Chan L, McGuinness OP, and Sun Y. Ablation of ghrelin receptor reduces adiposity and improves insulin sensitivity during aging by regulating fat metabolism in white and brown adipose tissues. *Aging Cell*. 2011; 10: 996–1010.
33. Tchkonina T, Morbeck DE, Von Zglinicki T, Van Deursen J, Lustgarten J, Scrbale H, Khosla S, Jensen MD, and Kirkland JL. Fat tissue, aging, and cellular senescence. *Aging Cell*. 2010; 9: 667–684.
34. Sun Y, Ahmed S, and Smith RG. Deletion of Ghrelin Impairs neither Growth nor Appetite. *Molecular and Cellular Biology*. 2003; 23: 7973–7981.
35. Murman DL. The Impact of Age on Cognition. *Seminars in Hearing*. 2015; 36: 111–121.
36. Morin V, Hozer F, and Costemale-Lacoste J-F. The effects of ghrelin on sleep, appetite, and memory, and its possible role in depression: A review of the literature. *L'Encéphale*. 2018; 44: 256–63.
37. Huang HJ, Zhu XC, Han QQ, Wang YL, Yue N, Wang J, Yu R, Li B, Wu GC, Liu Q, and Yu J. Ghrelin alleviates anxiety- and depression-like behaviors induced by chronic unpredictable mild stress in rodents. *Behavioural Brain Research*. 2017; 326: 33–43.
38. Tsubouchi H, Yanagi S, Miura A, Matsumoto N, Kangawa K, and Nakazato M. Ghrelin relieves cancer cachexia associated with the development of lung adenocarcinoma in mice. *European Journal of Pharmacology*. 2014; 743: 1–10.
39. Chen J, Splenser A, Guillory B, Luo J, Mendiratta M, Belinova B, Halder T, Zhang G, Li Y-P, and Garcia JM. Ghrelin prevents tumour- and cisplatin-induced muscle wasting:



- characterization of multiple mechanisms involved. *Journal of Cachexia, Sarcopenia and Muscle*. 2015; 6: 132–143.
40. Sun Y, Wang P, Zheng H, and Smith RG. Ghrelin stimulation of growth hormone release and appetite is mediated through the growth hormone secretagogue receptor. *Proc Natl Acad Sci U S A*. 2004; 101: 4679.
  41. Reano S, Graziani A, and Filigheddu N. Acylated and unacylated ghrelin administration to blunt muscle wasting. *Current Opinion in Clinical Nutrition & Metabolic Care*. 2014; 17: 236–40.
  42. Aderka D, Engelmann H, Maor Y, Brakebusch C, and Wallach D. Stabilization of the bioactivity of tumor necrosis factor by its soluble receptors. *Journal of Experimental Medicine*. 1992; 175: 323–329.
  43. Hassouna R, Zizzari P, Tomasetto C, Veldhuis JD, Fiquet O, Labarthe A, Cognet J, Steyn F, Chen C, Epelbaum J, and Tolle V. An Early Reduction in GH Peak Amplitude in Preproghrelin-Deficient Male Mice Has a Minor Impact on Linear Growth. *Endocrinology*. 2014; 155: 3561–3571.
  44. Balducci C, Beeg M, Stravalaci M, Bastone A, Scip A, Biasini E, Tapella L, Colombo L, Manzoni C, Borsello T, Chiesa R, Gobbi M, Salmona M, et al. Synthetic amyloid- $\beta$  oligomers impair long-term memory independently of cellular prion protein. *Proceedings of the National Academy of Sciences of the United States of America*. 2010; 107: 2295–2300.
  45. McMurphy T, Huang W, Liu X, Siu JJ, Queen NJ, Xiao R, and Cao L. Hypothalamic gene transfer of BDNF promotes healthy aging in mice. *Aging Cell*. 2019; 18: e12846.



## References

- Abbas MA. Physiological functions of Vitamin D in adipose tissue. *J Steroid Biochem Mol Biol*. 2017;165(Pt B):369-381. doi:10.1016/j.jsbmb.2016.08.004.
- Adunsky A, Chandler J, Heyden N, et al. MK-0677 (ibutamoren mesylate) for the treatment of patients recovering from hip fracture: a multicenter, randomized, placebo-controlled phase IIb study. *Arch Gerontol Geriatr*. 2011;53(2):183-189. doi:10.1016/j.archger.2010.10.004.
- Akamizu T, Kangawa K. Ghrelin for cachexia. *J Cachexia Sarcopenia Muscle*. 2010;1(2):169-176. doi:10.1007/s13539-010-0011-5.
- Akimoto Y, Kanai S, Ohta M, Akimoto S, Uematsu H, Miyasaka K. Age-associated reduction of stimulatory effect of ghrelin on food intake in mice. *Arch Gerontol Geriatr*. 2012;55(2):238-243. doi:10.1016/j.archger.2011.09.007.
- Ali S, Garcia JM. Sarcopenia, cachexia and aging: diagnosis, mechanisms and therapeutic options - a mini-review. *Gerontology*. 2014;60(4):294-305. doi:10.1159/000356760.
- Alvarez JA, Ashraf A. Role of vitamin d in insulin secretion and insulin sensitivity for glucose homeostasis. *Int J Endocrinol*. 2010;2010:351385. doi:10.1155/2010/351385.
- Andrews ZB. The extra-hypothalamic actions of ghrelin on neuronal function. *Trends Neurosci*. 2011;34(1):31-40. doi:10.1016/j.tins.2010.10.001
- Argilés JM, Busquets S, Stemmler B, López-Soriano FJ. Cachexia and sarcopenia: mechanisms and potential targets for intervention. *Curr Opin Pharmacol*. 2015;22:100-106. doi:10.1016/j.coph.2015.04.003.
- Argilés JM, Busquets S, Stemmler B, López-Soriano FJ. Cachexia and sarcopenia: mechanisms and potential targets for intervention. *Curr Opin Pharmacol*. 2015;22:100-106. doi:10.1016/j.coph.2015.04.003.
- Argilés JM, Stemmler B. The potential of ghrelin in the treatment of cancer cachexia. *Expert Opin Biol Ther*. 2013;13(1):67-76. doi:10.1517/14712598.2013.727390.
- Baatar D, Patel K, Taub DD. The effects of ghrelin on inflammation and the immune system. *Mol Cell Endocrinol*. 2011;340(1):44-58. doi:10.1016/j.mce.2011.04.019.

Baldanzi G, Filigheddu N, Cutrupi S, et al. Ghrelin and des-acyl ghrelin inhibit cell death in cardiomyocytes and endothelial cells through ERK1/2 and PI 3-kinase/AKT. *J Cell Biol.* 2002;159(6):1029-1037. doi:10.1083/jcb.200207165.

Beudart C, Buckinx F, Rabenda V, Gillain S, Cavalier E, Slomian J, et al. The effects of vitamin D on skeletal muscle strength, muscle mass, and muscle power: a systematic review and meta-analysis of randomized controlled trials. *J Clin Endocrinol Metab* 2014;99(11):4336–45.

Bischoff HA, Borchers M, Gudat F, et al. In situ detection of 1,25-dihydroxyvitamin D<sub>3</sub> receptor in human skeletal muscle tissue. *Histochem J.* 2001;33(1):19-24. doi:10.1023/a:1017535728844.

Bischoff-Ferrari HA, Borchers M, Gudat F, Dürmüller U, Stähelin HB, Dick W. Vitamin D receptor expression in human muscle tissue decreases with age. *J Bone Miner Res* 2004;19(2):265–9.

Bischoff-Ferrari HA, Kiel DP, Dawson-Hughes B, Orav JE, Li R, Spiegelman D, et al. Dietary calcium and serum 25-hydroxyvitamin D status in relation to BMD among U.S. adults. *J Bone Miner Res.* 2009;24:935–42.

Bischoff-Ferrari HA. Vitamin D and fracture prevention. *Rheum Dis Clin North Am.* 2012;38(1):107-113. doi:10.1016/j.rdc.2012.03.010.

Bodine SC, Stitt TN, Gonzalez M, et al. Akt/mTOR pathway is a crucial regulator of skeletal muscle hypertrophy and can prevent muscle atrophy in vivo. *Nat Cell Biol.* 2001;3(11):1014-1019. doi:10.1038/ncb1101-1014.

Boland R. Role of vitamin D in skeletal muscle function. *Endocr Rev.* 1986;7(4):434-448. doi:10.1210/edrv-7-4-434.

Bonaldo P, Sandri M. Cellular and molecular mechanisms of muscle atrophy. *Dis Model Mech.* 2013;6(1):25-39. doi:10.1242/dmm.010389.

Braga M, Simmons Z, Norris KC, Ferrini MG, Artaza JN. Vitamin D induces myogenic differentiation in skeletal muscle derived stem cells. *Endocr Connect.* 2017;6(3):139-150. doi:10.1530/EC-17-0008.

Broglio F, Arvat E, Benso A, et al. Ghrelin, a natural GH secretagogue produced by the stomach, induces hyperglycemia and reduces insulin secretion in humans. *J Clin Endocrinol Metab.* 2001;86(10):5083-5086. doi:10.1210/jcem.86.10.8098.

Buitrago CG, Arango NS, Boland RL.  $1\alpha,25(\text{OH})_2\text{D}_3$ -dependent modulation of Akt in proliferating and differentiating C2C12 skeletal muscle cells. *J Cell Biochem* 2012; 113: 1170-1181.

Bunout D, de la Maza MP, Barrera G, et al. Association between sarcopenia and mortality in healthy older people. *Australian J Ageing*. 2011;30(2):89-92.

Broglio F, Arvat E, Benso A, et al. Ghrelin, a natural GH secretagogue produced by the stomach, induces hyperglycemia and reduces insulin secretion in humans. *J Clin Endocrinol Metab*. 2001;86(10):5083-5086. doi:10.1210/jcem.86.10.8098.

Camperi A, Pin F, Costamagna D, Penna F, Menduina ML, Aversa Z *et al*. Vitamin D and VDR in cancer cachexia and muscle regeneration. *Oncotarget* 2017; 8: 21778-21793.

Cangussu LM, Nahas-Neto J, Orsatti CL, Bueloni-Dias FN, Nahas EA. Effect of vitamin D supplementation alone on muscle function in postmenopausal women: a randomized, double-blind, placebo-controlled clinical trial. *Osteoporos Int*.2015;26:2413-2421.

Caprio M, Infante M, Calanchini M, Mammi C, Fabbri A. Vitamin D: not just the bone. Evidence for beneficial pleiotropic extraskeletal effects. *Eat Weight Disord*. 2017;22(1):27-41. doi:10.1007/s40519-016-0312-6.

Caristia S, Filigheddu N, Barone-Adesi F, et al. Vitamin D as a Biomarker of Ill Health among the Over-50s: A Systematic Review of Cohort Studies. *Nutrients*. 2019;11(10):2384. Published 2019 Oct 6.

Casado E, Larrosa M. Skeletal and extraskeletal benefits of vitamin D. A Critical Evaluation of Vitamin D - Basic Overview. Sivakumar Gowder. 2017.

Chen JA, Splenser A, Guillory B, et al. Ghrelin prevents tumour- and cisplatin-induced muscle wasting: characterization of multiple mechanisms involved. *J Cachexia Sarcopenia Muscle* 2015;6:132-43.

Chopin LK, Seim I, Walpole CM, Herington AC: The ghrelin axis--does it have an appetite for cancer progression? *Endocr Rev* 2012;33:849-891.

Christakos S, Dhawan P, Verstuyf A, Verlinden L, Carmeliet G. Vitamin D: Metabolism, Molecular Mechanism of Action, and Pleiotropic Effects. *Physiol Rev*. 2016;96(1):365-408. doi:10.1152/physrev.00014.2015

Cruz-Jentoft AJ, Landi F, Schneider SM, Zuniga C, Arai H, Boirie Y, et al. Prevalence of and interventions for sarcopenia in ageing adults: a systematic review. Report of the International Sarcopenia Initiative (EWGSOP and IWGS). *Age Ageing*. 2014; 43(6):748–59. [PubMed: 25241753]

Cruz-Jentoft AJ, Sayer AA. Sarcopenia. *Lancet*. 2019 Jun 29;393(10191):2636-2646. doi: 10.1016/S0140-6736(19)31138-9. Epub 2019 Jun 3. Review. Erratum in: *Lancet*. 2019 Jun 29;393(10191):2590. PubMed PMID: 31171417.

Cruz-Jentoft AJ, Baeyens JP, Bauer JM, et al. Sarcopenia: European consensus on definition and diagnosis: Report of the European Working group on sarcopenia in older people. *Age Ageing*. 2010;39(4):412-23.

Currow D, Temel JS, Abernethy A, Milanowski J, Friend J, Fearon KC. ROMANA 3: a phase 3 safety extension study of anamorelin in advanced non-small-cell lung cancer (NSCLC) patients with cachexia. *Ann Oncol*. 2017;28(8):1949-1956. doi:10.1093/annonc/mdx192.

Dev R, Del Fabbro E, Schwartz GG, Hui D, Palla SL, Gutierrez N *et al*. Preliminary report: vitamin D deficiency in advanced cancer patients with symptoms of fatigue or anorexia. *Oncologist* 2011; 16: 1637-1641.

Dezaki K, Hosoda H, Kakei M, Hashiguchi S, Watanabe M, Kangawa K, Yada T. (2004). Endogenous ghrelin in pancreatic islets restricts insulin release by attenuating Ca<sup>2+</sup> signaling in beta-cells: implication in the glycemic control in rodents. *Diabetes*. 53(12):3142-51.

Dixit VD, Yang H, Cooper-Jenkins A, Giri BB, Patel K, Taub DD. Reduction of T cell-derived ghrelin enhances proinflammatory cytokine expression: implications for age-associated increases in inflammation. *Blood*. 2009;113(21):5202-5205. doi:10.1182/blood-2008-09-181255.

Dixit VD, Yang H, Sun Y, et al. Ghrelin promotes thymopoiesis during aging. *J Clin Invest*. 2007;117(10):2778-2790. doi:10.1172/JCI30248.

Dodson S, Baracos VE, Jatoi A, Evans WJ, Cella D, Dalton JT et al. Muscle wasting in cancer cachexia: clinical implications, diagnosis, and emerging treatment strategies. *Annu Rev Med* 2011; 62: 265-279.

Domingues-Faria C, Boirie Y, Walrand S. Vitamin D and muscle trophicity. *Curr Opin Clin Nutr Metab Care*. 2017;20(3):169-174. doi:10.1097/MCO.0000000000000358.

Drozdenco, G.; Scheel, T.; Heine, G.; Baumgrass, R.; Worm, M. Impaired T cell activation and cytokine production by calcitriol-primed human B cells. *Clin. Exp. Immunol.* 2014, 178, 364–372.

Eisman JA, Bouillon R. Vitamin D: direct effects of vitamin D metabolites on bone: lessons from genetically modified mice. *Bonekey Rep.* 2014;3:499. Published 2014 Feb 5. doi:10.1038/bonekey.2013.233

Fearon K, Strasser F, Anker SD, Bosaeus I, Bruera E, Fainsinger RL, Jatoi A, Loprinzi C, MacDonald N, Mantovani G, Davis M, Muscaritoli M, Ottery F, Radbruch L, Ravasco P, Walsh D, Wilcock A, Kaasa S, Baracos VE. Definition and classification of cancer cachexia: an international consensus. *The Lancet Oncology.* 2011;12(5):489–495.

Fearon KC, Baracos VE. Cachexia in pancreatic cancer: new treatment options and measures of success. *HPB (Oxford)* 2010; 12: 323-324.

Fearon KC, Glass DJ, Guttridge DC. Cancer cachexia: mediators, signaling, and metabolic pathways. *Cell Metab* 2012; 16: 153-166

Filigheddu N, Gnocchi VF, Coscia M, et al. Ghrelin and des-acyl ghrelin promote differentiation and fusion of C2C12 skeletal muscle cells. *Mol Biol Cell.* 2007;18(3):986-994. doi:10.1091/mbc.e06-05-0402.

Garcia JM, Boccia RV, Graham CD, et al. Anamorelin for patients with cancer cachexia: an integrated analysis of two phase 2, randomised, placebo-controlled, double-blind trials. *Lancet Oncol.* 2015;16(1):108-116. doi:10.1016/S1470-2045(14)71154-4.

Garcia JM, Garcia-Touza M, Hijazi RA, Taffet G, Epner D, Mann D, Smith RG, Cunningham GR, Marcelli M: Active ghrelin levels and active to total ghrelin ratio in cancer-induced cachexia. *J Clin Endocrinol Metab* 2005;90:2920-2926.

Garcia M, Seelaender M, Sotiropoulos A, Coletti D, Lancha AH Jr. Vitamin D, muscle recovery, sarcopenia, cachexia, and muscle atrophy. *Nutrition.* 2019;60:66-69. doi:10.1016/j.nut.2018.09.031.

Girgis CM, Clifton-Bligh RJ, Hamrick MW, Holick MF, Gunton JE. The roles of vitamin D in skeletal muscle: form, function, and metabolism. *Endocr Rev.* 2013;34(1):33-83. doi:10.1210/er.2012-1012

Girgis CM, Clifton-Bligh RJ, Mokbel N, Cheng K, Gunton JE. Vitamin D signaling regulates proliferation, differentiation, and myotube size in C2C12 skeletal muscle cells. *Endocrinology* 2014; 155: 347-357.

Gortan Cappellari G, Semolic A, Ruozi G, Vinci P, Guarnieri G, Bortolotti F, Barbetta D, Zanetti M, Giacca M, and Barazzoni R. Unacylated ghrelin normalizes skeletal muscle oxidative stress and prevents muscle catabolism by enhancing tissue mitophagy in experimental chronic kidney disease. *The FASEB Journal*. 2017; 31: 5159–5171.

Gortan Cappellari G, Zanetti M, Semolic A, Vinci P, Ruozi G, Falcione A, Filigheddu N, Guarnieri G, Graziani A, Giacca M, and Barazzoni R. Unacylated Ghrelin Reduces Skeletal Muscle Reactive Oxygen Species Generation and Inflammation and Prevents High-Fat Diet–Induced Hyperglycemia and Whole-Body Insulin Resistance in Rodents. *Diabetes*. 2016; 65: 874–86.

Graf SA, Garcia JM. (2017). Anamorelin hydrochloride in the treatment of cancer anorexia-cachexia syndrome: design, development, and potential place in therapy. *Drug Des Devel Ther*. 11:2325-2331.

Granata R, Settanni F, Biancone L, et al. Acylated and unacylated ghrelin promote proliferation and inhibit apoptosis of pancreatic beta-cells and human islets: involvement of 3',5'-cyclic adenosine monophosphate/protein kinase A, extracellular signal-regulated kinase 1/2, and phosphatidylinositol 3-Kinase/Akt signaling. *Endocrinology*. 2007;148(2):512-529. doi:10.1210/en.2006-0266.

Graumam RQ, Pinheiro MM, Nery LE, Castro C. Increased rate of osteoporosis, low lean mass, and fragility fractures in COPD patients: association with disease severity. *Osteoporos Int*. 2018;29:1457-1468.

Gutierrez JA, Solenberg PJ, Perkins DR, et al. Ghrelin octanoylation mediated by an orphan lipid transferase. *Proc Natl Acad Sci U S A*. 2008;105(17):6320-6325. doi:10.1073/pnas.0800708105.

Haqq AM, Stadler DD, Rosenfeld RG, et al. Circulating ghrelin levels are suppressed by meals and octreotide therapy in children with Prader-Willi syndrome. *J Clin Endocrinol Metab*. 2003;88(8):3573-3576. doi:10.1210/jc.2003-030205.

Howard AD, Feighner SD, Cully DF, et al. A receptor in pituitary and hypothalamus that functions in growth hormone release. *Science*. 1996;273(5277):974-977. doi:10.1126/science.273.5277.974.



- Hymøller L, Jensen SK. 25-hydroxyvitamin D circulates in different fractions of calf plasma if the parent compound is vitamin D<sub>2</sub> or vitamin D<sub>3</sub>, respectively. *J Dairy Res.* 2016;83(1):67-71. doi:10.1017/S0022029915000588.
- Iolascon G, Moretti A, de Sire A, Calafiore D, Gimigliano F. Effectiveness of calcifediol in improving muscle function in post-menopausal women: a prospective cohort study. *Adv Ther.* 2017;34:744-752.
- Janssen HC, Samson MM, Verhaar HJ. Vitamin D deficiency, muscle function, and falls in elderly people. *Am J Clin Nutr* 2002;75(4):611-5.
- Janssen I, Heymsfield SB, Wang ZM, Ross R. Skeletal muscle mass and distribution in 468 men and women aged 18-88 yr [published correction appears in *J Appl Physiol* (1985). 2014 May 15;116(10):1342]. *J Appl Physiol* (1985). 2000;89(1):81-88. doi:10.1152/jappl.2000.89.1.81.
- Jean G, Souberbielle JC, Chazot C. Vitamin D in chronic kidney disease and dialysis patients. *Nutrients.* 2017;9:328.
- Kang C, Chung E, Diffie G, Ji LL. Exercise training attenuates aging-associated mitochondrial dysfunction in rat skeletal muscle: Role of pgc-1alpha. *Exp Gerontol.* 2013
- Kang SY, Kang JH, Choi JC, Song SK, Oh JH. Low serum vitamin D levels in patients with myasthenia gravis. *J Clin Neurosci.* 2018;50:294-297.
- Kappeler L, Zizzari P, Grouselle D, Epelbaum J, Bluet-Pajot MT. Plasma and hypothalamic peptide-hormone levels regulating somatotroph function and energy balance in fed and fasted states: a comparative study in four strains of rats. *J Neuroendocrinol.* 2004;16(12):980-988. doi:10.1111/j.1365-2826.2004.01259.x.
- Kim MK, BaekKH, SongKH, Kang M, Park CY, LeeWY, OhKW (2011) Vitamin D deficiency is associated with sarcopenia in older Koreans, regardless of obesity: the fourth Korea National Health and Nutrition Examination Surveys (KNHANES IV) 2009. *J Clin Endocrinol Metab* 96:10.
- Kohno D, Gao HZ, Muroya S, Kikuyama S, Yada T. Ghrelin directly interacts with neuropeptide-Y-containing neurons in the rat arcuate nucleus: Ca<sup>2+</sup> signaling via protein kinase A and N-type channel-dependent mechanisms and cross-talk with leptin and orexin. *Diabetes.* 2003;52(4):948-956. doi:10.2337/diabetes.52.4.948
- Kojima M, Hosoda H, Date Y, Nakazato M, Matsuo H, Kangawa K. Ghrelin is a growth-hormone-releasing acylated peptide from stomach. *Nature.* 1999;402(6762):656-660. doi:10.1038/45230.

- Kojima M, Kangawa K. Ghrelin: structure and function. *Physiol Rev.* 2005;85(2):495-522. doi:10.1152/physrev.00012.2004.
- Kositsawat JMDM, Freeman VLM, Gerber BSMM, Geraci SM. Association of A1C levels with vitamin D status in U.S. adults: data from the National Health and Nutrition Examination Survey. *Diabetes Care* 2010;33:1236–1238
- Kunadian V, Ford GA, Bawamia B, Qiu W, Manson JE. Vitamin D deficiency and coronary artery disease: a review of the evidence. *Am Heart J.* 2014;167:283–91
- Labarthe A, Fiquet O, Hassouna R, et al. Ghrelin-Derived Peptides: A Link between Appetite/Reward, GH Axis, and Psychiatric Disorders?. *Front Endocrinol (Lausanne).* 2014;5:163. Published 2014 Oct 27. doi:10.3389/fendo.2014.00163.
- Lecker SH, Jagoe RT, Gilbert A, et al. Multiple types of skeletal muscle atrophy involve a common program of changes in gene expression. *FASEB J.* 2004;18(1):39-51. doi:10.1096/fj.03-0610com.
- Lin L, Lee JH, Bongmba OYN, Ma X, Zhu X, Sheikh-Hamad D, and Sun Y. The suppression of ghrelin signaling mitigates age-associated thermogenic impairment. *Aging.* 2014; 6: 1019–1032.
- Lin L, Saha PK, Ma X, et al. Ablation of ghrelin receptor reduces adiposity and improves insulin sensitivity during aging by regulating fat metabolism in white and brown adipose tissues. *Aging Cell.* 2011;10(6):996-1010. doi:10.1111/j.1474-9726.2011.00740.x.
- Luo Y, Yoneda J, Ohmori H, et al. Cancer usurps skeletal muscle as an energy repository. *Cancer Res.* 2014;74:330-340.
- MacDonald N, Easson AM, Mazurak VC, Dunn GP, Baracos VE. Understanding and managing cancer cachexia. *J Am Coll Surg* 2003; 197:143-161
- Mager DR, Carroll MW, Wine E, et al. Vitamin D status and risk for sarcopenia in youth with inflammatory bowel diseases. *Eur J Clin Nutr.* 2018;72:623-626.
- Mantovani G, Madeddu C. Cancer cachexia: medical management. *Support Care Cancer* 2010; 18: 1-9 [PMID: 19688225 DOI: 10.1007/s00520-009-0722-3]
- Marino R, Misra M. Extra-Skeletal Effects of Vitamin D. *Nutrients.* 2019;11(7):1460. Published 2019 Jun 27. doi:10.3390/nu11071460

- Mintz B, Baker WW. Normal mammalian muscle differentiation and gene control of isocitrate dehydrogenase synthesis. *Proc Natl Acad Sci U S A*. 1967;58(2):592-598. doi:10.1073/pnas.58.2.592.
- Mohr SB, Gorham ED, Kim J, Hofflich H, Cuomo RE, Garland CF. Could vitamin D sufficiency improve the survival of colorectal cancer patients? *J Steroid Biochem Mol Biol* 2015;148:239–44.
- Mondello P, Lacquaniti A, Mondello S, Bolignano D, Pitini V, Aloisi C, Buemi M: Emerging markers of cachexia predict survival in cancer patients. *BMC Cancer* 2014;14:828.
- Mosekilde L. Vitamin D and the elderly. *Clin Endocrinol* 2005;62(3):265–81.
- Nair R, Maseeh A. Vitamin D: The "sunshine" vitamin. *J Pharmacol Pharmacother*. 2012;3(2):118-126. doi:10.4103/0976-500X.95506
- Nass R, Farhy LS, Liu J, et al. Age-dependent decline in acyl-ghrelin concentrations and reduced association of acyl-ghrelin and growth hormone in healthy older adults. *J Clin Endocrinol Metab*. 2014;99(2):602-608. doi:10.1210/jc.2013-3158.
- Nesic DM, Stevanovic DM, Stankovic SD, et al. Age-dependent modulation of central ghrelin effects on food intake and lipid metabolism in rats. *Eur J Pharmacol*. 2013;710(1-3):85-91. doi:10.1016/j.ejphar.2013.03.052.
- Omdahl JL, Morris HA, May BK. Hydroxylase enzymes of the vitamin D pathway: expression, function, and regulation. *Annu Rev Nutr*.2002;22:139-166.
- Padrao AI, Oliveira P, Vitorino R, Colaco B, Pires MJ, Marquez M, Castellanos E, Neuparth MJ, Teixeira C, Costa C, Moreira-Goncalves D, Cabral S, Duarte JA, Santos LL, Amado F, Ferreira R. Bladder cancer-induced skeletal muscle wasting: Disclosing the role of mitochondria plasticity. *Int J Biochem Cell Biol*. 2013; 5:1399–1409.
- Penna F, Costamagna D, Pin F, Camperi A, Fanzani A, Chiarpotto EM, Cavallini G, Bonelli G, Baccino FM, Costelli P. Autophagic degradation contributes to muscle wasting in cancer cachexia. *Am J Pathol*. 2013; 182:1367–1378.
- Porporato PE, Filigheddu N, Reano S, et al. Acylated and unacylated ghrelin impair skeletal muscle atrophy in mice. *J Clin Invest* 2013; 123:611–622.

- Raisz LG, Kream BE, Smith MD, Simmons HA. Comparison of the effects of vitamin D metabolites on collagen synthesis and resorption of fetal rat bone in organ culture. *Calcif Tissue Int.* 1980;32(2):135-138. doi:10.1007/BF02408532
- Reano S, Angelino E, Ferrara M, et al. Unacylated Ghrelin Enhances Satellite Cell Function and Relieves the Dystrophic Phenotype in Duchenne Muscular Dystrophy mdx Model. *Stem Cells.* 2017;35(7):1733-1746. doi:10.1002/stem.2632.
- Reed JA, Benoit SC, Pfluger PT, Tschöp MH, D'Alessio DA, Seeley RJ. Mice with chronically increased circulating ghrelin develop age-related glucose intolerance. *Am J Physiol Endocrinol Metab.* 2008;294(4):E752-E760. doi:10.1152/ajpendo.00463.2007.
- Reimer MK, Pacini G, Ahrén B. Dose-dependent inhibition by ghrelin of insulin secretion in the mouse. *Endocrinology.* 2003;144(3):916-921. doi:10.1210/en.2002-220819
- Remelli F, Vitali A, Zurlo A, Volpato S. Vitamin D Deficiency and Sarcopenia in Older Persons. *Nutrients.* 2019;11(12):2861. Published 2019 Nov 21. doi:10.3390/nu11122861.
- Ryan ZC, Craig TA, Wang X, Delmotte P, Salisbury JL, Lanza IR, et al. 1 $\alpha$ ,25-dihydroxyvitamin D<sub>3</sub> mitigates cancer cell mediated mitochondrial dysfunction in human skeletal muscle cells. *Biochem Biophys Res Commun* 2018;496:746–52.
- Sacheck JM, Hyatt JP, Raffaello A, et al. Rapid disuse and denervation atrophy involve transcriptional changes similar to those of muscle wasting during systemic diseases. *FASEB J.* 2007;21(1):140-155. doi:10.1096/fj.06-6604com
- Sandri M. Autophagy in skeletal muscle. *FEBS Lett.* 2010;584(7):1411-1416.
- Sandri M. Protein breakdown in muscle wasting: role of autophagy-lysosome and ubiquitin-proteasome. *Int J Biochem Cell Biol.* 2013;45(10):2121-2129.
- Sandri M. Signaling in muscle atrophy and hypertrophy. *Physiology (Bethesda).* 2008; 23:160–170.
- A Sayer A, Stewart C, Patel H, Cooper C. The developmental origins of sarcopenia: from epidemiological evidence to underlying mechanisms. *J Dev Orig Health Dis.* 2010;1(3):150-157. doi:10.1017/S2040174410000097.

Scher HI, Jia X, Chi K, de Wit R, Berry WR, Albers P *et al.* Randomized, open-label phase III trial of docetaxel plus high-dose calcitriol versus docetaxel plus prednisone for patients with castration-resistant prostate cancer. *J Clin Oncol* 2011; 29: 2191-2198.

Schiaffino S, Mammucari C. Regulation of skeletal muscle growth by the IGF1-Akt/PKB pathway: insights from genetic models. *Skelet Muscle*. 2011;1(1):4. Published 2011 Jan 24. doi:10.1186/2044-5040-1-4.

Scott D, Daly RM, Sanders KM, Ebeling PR. Fall and Fracture Risk in Sarcopenia and Dynapenia With and Without Obesity: the Role of Lifestyle Interventions. *Curr Osteoporos Rep*. 2015;13(4):235-244. doi:10.1007/s11914-015-0274-z.

Sever S, White DL, Garcia JM. Is there an effect of ghrelin/ghrelin analogs on cancer? A systematic review. *Endocr Relat Cancer*. 2016;23(9):R393-R409. doi:10.1530/ERC-16-0130.

Sheriff S, Kadeer N, Joshi R, et al. Des-acyl ghrelin exhibits pro-anabolic and anticatabolic effects on C2C12 myotubes exposed to cytokines and reduces burn-induced muscle proteolysis in rats. *Mol Cell Endocrinol* 2012; 351:286–295.

Shimizu Y, Nagaya N, Isobe T, Imazu M, Okumura H, Hosoda H, Kojima M, Kangawa K, Kohno N: Increased plasma ghrelin level in lung cancer cachexia. *Clin Cancer Res* 2003;9:774-778.

Snijder MB, van Schoor NM, Pluijm SM, van Dam RM, Visser M, Lips P. Vitamin D status in relation to one-year risk of recurrent falling in older men and women. *J Clin Endocrinol Metab*. 2006;91:2980-2985.

Srikuea R, Zhang X, Park-Sarge OK, Esser KA. VDR and CYP27B1 are expressed in C2C12 cells and regenerating skeletal muscle: potential role in suppression of myoblast proliferation. *Am J Physiol Cell Physiol*. 2012;303:C396-405.

Sun Y, Garcia JM, Smith RG. Ghrelin and growth hormone secretagogue receptor expression in mice during aging. *Endocrinology*. 2007;148(3):1323-1329. doi:10.1210/en.2006-0782.

Sustova H, De Feudis M, Reano S, et al. Opposing effects of 25-hydroxy- and 1 $\alpha$ ,25-dihydroxy-vitamin D3 on pro-cachectic cytokine-and cancer conditioned medium-induced atrophy in C2C12 myotubes. *Acta Physiol (Oxf)*. 2019;226(3):e13269. doi:10.1111/apha.13269.

Suzuki T, Kwon J, Kim H, et al. Low serum 25-hydroxyvitamin D levels associated with falls among Japanese community-dwelling elderly. *J Bone Miner Res*. 2008;23:1309-1317.

- Taillandier D, Polge C. Skeletal muscle atrogenes: From rodent models to human pathologies. *Biochimie*. 2019;166:251-269. doi:10.1016/j.biochi.2019.07.014
- Teegarden D, Donkin SS. Vitamin D: emerging new roles in insulin sensitivity. *Nutr Res Rev* 2009;22:82–92
- Terawaki K, Kashiwase Y, Sawada Y, et al. Development of ghrelin resistance in a cancer cachexia rat model using human gastric cancer-derived 85As2 cells and the palliative effects of the Kampo medicine rikkunshito on the model. *PLoS One*. 2017;12(3):e0173113. doi:10.1371/journal.pone.0173113.
- Togliatto G, Trombetta A, Dentelli P, Cotogni P, Rosso A, Tschöp MH, Granata R, Ghigo E, and Brizzi MF. Unacylated ghrelin promotes skeletal muscle regeneration following hindlimb ischemia via SOD-2-mediated miR-221/222 expression. *Journal of the American Heart Association*. 2013; 2.
- Tsoli M, Robertson G. Cancer cachexia: malignant inflammation, tumorkines, and metabolic mayhem. *Trends Endocrinol Metab*. 2013;24(4):174-183.
- Tsoukas, C.D.; Provvedini, D.M.; Manolagas, S.C. 1,25-dihydroxyvitamin D<sub>3</sub>: A novel immunoregulatory hormone. *Science* 1984, 224, 1438–1440. [CrossRef] [PubMed]
- van der Meijden K, Bravenboer N, Dirks NF, et al. Effects of 1,25(OH)<sub>2</sub>D<sub>3</sub> and 25(OH)D<sub>3</sub> on C2C12 Myoblast Proliferation, Differentiation, and Myotube Hypertrophy. *J Cell Physiol*. 2016;231(11):2517-2528. doi:10.1002/jcp.25388.
- Van Kan GA. Epidemiology and consequences of sarcopenia. *J Nutr Health Aging*. 2009;13(8):708-712.
- Van Veldhuizen PJ, Taylor SA, Williamson S, Drees BM. Treatment of vitamin D deficiency in patients with metastatic prostate cancer may improve bone pain and muscle strength. *J Urol* 2000; 163: 187-190.
- Vaughan VC, Martin P, Lewandowski PA. Cancer cachexia: impact, mechanisms and emerging treatments. *J Cachexia Sarcopenia Muscle* 2013; 4: 95-109.
- Visser M, Schaap LA. Consequences of sarcopenia. *Clin Geriatric Med*. 2011;27(3):387-399.
- Vitale G, Cesari M, Mari D. Aging of the endocrine system and its potential impact on sarcopenia. *Eur J Intern Med*. 2016;35:10-15. doi:10.1016/j.ejim.2016.07.017

- Vitale G, Salvioli S, Franceschi C. Oxidative stress and the ageing endocrine system. *Nat Rev Endocrinol* 2013;9(4):228–40.
- Wagatsuma A, Sakuma K. Vitamin D signaling in myogenesis: potential for treatment of sarcopenia. *Biomed Res Intern* 2014;2014:121254.
- White HK, Petrie CD, Landschulz W, et al. Effects of an oral growth hormone secretagogue in older adults. *J Clin Endocrinol Metab*. 2009;94(4):1198-1206. doi:10.1210/jc.2008-0632.
- Wolden-Kirk H, Gysemans C, Verstuyf A, Mathieu C. Extraskeletal effects of vitamin D. *Endocrinol Metab Clin North Am*. 2012;41:571–94.
- Wu CS, Wei Q, Wang H, et al. Protective Effects of Ghrelin on Fasting-Induced Muscle Atrophy in Aging Mice. *J Gerontol A Biol Sci Med Sci*. 2020;75(4):621-630. doi:10.1093/gerona/gly256.
- Yang J, Zhao TJ, Goldstein JL, Brown MS. Inhibition of ghrelin O-acyltransferase (GOAT) by octanoylated pentapeptides. *Proc Natl Acad Sci U S A*. 2008;105(31):10750-10755. doi:10.1073/pnas.0805353105.
- Yin Y, Zhang W. The Role of Ghrelin in Senescence: A Mini-Review. *Gerontology*. 2016;62(2):155-162. doi:10.1159/000433533
- Youm YH, Yang H, Sun Y, et al. Deficient ghrelin receptor-mediated signaling compromises thymic stromal cell microenvironment by accelerating thymic adiposity. *J Biol Chem*. 2009;284(11):7068-7077. doi:10.1074/jbc.M808302200.
- Zanello SB, Collins ED, Marinissen MJ, Norman AW, Boland RL. Vitamin D receptor expression in chicken muscle tissue and cultured myoblasts. *Horm Metab Res*. 1997;29(5):231-236. doi:10.1055/s-2007-979027.
- Zeichner SB, Koru-Sengul T, Shah N, Liu Q, Markward NJ, Montero AJ, et al. Improved clinical outcomes associated with vitamin D supplementation during adjuvant chemotherapy in patients with HER2+ nonmetastatic breast cancer. *Clin Breast Cancer* 2015;15:e1–e11.
- Zhou X, Wang JL, Lu J, et al. Reversal of cancer cachexia and muscle wasting by ActRIIB antagonism leads to prolonged survival. *Cell*. 2010;142:531-543.

Zhu X, Cao Y, Voogd K, Steiner DF. On the processing of proghrelin to ghrelin [published correction appears in J Biol Chem. 2007 Jan 19;282(3):2124. Voodg, Keith [corrected to Voogd, Keith]]. J Biol Chem. 2006;281(50):38867-38870. doi:10.1074/jbc.M607955200.



## **Appendix**



# Ghrelin knockout mice display defective skeletal muscle regeneration and impaired satellite cell self-renewal

Elia Angelino<sup>1,2</sup> · Simone Reano<sup>1</sup> · Alessandro Bollo<sup>1,2</sup> · Michele Ferrara<sup>1,2</sup> · Marilisa De Feudis<sup>1</sup> · Hana Sustova<sup>1</sup> · Emanuela Agosti<sup>1</sup> · Sara Clerici<sup>1,2</sup> · Flavia Prodam<sup>3</sup> · Catherine-Laure Tomassetto<sup>4</sup> · Andrea Graziani<sup>1,2</sup> · Nicoletta Filigheddu<sup>1</sup> 

Received: 19 January 2018 / Accepted: 15 April 2018 / Published online: 30 May 2018  
© Springer Science+Business Media, LLC, part of Springer Nature 2018

## Abstract

**Purpose** Muscle regeneration depends on satellite cells (SCs), quiescent precursors that, in consequence of injury or pathological states such as muscular dystrophies, activate, proliferate, and differentiate to repair the damaged tissue. A subset of SCs undergoes self-renewal, thus preserving the SC pool and its regenerative potential. The peptides produced by the ghrelin gene, i.e., acylated ghrelin (AG), unacylated ghrelin (UnAG), and obestatin (Ob), affect skeletal muscle biology in several ways, not always with overlapping effects. In particular, UnAG and Ob promote SC self-renewal and myoblast differentiation, thus fostering muscle regeneration.

**Methods** To delineate the endogenous contribution of preproghrelin in muscle regeneration, we evaluated the repair process in *Ghrl*<sup>-/-</sup> mice upon CTX-induced injury.

**Results** Although muscles from *Ghrl*<sup>-/-</sup> mice do not visibly differ from WT muscles in term of weight, structure, and SCs content, muscle regeneration after CTX-induced injury is impaired in *Ghrl*<sup>-/-</sup> mice, indicating that ghrelin-derived peptides actively participate in muscle repair. Remarkably, the lack of ghrelin gene impacts SC self-renewal during regeneration.

**Conclusions** Although we cannot discern the specific *Ghrl*-derived peptide responsible for such activities, these data indicate that *Ghrl* contributes to a proper muscle regeneration.

**Keywords** Ghrelin knockout · Skeletal muscle regeneration · Satellite cells · Self-renewal

---

These authors contributed equally: Elia Angelino, Simone Reano.

---

These authors jointly supervised this work: Andrea Graziani, Nicoletta Filigheddu.

---

Elia Angelino, Simone Reano, Michele Ferrara, Marilisa De Feudis, Hana Sustova, Emanuela Agosti, Andrea Graziani, and Nicoletta Filigheddu are members of Istituto Interuniversitario di Miologia (IIM).

---

**Electronic supplementary material** The online version of this article (<https://doi.org/10.1007/s12020-018-1606-4>) contains supplementary material, which is available to authorized users.

---

✉ Andrea Graziani  
graziani.andrea@hsr.it

✉ Nicoletta Filigheddu  
nicoletta.filigheddu@med.uniupo.it

<sup>1</sup> Department of Translational Medicine, University of Piemonte Orientale, Novara, Italy

## Introduction

Skeletal muscle is a plastic tissue that regenerates upon injury through the activation, expansion, and differentiation of satellite cells (SCs), myogenic precursors characterized by the expression of the transcriptional factor Pax7 [1]. Muscle damage induces a local release of several factors that activate SCs, eventually leading to repair of the injured muscle. *Ghrl* and preproghrelin are induced by injury [2, 3], and both unacylated ghrelin (UnAG) and obestatin (Ob), two products of the ghrelin gene, are among the factors participating in muscle regeneration, as they increase SC

<sup>2</sup> Università Vita-Salute San Raffaele, Milano, Italy

<sup>3</sup> Department of Health Sciences, University of Piemonte Orientale, Novara, Italy

<sup>4</sup> IGBMC - Institut de Génétique et de Biologie Moléculaire et Cellulaire - Université de Strasbourg, Illkirch, France

activity [3, 4]. Also, their exogenous administration in vivo—via injection, electroporation, or AAV-mediated delivery—enhances muscle regeneration in several models of muscle injury, such as cardiotoxin (CTX)-induced or freeze-induced injury and hindlimb ischemia [4–6]. Consistently, muscle regeneration after CTX injury improves also in transgenic mice characterized by high levels of circulating UnAG [3].

Along with UnAG and Ob, also acylated ghrelin (AG) acts on muscle or muscle-derived cells. In particular, both AG and UnAG promote murine C2C12 myoblast differentiation [7], and Ob has a similar effect on human myoblasts [8]. Both UnAG and Ob foster skeletal muscle regeneration [2–6], and both AG and UnAG protect muscle from doxorubicin-induced apoptosis [9] and from wasting in numerous experimental models, such as burn injury [10, 11]; fasting and denervation [12], kidney disease-associated cachexia [13, 14], and, in vitro, on C2C12 myotubes treated with dexamethasone or co-cultured with CT26 colon carcinoma cells [12, 15]. Several studies evaluated the protective activity of AG alone and demonstrated its efficacy in protecting from hindlimb suspension- or angiotensin II-induced atrophy [16, 17], and from cancer cachexia [18, 19]. Although most of the reported activities of AG and UnAG in muscle-derived cells—both skeletal and cardiac—are overlapping, their effects on reactive oxygen species (ROS) production diverge, being UnAG the only peptide able to inhibit ROS accumulation [5, 6, 20]. Relevantly, UnAG, but not AG, induces skeletal muscle regeneration upon ischemia-induced injury [5].

Here we aim at establishing the impact of endogenous ghrelin in muscle regeneration using preproghrelin-deficient (*Ghrl*<sup>−/−</sup>) mice that do not produce any *Ghrl*-derived peptides.

## Materials and methods

### Animals

C57BL/6 male mice, matched for age and weight, were used for all experiments. C57BL/6 *Ghrl*<sup>−/−</sup> mice were generated as previously described [21]. Animals were fed ad libitum and had unrestricted access to drinking water. The light/dark cycle in the room consisted of 12/12 h with artificial light. Three mice had been estimated sufficient to detect 1 SD unit with 80% power and a significance level of 95% at Student's *T*-test in CSA frequency distribution experiments, according to previously published data (Porporato 2013). Five mice had been estimated sufficient to detect differences in Pax7+/BrdU+ cells according to the same model and previous data (Reano 2017). The number of mice was calculated with the program by R.V. Lenth

([www.stat.uiowa.edu/~rlenth/Power/index.html](http://www.stat.uiowa.edu/~rlenth/Power/index.html)). The investigators conducting the experiments were blind to the experimental group assessed. The investigators quantifying the experimental outcomes were maintained blinded to the animal group or intervention. Finally, the statistic evaluation of the experimental data was performed by another investigator not directly involved in data collection and parameter measurement.

### CTX-induced muscle regeneration

Experiments on muscle regeneration were conducted on adult male C57BL/6 and C57BL/6 *Ghrl*<sup>−/−</sup> mice matched for age and weight. CTX from *Naja mossaambica mossaambica* (Latoxan) was dissolved in sterile saline to a final concentration of 10 μM. Mice were anesthetized by isoflurane inhalation and hindlimbs were shaved and cleaned with alcohol. TA muscles were injected with 45 μl of CTX with a 30-gauge needle, with 15 microinjections of 3 μl CTX each in the mid-belly of the muscle to induce a homogeneous damage [3]. The TA muscles of the contralateral hindlimbs were injected with saline. After injection, animals were kept under a warming lamp until recovery.

For the experiments assessing SC self-renewal during muscle regeneration, immediately after each CTX administration, a single intraperitoneal injection of 5-bromo-2'-deoxyuridine (BrdU) (6 μg/g mouse) was given, followed by BrdU administered ad libitum in drinking water (2.5 mg/ml) for 17 days.

### Histological analysis

Muscles were trimmed of tendons and adhering non-muscle tissue, mounted in Killik embedding medium (Bio-optica), frozen in liquid-nitrogen-cooled isopentane, and stored at −80 °C. Transverse muscle sections (7 μm) were cryosectioned from the mid-belly of each muscle. Sections were stained with hematoxylin/eosin to reveal general muscle architecture. Images of whole muscle sections were acquired with the slide scanner Panoramic Midi 1.14 (3D Hitech) and cross-sectional areas (CSA) of centronucleated fibers quantified with ImageJ software (v1.49o). Muscle collagen content was assessed with Masson trichromic staining.

### Immunofluorescence

For Pax7 and BrdU detection, tissue sections were fixed in 4% PFA for 20 min, washed, permeabilized with cold methanol for 6 min, and then antigen-retrieved with sodium citrate (10 mM, 0.05% Tween in PBS) at 95 °C for 30 min. For blocking the unspecific binding sites, slices were

incubated in 4% BSA for 2 h at RT and then with M.O.M. blocking reagent (Vector) for 1 h at RT. Sections were stained with an anti-Pax7 antibody (1:100; Developmental Studies Hybridoma Bank) and with anti-BrdU antibody (1:300; Biorad) overnight at 4 °C. After washing, sections were incubated with the appropriate Alexa Fluor Dyes-

conjugated secondary antibody (488-anti-mouse/anti-rabbit or 568-anti-rabbit; Thermo Fisher Scientific) for 1 h at RT. DAPI was incubated for 5 min.

For immunofluorescence with anti-laminin (1:200; Dako), after fixing, slices were permeabilized with 0.2% Triton X-100 in 1% BSA for 15 min and blocked with 4% BSA for 30 min. One hour of incubation with primary antibodies was followed by 45 min of secondary antibody incubation at RT.

Images were acquired using the slide scanner Panoramic Midi Scanner 1.14 (3D Histech) and quantified with Panoramic viewer software or ImageJ v1.49o software.

**Table 1** Phenotypical characterization of *Ghrl*<sup>-/-</sup> mice

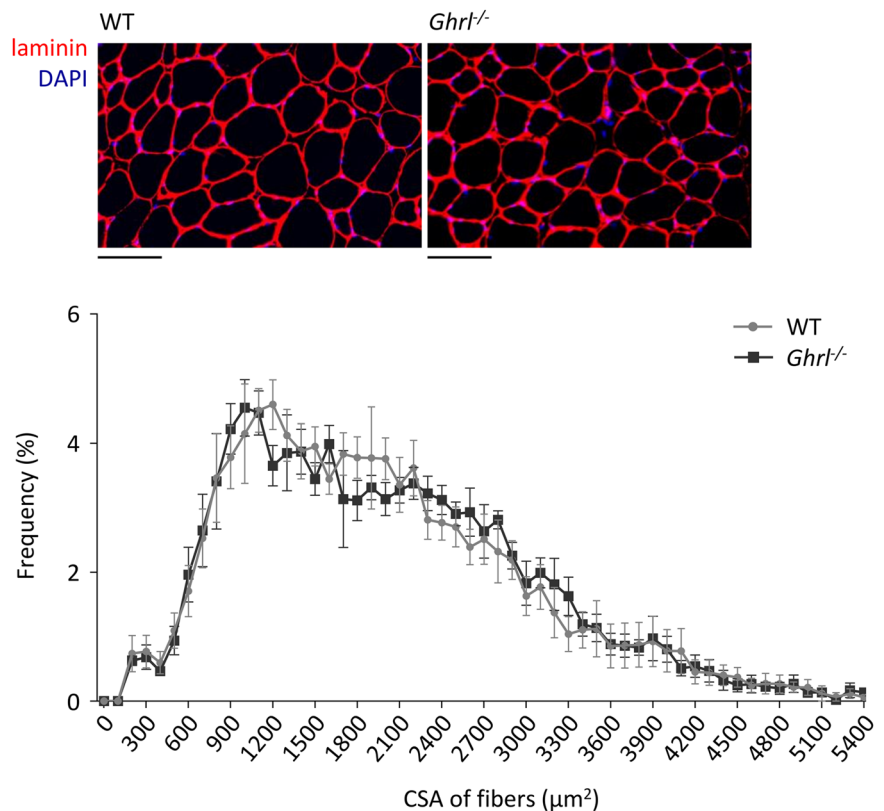
	WT	<i>Ghrl</i> <sup>-/-</sup>
Body weight (g)	30.69 ± 1.26	28.47 ± 0.65
Nose-to-anus length (mm)	93.59 ± 1.70	93.83 ± 0.75
Tibial length (mm)	19.60 ± 0.20	19.68 ± 0.13
Quadriceps weight (mg)	257.15 ± 13.21	244.15 ± 8.38
Gastrocnemius weight (mg)	167.40 ± 9.5	147.11 ± 16.72
Tibialis anterior weight (mg)	51.53 ± 2.62	51.80 ± 1.29
Extensor digitorum longus weight (mg)	10.59 ± 1.28	12.42 ± 0.45
Soleus weight (mg)	9.23 ± 0.49	8.85 ± 0.21
Heart weight (mg)	164.58 ± 11.68	138.30 ± 7.72

Measurements of the indicated parameters were performed as described in the Methods section. Data represent means ± S.E.M. (*N* = 5 for each group). The variation between groups was assessed by nonparametric Wilcoxon and Mann-Whitney U tests. No statistically significant differences were found in the analyzed features

## Statistical analysis

All data were expressed as mean ± SEM, absolute values, or percentages. For continuous variables, the variation between groups was compared by means of nonparametric Wilcoxon and Mann-Whitney U tests, as appropriate. When analyzing experiments acquired with different instruments, ANCOVA analysis was used to determine differences between groups by using the instrument as a covariate. Multiple logistic regression was used for trends. Statistical significance was assumed for *p* < 0.05. The statistical analysis was performed with SPSS for Windows version 17.0 (SPSS; Chicago, IL).

**Fig. 1** In not-injured conditions, the lack of *Ghrl* gene does not impact muscle morphology. Representative images (upper panels) of laminin IF and DAPI staining of not-injured TA muscle sections from WT and *Ghrl*<sup>-/-</sup> mice (scale bar, 100 μm) and myofiber CSA frequency distribution (lower panel). Chi-square test was used to compare distributions. (CSA mean ± S.E.M. μm<sup>2</sup>: WT 1941.63 ± 176.54; *Ghrl*<sup>-/-</sup> 1970.48 ± 80.92). *N* = 5 (WT) and 4 (*Ghrl*<sup>-/-</sup>)



## Results

### The lack of Ghrl gene impairs muscle regeneration

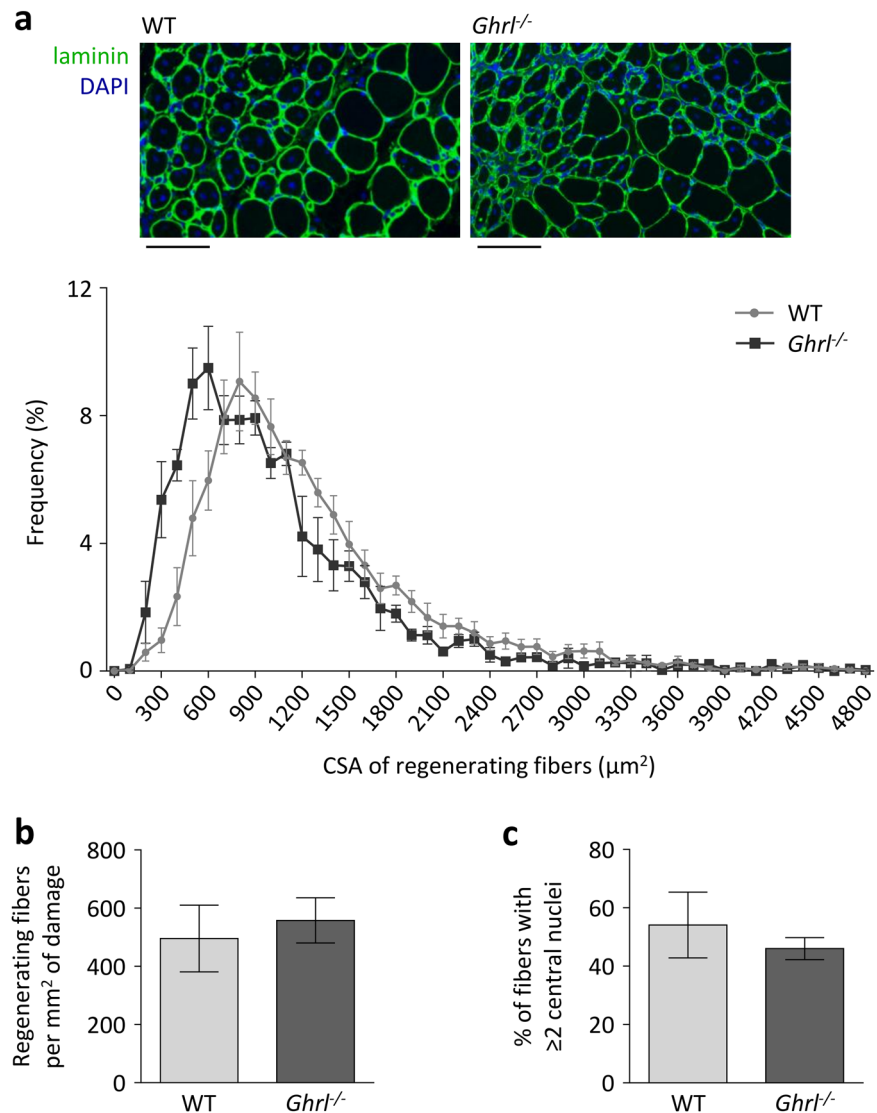
Ghrelin mRNA is rapidly and transiently induced in the injured muscle [2, 3], and preproghrelin-derived peptides UnAG and Ob contribute to the regenerative process [2, 3, 5, 6]. To further gain insight into the role of *Ghrl*-derived peptides in skeletal muscle regeneration, we induced injury in tibialis anterior (TA) muscle of *Ghrl*<sup>-/-</sup> mice by CTX injection. Although macroscopically *Ghrl*<sup>-/-</sup> mice did not show blatant differences in total body and muscle weight (Table 1), as well as in muscle morphology, number of Pax7 + SC (data not shown), and fiber CSA distribution (Fig. 1) compared with wild-type (WT) mice, at day 7 post CTX injury, regeneration in *Ghrl*<sup>-/-</sup> mice was impaired, as evidenced by a shift toward smaller CSA of regenerating (i.e., centronucleated) fibers (Fig. 2a). This shift was not

accompanied by an increase in the number of smaller fibers in the regenerating portion of the muscle, as the total number of regenerating fiber normalized to the damaged area was alike in *Ghrl*<sup>-/-</sup> and WT mice (Fig. 2b). Similarly, the number of regenerating fibers with ≥2 nuclei was similar in both *Ghrl*<sup>-/-</sup> and WT mice (Fig. 2c), suggesting that the lack of preproghrelin does not negatively impact on myoblast fusion during regeneration. The defect in regeneration observed in *Ghrl*<sup>-/-</sup> mice was not due to a basal deficit in the number of SCs either, as not-injured TA from *Ghrl*<sup>-/-</sup> and WT mice displayed a comparable number of Pax7+ cells (data not shown).

### The lack of Ghrl gene negatively impacts SC self-renewal during muscle regeneration

We have previously demonstrated that UnAG affects SC biology promoting their activation, stimulating their

**Fig. 2** The lack of *Ghrl* gene impairs muscle regeneration. **a** Representative images (upper panels) of laminin IF and DAPI staining of WT and *Ghrl*<sup>-/-</sup> TA muscle sections (scale bar, 100 μm) and quantification of CSA frequency distribution (lower panels) of regenerating (i.e., centronucleated) myofibers after 7 days from CTX injection. Chi-square test was used to compare distributions. Trend  $P < 0.01$ . (CSA mean ± S.E.M. μm<sup>2</sup>: WT 1254.80 ± 159.64; *Ghrl*<sup>-/-</sup> 1055.08 ± 103.78).  $N = 5$  (WT) and 4 (*Ghrl*<sup>-/-</sup>). **b** Number of regenerating fibers/mm<sup>2</sup> in the damaged area. Mean ± S.E.M.  $N = 5$  (WT) and 4 (*Ghrl*<sup>-/-</sup>). **c** Percentage of fibers with ≥2 central nuclei over the total of regenerating fibers. Mean ± S.E.M.  $N = 5$  (WT) and 4 (*Ghrl*<sup>-/-</sup>)



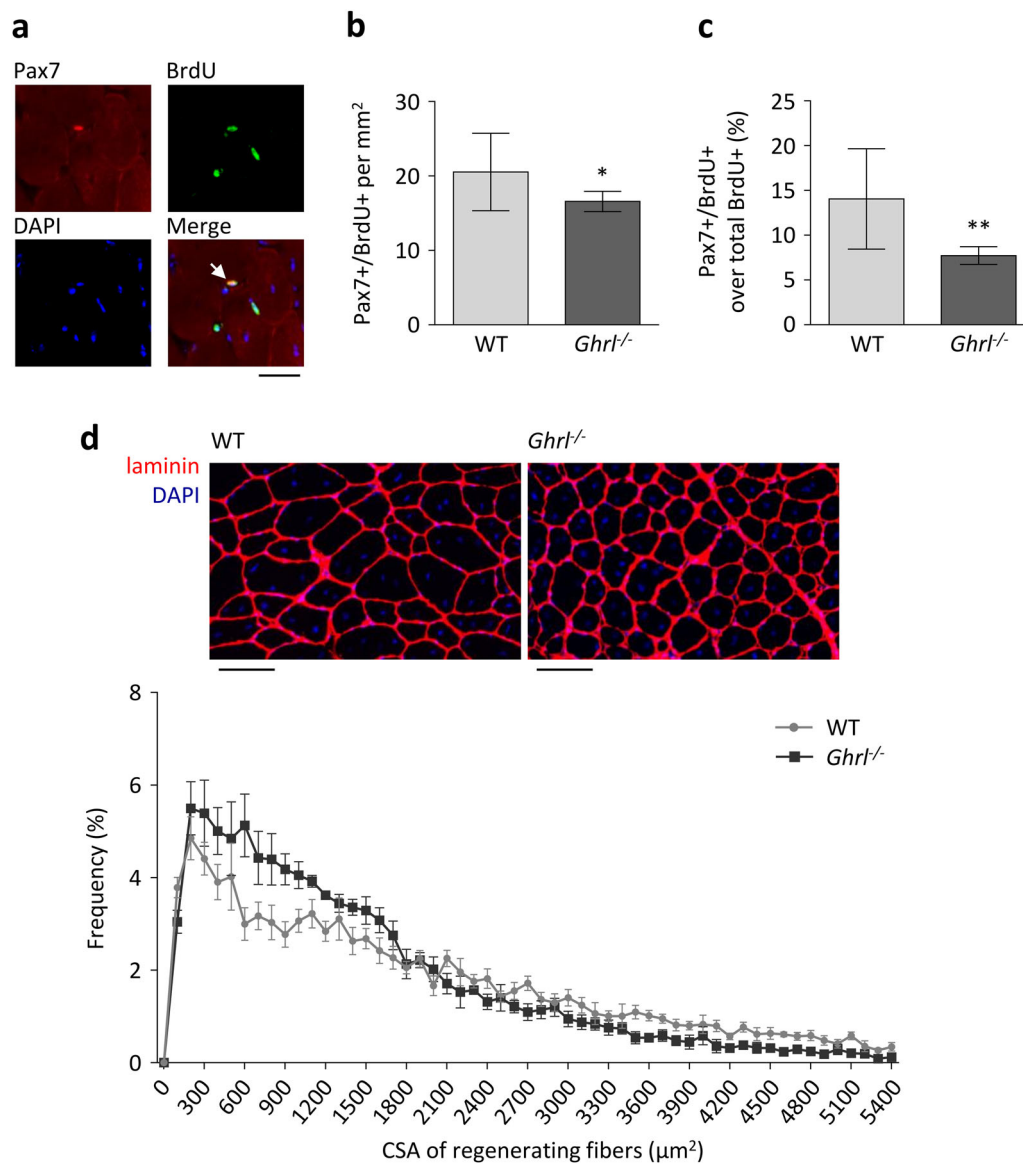


**Fig. 3** The lack of *Ghrl* gene impairs SC self-renewal during muscle regeneration. **a** Representative images of TA transverse sections stained with anti-Pax7, anti-BrdU, and DAPI after SC forced exhaustion procedure, arrow: Pax7+/BrdU+ nucleus (scale bar, 40 μm). **b** Pax7+/BrdU+ nuclei per mm<sup>2</sup>. Mean ± S.E.M.; \**P* < 0.05; *N* = 8 (WT) and 8 (*Ghrl*<sup>-/-</sup>). **c** Percentage of Pax7+/BrdU+ nuclei above the total number of BrdU+ cells. Mean ± S.E.M.; \*\**P* < 0.01; *N*

= 8 (WT) and 8 (*Ghrl*<sup>-/-</sup>). **d** Representative images (upper panels) of laminin IF and DAPI staining of WT and *Ghrl*<sup>-/-</sup> TA muscle sections (scale bar, 100 μm) after SC forced exhaustion procedure and quantification of CSA frequency distribution of myofibers. Chi-square test was used to compare distributions. Trend *P* < 0.05. (CSA mean ± S.E. M. μm<sup>2</sup>: WT 2054.35 ± 155.81; *Ghrl*<sup>-/-</sup> 1535.93 ± 145.37; *P* < 0.05). *N* = 5 (WT) and 5 (*Ghrl*<sup>-/-</sup>)

proliferation, and enhancing their self-renewal both in vitro and in vivo [3]. Similarly, Ob induces SC activation in freeze-injured muscles [4]. To further analyze the effect of the lack of *Ghrl*-derived peptides in SC self-renewal, we administered BrdU to WT and *Ghrl*<sup>-/-</sup> mice immediately after muscle injury and during the following phase of intense myoblast proliferation, in a system of forced regeneration consisting in three cycles of CTX injection [3]. Sixty days after the last injury, the number of Pax7+/BrdU + SCs, i.e., SCs that cycled at least once and then

underwent self-renewal [3, 22], was significantly reduced in *Ghrl*<sup>-/-</sup> muscle (Fig. 3a,b), demonstrating that preproghrelin deficiency compromises SC self-renewal in vivo. Noteworthy, the defect in self-renewal did not reflect an impairment of cell proliferation in *Ghrl*<sup>-/-</sup> muscle, as the number of Pax7+/BrdU+ cells normalized on the total of BrdU+ cells was further reduced in *Ghrl*<sup>-/-</sup> injured muscle (Fig. 3c), indicating that the lack of preproghrelin specifically affects SC self-renewal. Fiber CSA distribution analysis revealed that regenerating muscle from *Ghrl*<sup>-/-</sup> mice

had significantly smaller fibers compared to WT (Fig. 3d), indicating that the defect in regeneration persisted at 60 days.

## Discussion

In this study, we further extended the comprehension of the role of *Ghrl*-derived peptides on skeletal muscle regeneration by using *Ghrl*<sup>-/-</sup> mice and demonstrating that deletion of *Ghrl* impairs skeletal muscle regeneration. *Ghrl* codes for preproghrelin, which, in turn, give rise to different peptides, AG, UnAG, and Ob. All these peptides have activities on skeletal muscle; in particular, they promote skeletal muscle regeneration following CTX- or ischemia-induced damage [2–6]. The use of preproghrelin-deficient mice allowed us to demonstrate that muscle regeneration partly depends on endogenous *Ghrl*-derived peptides, and that preproghrelin is involved in the maintenance of the SC pool, by favoring SC self-renewal. These results are in line with previous data demonstrating that UnAG and Ob regulate multiple steps of muscle regeneration by directly acting on SCs, enhancing their proliferation and self-renewal [3, 4, 6]. Despite the direct effects of *Ghrl*-derived peptides on SCs, evidence that SCs isolated from *Ghrl*<sup>-/-</sup> mice differentiate and fuse exactly as WT SCs (data not shown) indicates the lack of an autocrine effect of these peptides on SCs.

Moreover, the effects on muscle regeneration as a whole can also result from the anti-inflammatory activity of *Ghrl*-derived peptides [23] on the immune cells that, following injury, infiltrate the muscle and release several factors that contribute to muscle repair [24]. Therefore, we can postulate that the impairment of regeneration in *Ghrl*<sup>-/-</sup> mice may in part reflect a dysregulated inflammatory response at the site of damage.

The lack of differences in the number of SCs in basal, not-injured condition, suggests that *Ghrl*-derived peptides might be noncompulsory for the biology of Pax3+ SCs responsible for the formation of the SC pool during muscle development. Nevertheless, *Ghrl*-derived peptides can affect these SCs, as shown in Tg mice overexpressing *Ghrl*, in which the high levels of circulating UnAG increase the basal number of quiescent SCs in not-injured muscles [3]. The impairment of SC self-renewal observed in *Ghrl*<sup>-/-</sup> mice, on the other hand, suggests that the role of *Ghrl*-derived peptides acquires relevance only in adult Pax7+ SCs. This is not totally unexpected, as many intrinsic and extrinsic factors are peculiar for embryonic and post-natal muscle formation versus adult muscle regeneration.

By using *Ghrl*<sup>-/-</sup> mice, we cannot discern the specific contribution of each peptide. However, evidence suggests that AG has a minor role, if any, in muscle regeneration. Indeed, in ischemia-induced muscle damage, UnAG but not

AG promotes regeneration by enhancing SC expansion [6]. In different systems of muscle wasting, such as denervation-induced or fasting-induced atrophy, both AG and UnAG act on skeletal muscle promoting signaling pathways leading to the maintenance of muscle mass [12]. This anti-atrophic effect was demonstrated in *Ghsr*<sup>-/-</sup> mice, ruling out the involvement of the canonical AG receptor in muscle activities elicited by both AG and UnAG. The findings gathered so far on the muscular effects of AG and UnAG led to the hypothesis of the existence of a common, yet to be identified, receptor for AG and UnAG. Data on muscle regeneration and SCs further suggest that another receptor—specific for UnAG—might be involved.

**Acknowledgements** This study was supported by research grants from the Muscular Dystrophy Association (grant MDA294617 to NF and AG), Association Française contre les Myopathies (Grant 16437 to AG), AIRC (to AG), and Fondazione Cariplo (Grant 2015\_0634 to NF).

## Compliance with ethical standards

**Conflict of interest** A.G. is a consultant to Helsinn (Lugano, Switzerland), N.F. is a consultant to Lyric Pharmaceuticals (South San Francisco, CA, USA).

**Ethical approval** This article does not contain any studies with human participants performed by any of the authors. Animal experiments were performed according to procedures approved by the Institutional Animal Care and Use Committee at the University of Piemonte Orientale.

## References

1. P. Seale, L.A. Sabourin, A. Girgis-Gabardo, A. Mansouri, P. Gruss, M.A. Rudnicki, Pax7 is required for the specification of myogenic satellite cells. *Cell* **102**, 777–786 (2000)
2. U. Gurriarán-Rodríguez, I. Santos-zas, O. Al-massadi, C.S. Mosteiro, R. Nogueiras, A.B. Crujeiras, L.M. Seoane, J. Señaris, R. Gallego, F. Felipe, Y. Pazos, J.P. Camiña, The obestatin/GPR39 system is up-regulated by muscle injury and functions as an autocrine regenerative system. *J. Biol. Chem.* **287**, 38379–38389 (2012)
3. S. Reano, E. Angelino, M. Ferrara, V. Malacarne, H. Sustova, O. Sabry, E. Agosti, S. Clerici, G. Ruozi, L. Zentilin, F. Prodam, S. Geuna, M. Giacca, A. Graziani, N. Filigheddu, Unacylated ghrelin enhances satellite cell function and relieves the dystrophic phenotype in Duchenne muscular dystrophy mdx model. *Stem Cells* **35**, 1733–1746 (2017)
4. U. Gurriarán-Rodríguez, I. Santos-zas, J. González-sánchez, D. Beiroa, V. Moresi, C.S. Mosteiro, W. Lin, J.E. Viñuela, J. Señaris, T. García-caballero, F.F. Casanueva, R. Nogueiras, R. Gallego, J. Renaud, S. Adamo, Y. Pazos, J.P. Camiña, Action of obestatin in skeletal muscle repair: stem cell expansion, muscle growth, and microenvironment remodeling. *Mol. Ther.* **23**, 1003–1021 (2015)
5. G. Ruozi, F. Bortolotti, A. Falcione, M.D. Ferro, L. Ukovich, A. Macedo, L. Zentilin, N. Filigheddu, G.G. Cappellari, G. Baldini, M. Zweyer, R. Barazzoni, A. Graziani, S. Zacchigna, M. Giacca, AAV-mediated in vivo functional selection of tissue-protective factors against ischaemia. *Nat. Commun.* **6**(6), 7388 (2015)
6. G.G. Togliatto, A. Trombetta, P. Dentelli, P. Cotogni, A. Rosso, H. Matthias, R. Granata, E. Ghigo, M.F. Brizzi, G. Togliatto, A.

- Trombetta, P. Dentelli, P. Cotogni, A. Rosso, Unacylated ghrelin promotes skeletal muscle regeneration following hindlimb ischemia via SOD-2-mediated miR-221/222 expression. *J. Am. Heart Assoc.* **2**, e000376 (2013)
7. N. Filigheddu, V.F. Gnocchi, M. Coscia, M. Cappelli, P.E. Porporato, R. Taulli, S. Traini, G. Baldanzi, F. Chianale, S. Cutrupi, E. Arnoletti, C. Ghe, A. Fubini, N. Surico, F. Sinigaglia, C. Ponzetto, G. Muccioli, T. Crepaldi, A. Graziani, Ghrelin and des-acyl ghrelin promote differentiation and fusion of C2C12 skeletal muscle cells. *Mol. Biol. Cell* **18**, 986–994 (2007).
  8. I. Santos-Zas, U. Gurriarán-Rodríguez, T. Cid-Díaz, G. Figueroa, J. González-Sánchez, M. Bouzo-Lorenzo, C.S. Mosteiro, J. Señarís, F.F. Casanueva, X. Casabiell, R. Gallego, Y. Pazos, V. Mouly, J.P. Camiña,  $\beta$ -Arrestin scaffolds and signaling elements essential for the obestatin/GPR39 system that determine the myogenic program in human myoblast cells. *Cell. Mol. Life. Sci.* **73**, 617–635 (2016)
  9. A.P. Yu, X.M. Pei, T.K. Sin, S.P. Yip, B.Y. Yung, L.W. Chan, C. S. Wong, P.M. Siu, Acylated and unacylated ghrelin inhibit doxorubicin-induced apoptosis in skeletal muscle. *Acta Physiol.* **211**, 201–213 (2014)
  10. A. Balasubramaniam, R. Joshi, C. Su, L.A. Friend, S. Sheriff, R.J. Kagan, J.H. James, Ghrelin inhibits skeletal muscle protein breakdown in rats with thermal injury through normalizing elevated expression of E3 ubiquitin ligases MuRF1 and MAFbx. *Am. J. Physiol. Regul. Integr. Comp. Physiol.* **296**, R893 (2009)
  11. S. Sheriff, N. Kadeer, R. Joshi, L. Ann, J.H. James, A. Balasubramaniam, Des-acyl ghrelin exhibits pro-anabolic and anti-catabolic effects on C2C12 myotubes exposed to cytokines and reduces burn-induced muscle proteolysis in rats. *Mol. Cell. Endocrinol.* **351**, 286–295 (2012)
  12. P.E. Porporato, N. Filigheddu, S. Reano, M. Ferrara, E. Angelino, V.F. Gnocchi, F. Prodam, G. Ronchi, S. Fagoonee, M. Fornaro, F. Chianale, G. Baldanzi, N. Surico, F. Sinigaglia, I. Perroteau, R.G. Smith, Y. Sun, S. Geuna, A. Graziani, Acylated and unacylated ghrelin impair skeletal muscle atrophy in mice. *J. Clin. Invest.* **123**, 611–622 (2013)
  13. M. Tamaki, A. Hagiwara, K. Miyashita, S. Wakino, H. Inoue, K. Fujii, C. Fujii, M. Sato, M. Mitsuishi, A. Muraki, K. Hayashi, T. Doi, H. Itoh, Improvement of physical decline through combined effects of muscle enhancement and mitochondrial activation by a gastric hormone ghrelin in male 5/6Nx CKD model mice. *Endocrinology* **156**, 3638–3648 (2015)
  14. G.G. Cappellari, A. Semolic, G. Ruozi, P. Vinci, G. Guarnieri, F. Bortolotti, D. Barbetta, M. Zanetti, M. Giacca, R. Barazzoni, Unacylated ghrelin normalizes skeletal muscle oxidative stress and prevents muscle catabolism by enhancing tissue mitophagy in experimental chronic kidney disease. *FASEB J.* **31**, 5159–5171 (2017)
  15. X. Zeng, S. Chen, Y. Yang, Z. Ke, Acylated and unacylated ghrelin inhibit atrophy in myotubes co-cultured with colon carcinoma cells. *Oncotarget* **8**, 72872–72885 (2017)
  16. K. Koshinaka, K. Toshinai, A. Mohammad, K. Noma, M. Oshikawa, H. Ueno, H. Yamaguchi, M. Nakazato, Therapeutic potential of ghrelin treatment for unloading-induced muscle atrophy in mice. *Biochem. Biophys. Res. Commun.* **412**, 296–301 (2011)
  17. M. Sugiyama, A. Yamaki, M. Furuya, N. Inomata, Y. Minamitake, K. Ohsuye, K. Kangawa, Ghrelin improves body weight loss and skeletal muscle catabolism associated with angiotensin II-induced cachexia in mice. *Regul. Pept.* **178**, 21–28 (2012)
  18. H. Tsubouchi, S. Yanagi, A. Miura, N. Matsumoto, K. Kangawa, M. Nakazato, Ghrelin relieves cancer cachexia associated with the development of lung adenocarcinoma in mice. *Eur. J. Pharmacol.* **743**, 1–10 (2014)
  19. J. Chen, A. Splenser, B. Guillory, J. Luo, M. Mendiratta, B. Belinova, T. Halder, G. Zhang, Y. Li, J.M. Garcia, Ghrelin prevents tumour and cisplatin-induced muscle wasting: characterization of multiple mechanisms involved. *J. Cachexia Sarcopenia Muscle* **6**, 132–143 (2015).
  20. G.G. Cappellari, M. Zanetti, A. Semolic, P. Vinci, G. Ruozi, A. Falcione, N. Filigheddu, G. Guarnieri, A. Graziani, M. Giacca, R. Barazzoni, Unacylated ghrelin reduces skeletal muscle reactive oxygen species generation and inflammation and prevents high-fat diet-induced hyperglycemia and whole-body insulin resistance in rodents. *Diabetes* **65**, 874–886 (2016)
  21. R. Hassouna, P. Zizzari, C. Tomasetto, J.D. Veldhuis, O. Fiquet, A. Labarthe, J. Cognet, F. Steyn, C. Chen, J. Epelbaum, V. Tolle, An early reduction in GH peak amplitude in preproghrelin-deficient male mice has a minor impact on linear growth. *Endocrinology* **155**, 3561–3571 (2014)
  22. K.L. Shea, W. Xiang, V.S. Laporta, J.D. Licht, C. Keller, M.A. Basson, A.S. Brack, Sprouty1 regulates reversible quiescence of a self-renewing adult muscle stem cell pool during regeneration. *Cell Stem Cell* **6**, 117–129 (2010)
  23. F. Prodam, N. Filigheddu, Ghrelin gene products in acute and chronic inflammation. *Arch. Immunol. Ther. Exp. (Warsz.)* **62**, 369–384 (2014)
  24. H. Yin, F. Price, M.A. Rudnicki, Satellite cells and the muscle stem cell niche. *Physiol. Rev.* **93**, 23–67 (2013)



## Identification of Haptoglobin as a Readout of rhGH Therapy in GH Deficiency

Marilisa De Feudis,<sup>1</sup> Gillian Elisabeth Walker,<sup>2</sup> Giulia Genoni,<sup>2</sup> Marcello Manfredi,<sup>3,4</sup> Emanuela Agosti,<sup>1</sup> Mara Giordano,<sup>2</sup> Marina Caputo,<sup>1</sup> Luisa Di Trapani,<sup>5</sup> Emilio Marengo,<sup>6</sup> Gianluca Aimaretti,<sup>1</sup> Nicoletta Filigheddu,<sup>1</sup> Simonetta Bellone,<sup>2</sup> Gianni Bona,<sup>2</sup> and Flavia Prodam<sup>2,3</sup>

<sup>1</sup>Department of Translational Medicine, University of Piemonte Orientale, 28100 Novara, Italy; <sup>2</sup>Department of Health Sciences, University of Piemonte Orientale, 28100 Novara, Italy; <sup>3</sup>Interdisciplinary Research Center of Autoimmune and Allergic Diseases, University of Piemonte Orientale, 28100 Novara, Italy; <sup>4</sup>Innovative Solutions and Advanced LED Imaging Techniques s.r.l., Spin-off of Department of Sciences and Technological Innovation, University of Piemonte Orientale, 15121 Alessandria, Italy; <sup>5</sup>Clinical Biochemistry, Maggiore della Carità Hospital, 28100 Novara, Italy; and <sup>6</sup>Department of Sciences and Technological Innovation, University of Piemonte Orientale, 15121 Alessandria, Italy

**ORCID numbers:** 0000-0001-9660-5335 (F. Prodam).

**Background:** GH deficiency (GHD) is characterized by a cluster of cardiovascular risk factors and subtle inflammation. We aimed to demonstrate, through a proteomic approach, molecules directly modulated by GHD and involved in the inflammatory state.

**Methods:** Ten children with isolated GHD were studied before and after 1 year of treatment with rhGH and compared with 14 matched controls. A two-dimensional electrophoresis plasma proteomics analysis was performed at baseline and after GH treatment to identify the top molecules modulated by GH. *In vitro* studies on human hepatoma (HepG2) cells were performed to validate the data.

**Results:** Twelve of 20 proteomic spots were predicted to be isoforms  $\alpha$  and  $\beta$  of haptoglobin (Hp) and confirmed by liquid chromatography tandem mass spectrometry and Western immunoblot analyses. Hp levels were higher in patients with GHD than controls at baseline ( $P < 0.001$ ) and were reduced following GH treatment ( $P < 0.01$ ). In HepG2 cells, both GH and IGF-1 were able to downregulate IL-6-induced Hp secretion. Moreover, Hp secretion was restored in pegvisomant-treated HepG2 cells.

**Conclusions:** Hp is a molecule acting in the inflammatory state of GHD and a possible biomarker for GH treatment. Nevertheless, the contribution of other factors and the molecular pathways involved in the GH downregulation of Hp remain to be clearly defined. (*J Clin Endocrinol Metab* 104: 5263–5273, 2019)

**G**H, beyond its main action on growth, is a pleiotropic hormone, with a pivotal metabolic role. It antagonizes insulin action, stimulates lipolysis, gluconeogenesis, and glycogenolysis either directly or indirectly by IGF-1 (1–5).

GH deficiency (GHD) is a condition of metabolic dysregulation, which is coupled to a cluster of cardiovascular risk factors (6–8), including central adiposity

(9–12) and insulin resistance (13). Subjects with GHD exhibit the same metabolic risk factors of patients with metabolic syndrome (5–15). An increasing number of studies have indicated that subjects affected by GHD are more inflamed compared with controls, most likely because of the immunomodulatory role of GH (9, 16–18). It is noteworthy that the major part of the studies on the

metabolic and inflammatory role of GH concerns GHD adults or adolescents, whereas children have been largely disregarded (19–23). Considering the lack of targets that characterize the metabolic and inflammatory state in pediatric subjects with GHD, we used a proteomic approach to identify broad-spectrum changes in plasmatic protein profile in children affected by isolated GHD. Indeed, clinical proteomic has acquired increased importance as a high throughput tool for identification of putative key proteins in many diseases and target organs, allowing the comprehension of complex pictures (24–26).

This analysis highlighted differences between pre- and posttreatment with GH in many plasma proteins. Because the most considerable identified proteins are acute phase proteins, *in vitro* functional studies were performed to further investigate the interplay between GH/IGF-1 axis and inflammation.

## Subjects and Methods

### Patients and controls

A total of 10 patients (7 males/3 females) with a mean age at diagnosis of  $11.5 \pm 2.9$  years were enrolled according to selection criteria: (i) isolated GHD; (ii) no family history of pituitary dysfunction; (iii) no history of traumatic brain injury; (iv) prepuberty or starting puberty (Tanner stage 2); (v) naive to rhGH treatment; and (vi) no chronic treatments with therapies that interfere with GH or IGF-1 secretion. GHD was diagnosed in the presence of clinical and auxological criteria, low-normal IGF-1 levels according to sex and age cutoffs, and impaired GH response to two consecutive provocative tests (27). An impaired response was defined as a peak GH concentration below  $8 \mu\text{g/L}$  for arginine and clonidine and below  $20 \mu\text{g/L}$  for GHRH + arginine (28). Combined hypopituitarism was excluded in all patients (29).

Fourteen healthy children with normal height, growth velocity, and IGF-I values, matched for age (mean age,  $12.7 \pm 1.1$  years), sex (10 males/4 females), pubertal status, and body mass index were enrolled as controls. All children and their parents gave their written informed consent to participate in this study, which was approved by the local Ethical Committee of our Hospital (CE number 14/11).

All subjects with GHD and controls underwent a complete clinical and auxological evaluation by a trained research team. Height was measured by the Harpenden stadiometer and weight with light clothing by using an electronic scale. Mean height SD score (SDS) for chronological age was calculated according to Tanner national standards (30). Italian growth charts were used for height and weight (31).

MRI of the hypothalamopituitary region was obtained in all patients with GHD at the time of diagnosis (27). In subjects with pituitary anomalies at MRI, genetic causes of isolated GHD (GH1 and GHRHR mutations) were excluded.

After a 12-hour overnight fast, morning blood samples were taken, with patients with GHD undergoing a further sample for proteomic evaluation at baseline (T0) and 12 months (T12) after the beginning of rhGH treatment. Blood samples for confirmation of the proteomic results were also collected from control children.

All biochemical measurements were performed at the Clinical Laboratory of Novara Hospital. GH and IGF-1 serum levels were measured by Liason hGH e IGF-1 immunoassay (DiaSorin S.p.A., Saluggia, Italy) with a sensibility of 0.009 to 0.052 ng/mL, and  $<3$  ng/mL, respectively.

Serum haptoglobin (Hp; mg/mL) was evaluated by immunonephelometry, using as reagent the N antisera antihuman haptoglobin (Siemens Healthcare Diagnostics, Deerfield, IL), with a sensibility of 0.26 to 8.3 g/L, coefficients of variation intercycle 2.3%, intracycle 3.5% and total 3.9%. C-reactive protein (CRP) was evaluated by Siemens Advia Chemistry 1200 (Siemens Healthcare Diagnostics) with a sensibility of 0.002 to 16.4 mg/dL, and coefficients of variation intracycle 2.6% and total 2.7%.

Ferritin was evaluated by chemiluminescence immunoassay (ADVIA Centaur XPT; Siemens Healthcare Diagnostics) with a sensibility of 0.5 to 1650 ng/mL.

Platelets counting and hemoglobin assessment were performed using Sysmex XN2000 (Sysmex Corporation, Kobe, Japan) by direct current hydrodynamic focusing principle and spectrophotometry reading the absorbance at 555 nm, respectively.

### Two-dimensional electrophoresis

Platelet-free plasma samples were obtained by centrifugation at 1300 rpm for 10 minutes at  $4^\circ\text{C}$ , followed by a second centrifugation at 2400 g for 15 minutes at  $4^\circ\text{C}$ . Samples were then stored at  $-80^\circ\text{C}$  until analysis. Plasma proteins concentration were determined by using the DC Protein Assay (Bio-Rad, Hercules, CA). For the first dimension analysis,  $50 \mu\text{g}$  of protein were resuspended in a rehydration buffer, according to the method of de Roos *et al.* (32) and loaded into the Immobilized pH Gradient (IPG; 7 cm) 4–7 strip, for an active overnight (O/N) in-gel rehydration (Bio-Rad). Isoelectric focusing was performed at  $20^\circ\text{C}$  with a Protean IEF Cell (Bio-Rad) using a total of maximum of 8000 V. For the second dimensional separation, IPG strips were soaked, first in a reduction equilibration buffer (6M urea, 2% SDS, 0.375M Tris-HCl pH 8.8, 20% glycerol, and 2% w/v

DTT), followed by an alkylation buffer (6M urea, 2% SDS, 0.375M Tris-HCl pH 8.8, 20% glycerol, and 2.5% w/v iodoacetamide). The strips were then positioned in a 10% SDS-Polyacrylamide gels and run at 200 V for 40 minutes. Finally, polyacrylamide gels were fixed in a solution of 10% methanol and 7% acetic acid and resolved protein spots visualized with an O/N incubation in Sypro-Ruby fluorescent total protein stain (Bio-Rad). All samples were evaluated in duplicate.

### Image analysis

Fluorescent images of individual IPG 4-7 gels were captured with a ChemiDoc Imager using a 615- to 645-nM filter (630BP30; BioRad) and analyzed using PDQuest software (version 8.0) according to the manufacturer's recommendations. Briefly, the software performs an automated detection and matching of spots from all gels, calculating individual spot "volumes" by density/area integration with Sypro-Ruby filtration and Gaussian modeling. To control for slight differences in protein loading across gels, the individual spot volumes were also normalized to the total spot volume for each gel. For each protein spot, an average value for T0 and T12 were compared and subjected to Student *t* test to determine the spots that were significantly different between the two time points for each subject. Only those spots that showed a statistically significant difference with a  $P < 0.05$  and were consistently replicated between the cohort of subjects with GHD were chosen for PDQuest isoelectric point (pI) and molecular weight (MW) estimations and eventual mass spectrometry (MS) identification.

### MS analysis

Selected spots were cut and digested in-gel with 20  $\mu\text{g}/\text{mL}$  trypsin (sequencing grade; Promega, Madison, WI) at 37°C O/N for liquid chromatography tandem MS (LC-MS/MS) analysis. The LC-MS/MS analyses were performed by a micro-LC (Eksigent Technologies, Dublin, CA) system that included a micro LC200 Eksigent pump with flow module 5 to 50  $\mu\text{L}$ , a programmable autosampler CTC PAL with a Peltier unit (1.0 to 45.0°C). The LC system was interfaced with a 5600<sup>+</sup> TripleTOF<sup>TM</sup> system (AB Sciex, Concord, Canada) equipped with DuoSpray<sup>TM</sup> Ion Source and Calibrant Delivery System. Data were acquired with Analyst TF 1.7 (AB Sciex). The MS files were searched using ProteinPilot software, version 4.2 (AB Sciex), with the Paragon algorithm. Samples were input with the following parameters: cysteine alkylation, digestion by trypsin, no special factors, and false discovery rate at 1%. The search was conducted using a thorough identification effort of a UniProt Swiss-Prot database containing human

proteins (version 2015.06.09 reviewed, containing 20207 sequence entries).

### HepG2 cell culture and treatments

HepG2 (human hepatoma) cells were cultured in Dulbecco's Modified Eagle Medium (Sigma-Aldrich, St. Louis, MO), supplemented with 10% fetal bovine serum and 1% penicillin-streptomycin solution (Sigma-Aldrich), in a humidified 5% CO<sub>2</sub> incubator at 37°C. Before treatments, cells were cultured O/N in serum-free medium. HepG2 cells were treated for 24 hours with 20 ng/mL of IL-6 (Sigma-Aldrich) alone or in combination with 2  $\mu\text{g}/\text{mL}$  of rhGH (Genotropin, Pfizer, New York, NY) or 5  $\mu\text{g}/\text{mL}$  of IGF-1 (Increlex, Ipsen, Boulogne-Billancourt, France). HepG2 cells were also treated with pegvisomant (25  $\mu\text{g}/\text{mL}$ ; Pfizer), a specific GH receptor-inhibitor. After 24 hours of incubation, the conditioned medium was collected and centrifuged at 1000 g for 10 minutes. Proteins were precipitated with 10% of trichloroacetic acid (Sigma-Aldrich), washed with cold Acetone (Sigma-Aldrich), resuspended in 6M Urea (Sigma-Aldrich) and quantified with the Bio-Rad Protein Assay according to the manufacturer's instructions (Bio-Rad).

### WIB analysis

Plasma or conditioned medium sample proteins were size-fractionated under reduction conditions on a 10% SDS- Polyacrylamide gels and electro-transferred to an immunoblot polyvinylidene difluoride membrane (Bio-Rad). Membranes were then blocked for 1 hour in a solution of Tris-buffered saline - 0.1% Tween-20 containing 5% of nonfat milk and then incubated with 2F4, a primary antibody against Hp (1:20,000 or 1:5000; Santa Cruz Biotechnology, Dallas, TX) and detected with a horseradish peroxidase-conjugated secondary antimouse IgG (1:5000; Merck Millipore, Darmstadt, Germany). Immunoreactive proteins were detected using enhanced chemiluminescence (Pierce Biotechnology Inc, Rockford, IL) with image capture performed using a CCD-camera linked to the ChemiDoc (Bio-Rad). Results were quantified using the QuantityOne software with values presented as arbitrary units.

### Amplification and sequencing of the Hp gene: exon 1 and the junction region of Hp<sup>del</sup> allele

Genomic DNA was extracted from peripheral blood of case-subjects and three healthy controls using the QIAamp DNA Mini Kit (Qiagen, Hilden, Germany) according to the manufacturer's instructions.

The junction region of the Hp<sup>del</sup> allele was amplified by using PCR. In addition, exon 1 of the Hp gene was coamplified as an amplification control. Primer

sequences used for the amplification of the junction region are localized in the exon 5 of the haptoglobin-related gene (33).

Primer sequences were as follows: -Hp<sup>del</sup>-U: 5'-CTTTATGGCACTGGGGAACAAGCATTTTG-3'; -Hp<sup>del</sup>-L 5'-CAG GAGGAAATTTTGTAGCCGTGGTCAGCAG-3'; -Hp-Ex1-U 5'-GCAGTGTGAAAATCCTCCAAGATAA-3'; -Hp-Ex1-L 5'-AATTTAGCCCATTTGCCCGTTT CTT-3'. PCR reactions were performed with 100 ng of genomic DNA and 0.18  $\mu$ L of AmpliTaq Gold Polymerase (Life Technologies, Foster City, CA), in a total reaction volume of 30  $\mu$ L. The temperature protocol was: initial denaturation at 95°C for 10 minutes followed by 35 cycles with denaturation at 95°C for 30 seconds, annealing at 60°C for 30 seconds and an extension at 72°C for 1 minute, with a final extension at 72°C for 10 minutes.

The PCR products were then visualized on a 2% agarose gel before bidirectional sequencing using the BigDye Terminator v1.1 Cycle Sequencing Kit and an ABI PRISM 3130xl automated sequencer (Life Technologies). Finally, the resulting electropherograms were aligned with the wild-type human Hp sequence (NM\_005143) using the Multiple Sequence Alignment Clustalw software ([www.genome.jp/tools/clustalw/](http://www.genome.jp/tools/clustalw/)).

### Statistical analysis

All the data were expressed as mean  $\pm$  SD. For continuous variables, the variation between groups was calculated by means of Student *t* test. Statistical significance was assumed for  $P < 0.05$ . All statistical analyses were performed with SPSS for Windows version 17.0 (IBM, Chicago, IL).

## Results

### Clinical characteristics

At diagnosis, patients showed lower height SDS ( $-2.23 \pm 0.33$  vs  $0.91 \pm 1.02$  SDS;  $P < 0.001$ ) and IGF-1 SDS ( $-1.50 \pm 0.11$  vs  $0.13 \pm 0.59$  SDS;  $P < 0.001$ ) compared with controls, whereas no difference was found in hemoglobin levels ( $13.5 \pm 0.9$  mg/dL vs  $13.1 \pm 0.9$  mg/dL). In cases, the GH peak at provocative tests with GHRH + arginine and with arginine/clonidine was  $14.3 \pm 1.7$  and  $4.3 \pm 1.1$  ng/mL, respectively, and seven patients had a normal pituitary morphology at MRI, whereas three showed anterior pituitary hypoplasia.

After 12 months of rhGH treatment, nobody developed other pituitary deficiencies. The mean rhGH dose was  $7.9 \pm 2.6$  mg/wk ( $33 \pm 5$   $\mu$ g/kg/day). Compared with T0, at T12 height SDS ( $-2.23 \pm 0.33$  vs  $-1.61 \pm 0.22$  SDS;  $P < 0.001$ ) and IGF-1 SDS ( $-1.50 \pm 0.11$  vs  $0.12 \pm 0.53$  SDS;  $P < 0.001$ ) significantly

improved, with a mean growth velocity of  $8.3 \pm 0.7$  cm per year.

### Two-dimensional electrophoresis analysis: GHD pediatric subjects treated with rhGH

At T0 and T12 of rhGH treatment, plasma samples from each subject were analyzed by two-dimensional-electrophoresis (2-DE) to evaluate comprehensive changes in the expression of circulating proteins. By PDQuest analysis, protein spots significantly altered between T0 and T12 in all subjects with GHD were identified ( $P < 0.05$ ). A prediction of the “top 20” spots was made on the basis of their pI and MW, in combination with the Swiss-Prot human plasma database and the TagIdent Searches (<http://web.expasy.org>) (Table 1). Interestingly, the protein spot predictions highlighted a predominance of Hp with 12 of the top 20 spots predicted to be isoforms  $\alpha$  and  $\beta$  of Hp, which showed significantly reduced levels following GH treatment (Fig. 1 and Fig. 2). The predicted identity of Hp was confirmed by LC-MS/MS (Table 2) and by WIB on 2D gels using the specific antibody anti-Hp  $\beta$ .

### Confirmation of GH-induced downregulation of Hp

The analysis of the individual data demonstrated the likely existence of a GH regulation of Hp levels. Indeed, both the WIB analysis on 2-DE and on plasma samples using specific anti-Hp  $\beta$  antibody showed a clear reduction of Hp levels [Fig. 3(a)–3(b)]. Because it is now

**Table 1. Top 20 Plasma Protein Spots With Expression Significantly Regulated by rhGH in Subjects With GHD**

SSP	pI <sup>a</sup>	MW (kDa) <sup>a</sup>	Protein Prediction
202	4.29	42.9	A1AG
306	4.67	52.4	Unknown
604	4	73.9	Unknown
1102	4.84	37.9	Clusterin
1103	4.91	36.5	Clusterin
1104	4.96	46.4	Clusterin
1201	4.97	42	<b>Hp b</b>
1202	5.1	41.4	<b>Hp b</b>
1203	5.21	41.3	<b>Hp b</b>
2102	5.21	40.6	<b>Hp b</b>
3101	5.36	40.8	<b>Hp b</b>
3102	5.38	37.7	<b>Hp b cleaved</b>
3701	5.2	93.7	IGSA
4101	5.5	40.4	<b>Hp b</b>
4102	5.55	38.5	<b>Hp b cleaved</b>
6002	5.68	17.07	<b>Hp a</b>
6103	5.69	40.3	<b>Hp b</b>
6104	5.69	38.2	<b>Hp b cleaved</b>
8001	6.07	16.88	<b>Hp a</b>
9304	6.1	56.1	Unknown

Boldface type highlights predicted Hp isoforms.

Abbreviation: SSP, PDQuest identification.

<sup>a</sup>PDQuest estimates.

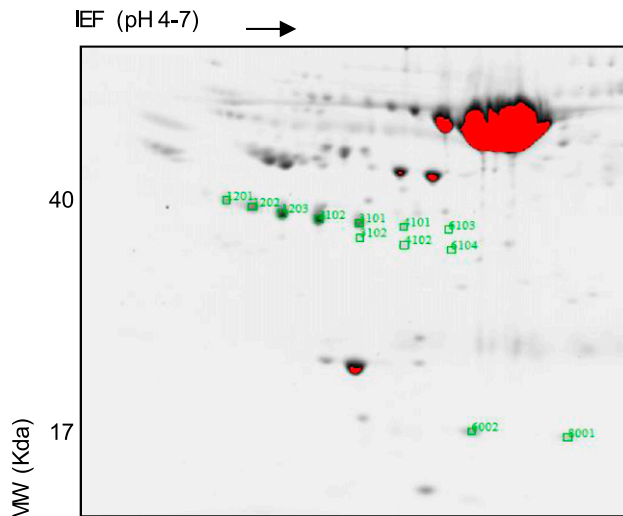


**Figure 1.** 2D-polyacrylamide gel electrophoresis of plasma protein from patients with GHD. The predicted 12 spots to be hp isoforms are highlighted by green squares and PDQuest identification number. IEF, isoelectric focusing; MW, molecular weight.

well demonstrated that CRP levels are negatively regulated by GH in adults (34), to further confirm the GH-dependent regulation of Hp levels, we used standard biochemical methods to evaluate both Hp ( $64.5 \pm 39.8$  vs  $3.14 \pm 5.00$  mg/dL,  $P < 0.001$ ) and CRP levels ( $0.124 \pm 0.174$  vs  $0.008 \pm 0.004$ ,  $P < 0.05$ ) in subjects with GHD at T0 compared with controls [Fig. 3(c)]. Furthermore, in patients with GHD, Hp ( $64.5 \pm 39.8$

$30.1 \pm 31.5$  mg/dL,  $P < 0.01$ ) and CRP levels ( $0.124 \pm 0.174$  vs  $0.04 \pm 0.119$  mg/dL,  $P < 0.05$ ) decreased at T12 compared with T0 [Fig. 3(d)]. The reduction of Hp respect to baseline was of  $48.0 \pm 24.4\%$ . We also aimed to evaluate other acute phase markers and found no difference in ferritin levels in GHD patients compared with controls at T0 ( $25.3 \pm 8.0$  ng/mL vs  $28.8 \pm 10.5$  ng/mL) and in GHD subjects at T0 vs T12 ( $25.3 \pm 8.0$  ng/mL vs  $24.7 \pm 10.2$  ng/mL), whereas platelets were higher in GHD children than in controls at baseline ( $299.5 \pm 44.5$   $10^3/\mu\text{L}$  vs  $247.8 \pm 59.5$   $10^3/\mu\text{L}$ ,  $P < 0.05$ ) and no difference was found in GHD patients between T0 and T12 ( $299.5 \pm 44.5$   $10^3/\mu\text{L}$  vs  $315.9 \pm 74.5$   $10^3/\mu\text{L}$ ; not significant).

Interestingly, we observed that one patient, although showing modest GH regulation, overall demonstrated extremely low to undetectable levels of Hp. This subject showed the presence of only three Hp  $\beta$  isoforms, with levels at the limit of detection. Despite this result, however, the data were suggestive of a reduction of all these three isoforms at T12 at WIB and 2D-E analyses. A preliminary genetic analysis was performed in this subject to better investigate this condition of hypohaptoglobinemia. The direct sequencing of the promoter region highlighted the presence of three single nucleotide polymorphisms in the heterozygous state (rs5467, rs5469, rs5472) associated with the Hp deficiency (35, 36).

### GH downregulates the expression of Hp in HepG2 cells

IL-6-treated HepG2 cells are a widely used *in vitro* model to study Hp expression (37–39). To confirm the proteomic results from subjects with GHD, HepG2 cells were treated with IL-6 in the presence or absence of GH. The analysis of the conditioned medium demonstrated that treatment of HepG2 cells with the combination of IL-6 and GH resulted in a reduction of Hp  $\beta$  secretion compared with HepG2 treated with IL-6 alone [Fig. 4(a)]. Overall, the secretion of Hp  $\beta$  is in accordance with our proteomic data, demonstrating a GH-induced regulation of Hp  $\beta$  secretion. In addition, to validate the specificity of the GH effect on IL-6-induced increase of Hp levels, HepG2 cells were treated with pegvisomant, a GH receptor inhibitor (40, 41) [Fig. 4(b)]. We observed that, although GH was able to downregulate IL-6-induced Hp secretion, Hp  $\beta$  secretion was restored in pegvisomant-treated HepG2 cells.

### Effects of IGF-1 on IL-6-induced secretion of Hp in HepG2 cells

The results obtained by treating HepG2 cells with pegvisomant demonstrated a direct and specific effect of rhGH on haptoglobin in an *in vitro* system, without

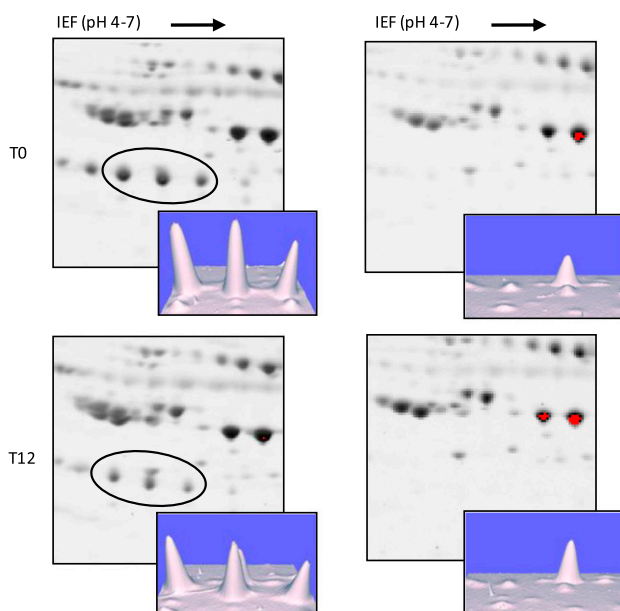


**Figure 2.** rhGH treatment in subjects with GHD reduced Hp spot intensity. A focus and 3D-image of haptoglobin spots at baseline (T0) and following 12 mos (T12) of rhGH therapy showed a reduction of the intensities of haptoglobin spots after treatment. The circled spots are represented in 3D. Subject 1 was representative of the GHD cohort selected; subject 2 showed a very low protein expression. 3D, three-dimensional.

**Table 2. Hp Identity Confirmation by LC-MS/MS Analysis**

SSP 1203				
Protein	Sequence	Mass (Da)	Sequence Coverage	UniProt Accession No.
Hp	MSALGAVIALLLWGQLFAVDSG NDVTDIADDGCPKPEIAHGY VEHSVRYQCKNYYKLRTGDGV YTLNKKQWINKAVGDKLPE CEADDGCPKPEIAHGYVE HSVRYQCKNYYKLRTGDGVY TLNNEKQWINKAVGDKLPECEA VCGKPKNPANPVQRILGGHLD AKGSFPWQAKMVSHHLLTTG ATLINEQWLLTTAKNLF LNHSENAKDIAPTLT YVGKKQLVEIEKVVLPNYSQVDI GLIKLKQKVSNERVMPICLPSK DYAEVGRVGYVSGWGRNANF KFTDHLKYVMLPVADQDQCIR HYEGSTVPEKKTTPKSPVGV QPILNEHTFCAGMSKYQED TCYGDAGSAFAVHDLLEEDTW YATGILSFDKSCAVAEYGV YVKVTSIQDWWQKTIAEN	45205	37%	P00738
SSP 2102				
Hp	MSALGAVIALLLWGQLFAV DSGNDVTDIADDGCPKPE IAHGYVEHSVRYQCKNYYKLRT EGDGVYTLNKKQWINKAVGDK LPECEADDGCPKPEIAHGYV EHSVRYQCKNYYKLRTGDGV YTLNNEKQWINKAVGDKLPE CEAVCGKPKNPANPVQR ILGGHLDKGSFPWQAKM VSHHLLTTGATLINEQ WLLTTAKNLFNLHSENAK DIAPTLTYVGKKQLVEIEKVV LHPNYSQVDIGLIKQKVS NERVMPICLPSKDYAEVGRV YVSGWGRNANFKFTDHLKYV MLPVADQDQCIRHYEGSTVPE KKTTPKSPVGVQPILNEHTFCAGM SKYQEDTCYGDAGSAFAVH DLEEDTWYATGILSFDKS CAVAEYGVYKVTIQDWWQKTIAEN	45205	34%	P00738

Trypsin-digested protein spots 1203, 2102 were resolved with LC-MS/MS. The analyzed peptides were identified with UniProt Swiss-Prot database. Abbreviation: SSP, PDQuest identification.

giving information about the possible involvement of IGF-1. Therefore, to understand if IGF-1 can directly influence the secretion of Hp induced by IL-6, HepG2 cells were treated with IGF-1 in combination with 20 ng/mL of IL-6. The data demonstrated that also IGF-1 was able to reduce IL-6–induced Hp secretion (Fig. 5).

## Discussion

GH is a multitask hormone whose lack, as in GHD, is responsible for a syndrome of metabolic dysregulation. This condition is accompanied by high cardiovascular risk and a

chronic inflammatory state, because of the presence of central adiposity, increased visceral fat, insulin resistance, and dyslipoproteinemia (10, 42). Although there are no good biomarkers for the assessment of GH therapy, patients subjected to rhGH substitutive treatment exhibit a reduction of all risk factors that are associated with the lack of GH (43). The data here presented identified Hp as potential biomarker regulated by GH. Indeed, plasmatic levels of Hp are significantly higher in pediatric patients with GHD compared with healthy controls, and a substantial reduction of Hp is visible in GHD subjects after 12 months of rhGH treatment.

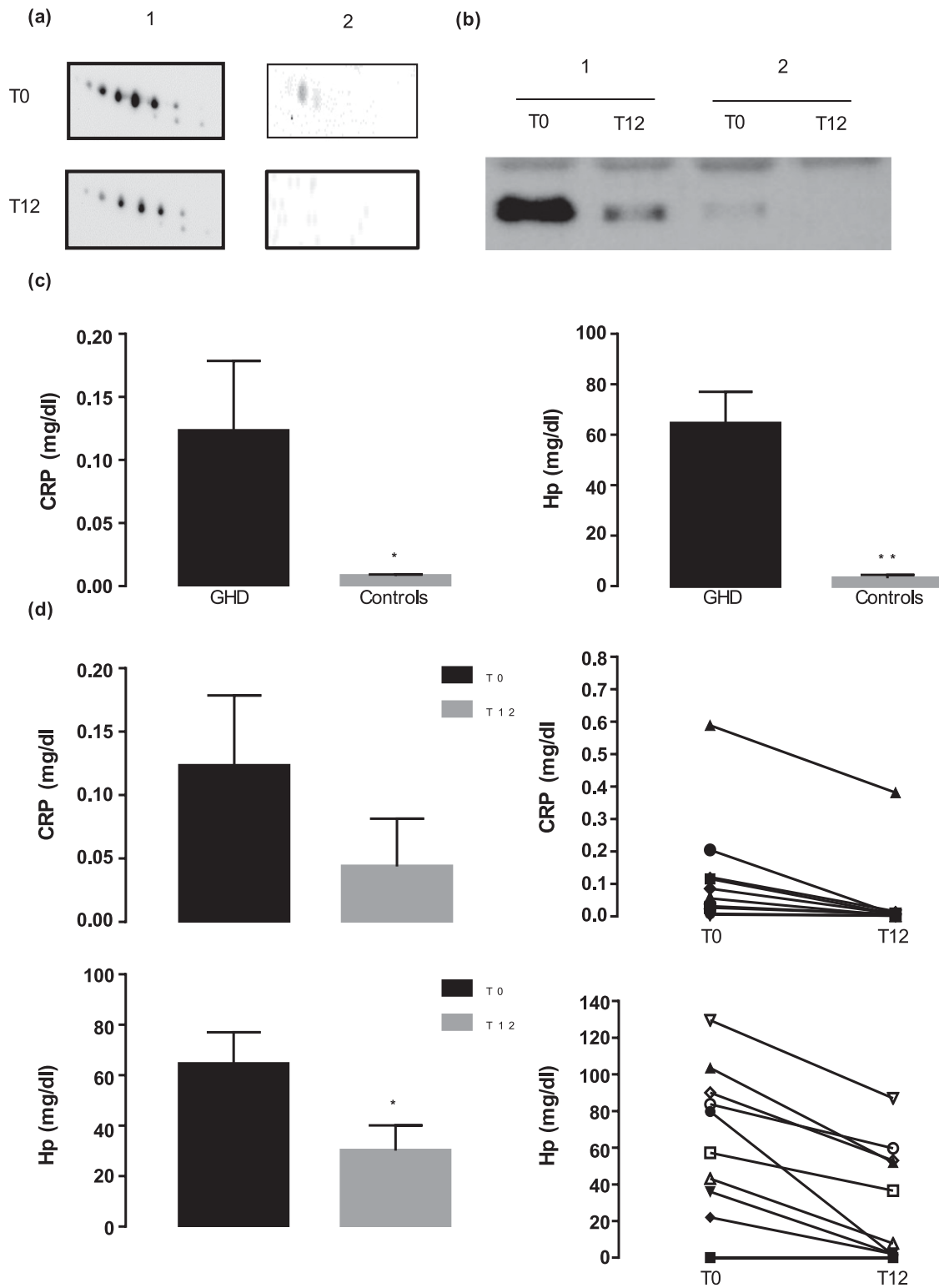


**Figure 3.** WIB and biochemical analysis confirm the Hp downregulation by rhGH in pediatric subjects with GHD. (a) A WIB on a 2D gel was performed for subjects with GHD (n = 10) at T0 and T12 using a specific antihaptoglobin  $\beta$  antibody. Two representative subjects are shown. (b) A representative WIB for Hp  $\beta$  in the plasma of patients with GHD under reduced conditions. (c) Biochemical evaluation of both Hp and CRP circulating levels in GHD (n = 10) and control subjects (n = 14) at T0. \* $P < 0.05$  and \*\* $P < 0.01$  control subjects vs subjects with GHD. (d) Biochemical analysis of circulating Hp and CRP in subjects with GHD (n = 10); the left panel shows the average of all subjects with GHD for both Hp and CRP before and after rhGH treatment (T0/T12); the right panel shows the downward trend of both circulating proteins level for each subject. \* $P < 0.05$  T12 vs T0.

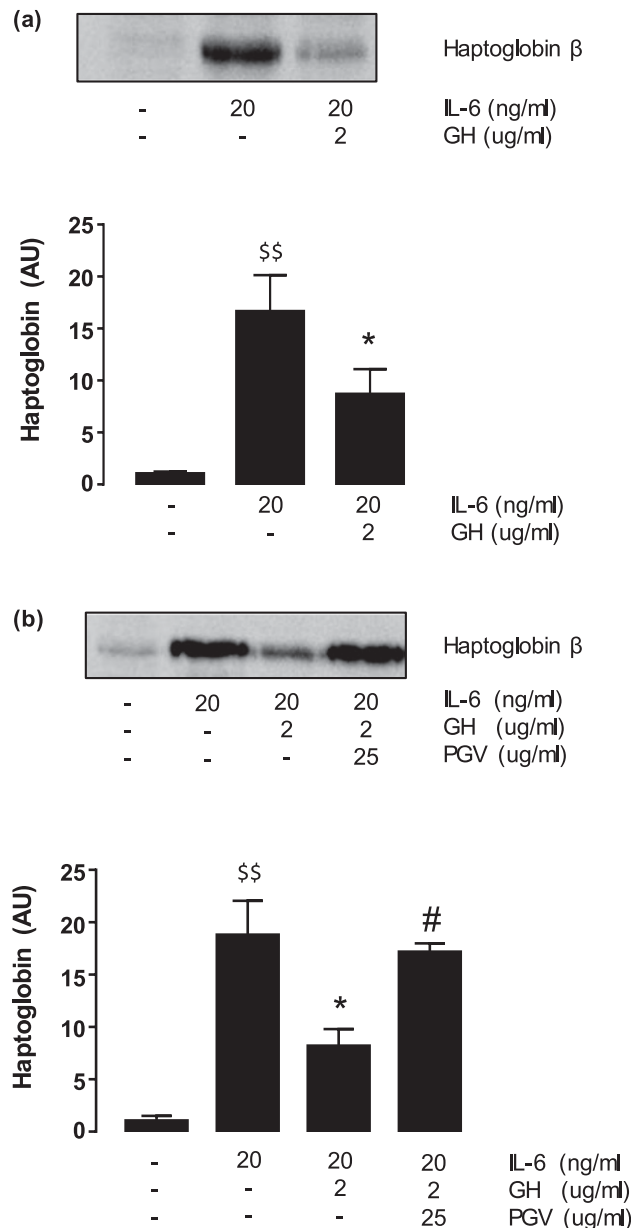


**Figure 4.** GH directly downregulates Hp secretion in HepG2 cells. HepG2 cells were treated with IL-6 alone, combined with (a) only GH or with (b) GH plus PGV in serum-free medium for 24 hours. The proteins were precipitated from conditioned medium and were separated by WIB under reduced conditions and analyzed densitometrically for the secretion of Hp  $\beta$  ( $n = 3$ ).  $$$P < 0.01$  vs control cells;  $*P < 0.05$  vs IL-6-treated cells;  $\#P < 0.05$  vs cells treated with IL-6 and GH combination. PGV, pegvisomant.

Hp is an abundant acute phase plasma glycoprotein of the  $\alpha_2$ -globulin, synthesized predominantly in the liver. Giving its well-established role as a hemoglobin-scavenging molecule, Hp protects against toxic effects associated with intravascular hemolysis-induced hemoglobin release, facilitating its clearance and preventing the formation of free radicals mediated by heme iron (44, 45). Acting as an acute phase protein, circulating levels of Hp increase in response to inflammatory cytokines, such

as IL-6 and IL-1 (46–48). For this reason, Hp is a clinical marker of the acute-phase response besides being a routine clinical marker of intravascular hemolysis (49).

The proteomic data presented here on Hp are intriguing in view of the pleiotropic effects of GH and on the chronic inflammation observed in GHD. Indeed, rhGH supplementation in pediatric subjects with GHD resulted in a reduction of the plasmatic Hp levels after 12 months of treatment. This result is supported by the well-known immunomodulatory effect of GH (16–18). In particular, long-term GH replacement therapy in adult-onset subjects with GHD modulates inflammatory activity, reducing IL-6 levels and the synthesis of acute phase reactants in the liver (43). Because IL-6 is the major inducing cytokine of Hp, GH-mediated reduction of its circulating levels supports the results presented here on Hp, suggesting its use as a possible clinical marker in pediatric subjects with GHD under GH replacement therapy. It is interesting to note that the GH effect on Hp is visible also in a patient with GHD characterized by extremely low levels of circulating Hp. Genetic analysis of the promoter region of Hp gene of this patient showed the presence of three polymorphism (rs5467, rs5469, rs5472): rs5472 was reported to be significantly associated with Hp expression, affecting the serum protein levels (35), whereas the rs5467 has been demonstrated to be associated with Hp concentrations (36). Further analyses are needed to confirm the absence of these single nucleotide polymorphisms in the GHD population characterized by normal Hp expression.

Although Hp may be a biomarker of GH therapy, it has to be considered that Hp is a hemoglobin-scavenging molecule and that it is primarily regulated by an acute phase inflammation, introducing an important bias during the follow up of patients. On the other hand, our results suggest a clear link between GHD and the associated inflammatory state, as reported by several epidemiological studies (50, 51). Furthermore, in the current study, we have not found any difference either in baseline hemoglobin levels between patients and controls or in other acute phase markers (ferritin and platelets) during GH treatment, further highlighting the potential role of Hp. Indeed, the present data increase the knowledge regarding the role of GH in inflammation and can assist in the decision to treat patients in which height was achieved. In contrast to our results, Cruz-Topete *et al.* exclude Hp as a possible biomarker of GH replacement therapy in those with GHD (52). Despite the proteomic evaluation demonstrating Hp spot intensities to be significantly modified with GH treatment, they found no important differences in the total concentration of Hp by conventional techniques such as ELISA or WIB. On the contrary, our data demonstrate substantial differences in



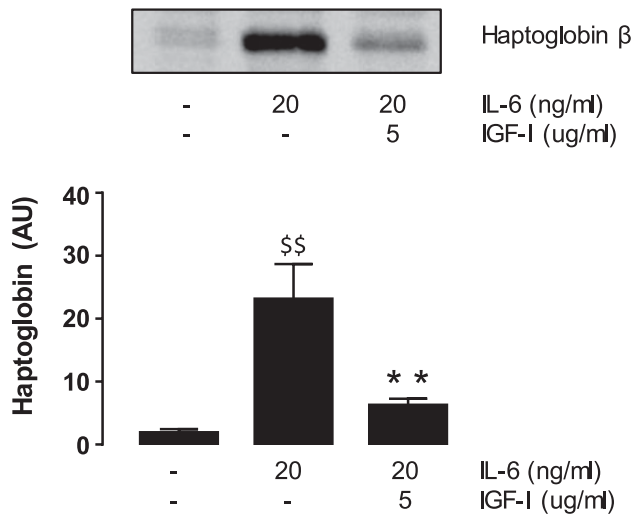


**Figure 5.** IGF-1 downregulates Hp secretion in HepG2 cells. HepG2 cells were treated with IL-6 alone or combined with IGF-1 in serum-free medium for 24 hrs. The proteins were precipitated from conditioned medium and were separated by WIB under reduced conditions and analyzed densitometrically for the secretion of Hp  $\beta$ . (n=3).  $$$P < 0.01$  vs control cells;  $**P < 0.01$  vs IL-6-treated cells.

the total Hp concentration by WIB, and these findings are confirmed by immunonephelometry. These incongruences may be explained by differences in study population because they selected an adult GHD population with a combined pituitary deficiency in which it is well known that both a not-complete substitutive treatment or an overtreatment with glucocorticoids, resulting from the formulations of therapies, constitute an important confounding factor. Given these premises, we investigated pediatric subjects with an idiopathic and isolated GHD. Moreover, their investigation was relatively short, with a follow up of 3 to 4 months. It is well known that the titration of rhGH treatment is after 6 months, and stability is more frequently reached after 12 months. In addition, GH treatment, as demonstrated on bone and glucose metabolism, frequently has a biphasic effect with a relatively short acute action completely opposed to that reported in chronic conditions (53). With this observation, we believe that Hp might be a possible additional candidate biomarker of the response to GH treatment, even if the small size of the population enrolled does not allow us to draw definitive conclusions. In accordance with the incidence of GHD in childhood (1:4000 to 1:10,000) (54), we were able to select only 10 subjects characterized by a severe GHD condition. Giving the statistical validity of these preliminary data, a multicenter longitudinal study is needed to enroll a greater number of patients and increase knowledge on the relationship between Hp and GH.

The data presented on HepG2 cells, showing the relationship between GH and Hp, support the result obtained by treating patients with GHD with rhGH,

justifying future clinical studies on a larger number of patients. Consistent with data already published, HepG2 cells express acute phase proteins in response to IL-6 treatment (38, 39) and, among them, we were able to observe Hp secretion in a short time after treatment. The use of pegvisomant, a specific and direct inhibitor of GHR, demonstrates a direct effect of GH on IL-6-mediated Hp secretion because treatment with this drug abolishes the inhibition of Hp production. On the contrary, although IGF-1 shows an effect similar to GH on Hp release, further studies are needed to evaluate the direct involvement of its receptor in Hp downregulation.

Although a direct inhibitory effect of GH on IL-6-induced Hp secretion is supported by the present data, the molecular mechanisms mediating GH actions are still unknown, and the involvement of different molecular pathways may be considered. It is known that GHR belongs to the superfamily of cytokines receptors. This assumption led us to speculate on the possibility that GH may bind to the IL-6 receptor, or *vice versa*, thus blocking the respective receptor activation, reducing Hp secretion. Wu *et al.* (55) have suggested that SOCS-3 may play an important role in the suppression of cytokines signaling mediated by GH, resulting in the downregulation of acute phase response after injury. It is possible that GH may exert an indirect action on IL-6, mediated by SOCS-3, which belongs to the SOCS protein family, whose members inhibit signal transduction by combining with JAK kinase and competing for binding with STAT (56, 57). Further studies are needed to dispel the involvement of these elements in GH action on IL-6-mediated Hp secretion.

### Study limitations

Our study has several potential limitations. It is a pilot study, and the major limit is the small size of the population. For these two reasons, we are not able to investigate the possible correlations between Hp and clinical (growth velocity) and biochemical (IGF-1) biomarkers of rhGH treatment response. Moreover, the molecular mechanisms beyond our observations remain to be clarified. Future studies on molecular pathways involved in the GH-mediated downregulation of Hp and larger longitudinal studies and randomized trials to evaluate the relationship between Hp and other markers, used in clinical practice, to assess the response to rhGH therapy are warranted to confirm our findings. Finally, a more extensive hormonal evaluation, including sex hormones, could highlight the influence of sex and puberty on Hp status.

### Conclusions

In the current study, we used a proteomic approach to analyze the global plasmatic changes between subjects

with GHD at baseline conditions and after 12 months of rhGH treatment, identifying Hp as a possible biomarker for GH treatment because its total plasma levels decrease after treatment. By using the *in vitro* HepG2 hepatocyte cell model system, we demonstrated the impact that the GH-IGF-1 axis could have on Hp secretion.

## Acknowledgment

The authors thank Umberto Dianzani for technical support.

**Financial Support:** This work was supported by Research Projects of National Interest 2008 protocol 20082P8CCE (to G.B.).

## Additional Information

**Correspondence and Reprint Requests:** Flavia Prodam, MD, PhD, Department of Health Sciences, University of Piemonte Orientale, Via Solaroli 17, 28100 Novara, Italy. E-mail: [flavia.prodam@med.uniupo.it](mailto:flavia.prodam@med.uniupo.it).

**Disclosure Summary:** The authors have nothing to disclose.

**Data Availability:** The datasets generated during and/or analyzed during the current study are not publicly available but are available from the corresponding author on reasonable request.

## References and Notes

- Møller N, Jørgensen JO, Alberti KG, Flyvbjerg A, Schmitz O. Short-term effects of growth hormone on fuel oxidation and regional substrate metabolism in normal man. *J Clin Endocrinol Metab.* 1990;70(4):1179–1186.
- Laron Z, Klingler B, Silbergeld A. Serum insulin-like growth factor-I (IGF-I) levels during long-term IGF-I treatment of children and adults with primary GH resistance (Laron syndrome). *J Pediatr Endocrinol Metab.* 1999;12(2):145–152.
- Hansen TK, Gravholt CH, ØRskov H, Rasmussen MH, Christiansen JS, Jørgensen JO. Dose dependency of the pharmacokinetics and acute lipolytic actions of growth hormone. *J Clin Endocrinol Metab.* 2002;87(10):4691–4698.
- Krag MB, Gormsen LC, Guo Z, Christiansen JS, Jensen MD, Nielsen S, Jørgensen JO. Growth hormone-induced insulin resistance is associated with increased intramyocellular triglyceride content but unaltered VLDL-triglyceride kinetics. *Am J Physiol Endocrinol Metab.* 2007;292(3):E920–E927.
- Prodam F, Zavattaro M, Caputo M, Marzullo P, Aimaretti G. In: Ghigo E, Porta M, eds. *Diabetes in growth hormone deficiency. Diabetes Secondary to Endocrine and Pancreatic Disorders. Vol 22.* Basel, Switzerland: Karger; 2014:10–21.
- Beshyah SA, Johnston DG. Cardiovascular disease and risk factors in adults with hypopituitarism. *Clin Endocrinol (Oxf).* 1999;50(1):1–15.
- Gazzaruso C, Gola M, Karamouzis I, Giubbini R, Giustina A. Cardiovascular risk in adult patients with growth hormone (GH) deficiency and following substitution with GH—an update. *J Clin Endocrinol Metab.* 2014;99(1):18–29.
- Isgaard J, Arcopinto M, Karason K, Cittadini A. GH and the cardiovascular system: an update on a topic at heart. *Endocrine.* 2015;48(1):25–35.
- Leonsson M, Hulthe J, Johannsson G, Wiklund O, Wikstrand J, Bengtsson BA, Oscarsson J. Increased interleukin-6 levels in pituitary-deficient patients are independently related to their carotid intima-media thickness. *Clin Endocrinol (Oxf).* 2003;59(2):242–250.
- Cuneo RC, Salomon F, McGauley GA, Sönksen PH. The growth hormone deficiency syndrome in adults. *Clin Endocrinol (Oxf).* 1992;37(5):387–397.
- De Boer H, Blok GJ, Voerman HJ, De Vries PM, van der Veen EA. Body composition in adult growth hormone-deficient men, assessed by anthropometry and bioimpedance analysis. *J Clin Endocrinol Metab.* 1992;75(3):833–837.
- Binnerts A, Deurenberg P, Swart GR, Wilson JH, Lamberts SW. Body composition in growth hormone-deficient adults. *Am J Clin Nutr.* 1992;55(5):918–923.
- Weaver JU, Monson JP, Noonan K, John WG, Edwards A, Evans KA, Cunningham J. The effect of low dose recombinant human growth hormone replacement on regional fat distribution, insulin sensitivity, and cardiovascular risk factors in hypopituitary adults. *J Clin Endocrinol Metab.* 1995;80(1):153–159.
- Johannsson G, Oscarsson J, Rosén T, Wiklund O, Olsson G, Wilhelmson L, Bengtsson BA. Effects of 1 year of growth hormone therapy on serum lipoprotein levels in growth hormone-deficient adults. Influence of gender and Apo(a) and ApoE phenotypes. *Arterioscler Thromb Vasc Biol.* 1995;15(12):2142–2150.
- Bengtsson BA, Edén S, Lönn L, Kvist H, Stokland A, Lindstedt G, Bosaeus I, Tölli J, Sjöström L, Isaksson OG. Treatment of adults with growth hormone (GH) deficiency with recombinant human GH. *J Clin Endocrinol Metab.* 1993;76(2):309–317.
- Inoue T, Saito H, Fukushima R, Inaba T, Lin MT, Fukatsu K, Muto T. Growth hormone and insulinlike growth factor I enhance host defense in a murine sepsis model. *Arch Surg.* 1995;130(10):1115–1122.
- Jarrar D, Wolf SE, Jeschke MG, Ramirez RJ, DebRoy M, Ogle CK, Papaconstantinou J, Herndon DN. Growth hormone attenuates the acute-phase response to thermal injury. *Arch Surg.* 1997;132(11):1171–1175, discussion 1175–1176.
- Geffner M. Effects of growth hormone and insulin-like growth factor I on T- and B-lymphocytes and immune function. *Acta Paediatr Suppl.* 1997;423(S423):76–79.
- Pagani S, Meazza C, Travaglini P, De Benedetti F, Tinelli C, Bozzola M. Serum cytokine levels in GH-deficient children during substitutive GH therapy. *Eur J Endocrinol.* 2005;152(2):207–210.
- Salerno M, Esposito V, Farina V, Radetti G, Umbaldo A, Capalbo D, Spinelli L, Muzzica S, Lombardi G, Colao A. Improvement of cardiac performance and cardiovascular risk factors in children with GH deficiency after two years of GH replacement therapy: an observational, open, prospective, case-control study. *J Clin Endocrinol Metab.* 2006;91(4):1288–1295.
- Andiran N, Yordam N. TNF-alpha levels in children with growth hormone deficiency and the effect of long-term growth hormone replacement therapy. *Growth Horm IGF Res.* 2007;17(2):149–153.
- Cañete R, Valle M, Martos R, Sánchez-Carrión A, Cañete MD, van Donkelaar EL. Short-term effects of GH treatment on coagulation, fibrinolysis, inflammation biomarkers, and insulin resistance status in prepubertal children with GH deficiency. *Eur J Endocrinol.* 2012;167(2):255–260.
- Capalbo D, Barbieri F, Improda N, Giallauria F, Di Pietro E, Rapacciuolo A, Di Mase R, Vigorito C, Salerno M. Growth hormone improves cardiopulmonary capacity and body composition in children with growth hormone deficiency. *J Clin Endocrinol Metab.* 2017;102(11):4080–4088.
- Chung CH, Levy S, Chaurand P, Carbone DP. Genomics and proteomics: emerging technologies in clinical cancer research. *Crit Rev Oncol Hematol.* 2007;61(1):1–25.
- Walker GE, De Feudis M, Roccio M, Bona G, Prodam F. Proteomics in the characterization of new target therapies in pediatric obesity treatment. In Rehman A, Choudhary MI, eds. *Anti-Obesity Drug Discovery and Development.* Sharjah, UAE: Bentham Science Publishers; 2017:3–85.

26. Sackmann-Sala L, Ding J, Frohman LA, Kopchick JJ. Activation of the GH/IGF-1 axis by CJC-1295, a long-acting GHRH analog, results in serum protein profile changes in normal adult subjects. *Growth Horm IGF Res.* 2009;19(6):471–477.
27. Growth Hormone Research Society; GH Research Society. Consensus guidelines for the diagnosis and treatment of growth hormone (GH) deficiency in childhood and adolescence: summary statement of the GH Research Society. *J Clin Endocrinol Metab.* 2000;85(11):3990–3993.
28. Schneider HJ, Kreitschmann-Andermahr I, Ghigo E, Stalla GK, Agha A. Hypothalamopituitary dysfunction following traumatic brain injury and aneurysmal subarachnoid hemorrhage: a systematic review. *JAMA.* 2007;298(12):1429–1438.
29. Godi M, Mellone S, Tiradani L, Marabese R, Bardelli C, Salerno M, Prodam F, Bellone S, Petri A, Momigliano-Richiardi P, Bona G, Giordano M. Functional SNPs within the intron 1 of the PROP1 gene contribute to combined growth hormone deficiency (CPHD). *J Clin Endocrinol Metab.* 2012;97(9):E1791–E1797.
30. Tanner JM, Whitehouse RH, Cameron N, Marshall WA, Healy WA, Goldstein H. *Assessment of Skeletal Maturity and Prediction of Adult Height (TW2 Method)*. San Diego: Academic Press; 1988.
31. Cacciari E, Milani S, Balsamo A, Spada E, Bona G, Cavallo L, Cerutti F, Gargantini L, Greggio N, Tonini G, Cicognani A. Italian cross-sectional growth charts for height, weight and BMI (2 to 20 yr). *J Endocrinol Invest.* 2006;29(7):581–593.
32. de Roos B, Duthie SJ, Polley AC, Mulholland F, Bouwman FG, Heim C, Rucklidge GJ, Johnson IT, Mariman EC, Daniel H, Elliott RM. Proteomic methodological recommendations for studies involving human plasma, platelets, and peripheral blood mononuclear cells. *J Proteome Res.* 2008;7(6):2280–2290.
33. Lee CC, Lee MS, Ho HC, Hung SK, Tung YT, Chou P, Su YC. The prognostic utility of haptoglobin genotypes in squamous cell carcinoma of the head and neck. *Clin Chem Lab Med.* 2009;47(10):1277–1283.
34. McCallum RW, Sainsbury CA, Spiers A, Dominiczak AF, Petrie JR, Sattar N, Connell JM. Growth hormone replacement reduces C-reactive protein and large-artery stiffness but does not alter endothelial function in patients with adult growth hormone deficiency. *Clin Endocrinol (Oxf).* 2005;62(4):473–479.
35. Soejima M, Sagata N, Komatsu N, Sasada T, Kawaguchi A, Itoh K, Koda Y. Genetic factors associated with serum haptoglobin level in a Japanese population. *Clin Chim Acta.* 2014;433:54–57.
36. Maeda N. DNA polymorphisms in the controlling region of the human haptoglobin genes: a molecular explanation for the haptoglobin 2-1 modified phenotype. *Am J Hum Genet.* 1991;49(1):158–166.
37. Mackiewicz A, Schooltink H, Heinrich PC, Rose-John S. Complex of soluble human IL-6-receptor/IL-6 up-regulates expression of acute-phase proteins. *J Immunol.* 1992;149(6):2021–2027.
38. Amit T, Hacham H, Daily O, Hertz P, Barkey RJ, Hochberg Z. The Hep G2 cell line in the study of growth hormone receptor/binding protein. *Mol Cell Endocrinol.* 1994;101(1-2):29–36.
39. Boe A, Canosi U, Donini S, Mastrangeli R, Ythier A, Crescenzi OS. Determination of haptoglobin expression in IL-6 treated HepG2 cells by ELISA and by RNA hybridization—evaluation of a quantitative method to measure IL-6. *J Immunol Methods.* 1994;171(2):157–167.
40. Trainer PJ, Drake WM, Katznelson L, Freda PU, Herman-Bonert V, van der Lely AJ, Dimaraki EV, Stewart PM, Friend KE, Vance ML, Besser GM, Scarlett JA, Thorner MO, Parkinson C, Klibanski A, Powell JS, Barkan AL, Sheppard MC, Malsonado M, Rose DR, Clemmons DR, Johannsson G, Bengtsson BA, Stavrou S, Kleinberg DL, Cook DM, Phillips LS, Bidlingmaier M, Strasburger CJ, Hackett S, Zib K, Bennett WF, Davis RJ. Treatment of acromegaly with the growth hormone-receptor antagonist pegvisomant. *N Engl J Med.* 2000;342(16):1171–1177.
41. van der Lely AJ, Hutson RK, Trainer PJ, Besser GM, Barkan AL, Katznelson L, Klibanski A, Herman-Bonert V, Melmed S, Vance ML, Freda PU, Stewart PM, Friend KE, Clemmons DR, Johannsson G, Stavrou S, Cook DM, Phillips LS, Strasburger CJ, Hackett S, Zib KA, Davis RJ, Scarlett JA, Thorner MO. Long-term treatment of acromegaly with pegvisomant, a growth hormone receptor antagonist. *Lancet.* 2001;358(9295):1754–1759.
42. Bates AS, Van't Hoff W, Jones PJ, Clayton RN. The effect of hypopituitarism on life expectancy. *J Clin Endocrinol Metab.* 1996;81(3):1169–1172.
43. Sesmilo G, Biller BM, Llevadot J, Hayden D, Hanson G, Rifai N, Klibanski A. Effects of growth hormone administration on inflammatory and other cardiovascular risk markers in men with growth hormone deficiency. A randomized, controlled clinical trial. *Ann Intern Med.* 2000;133(2):111–122.
44. Moreira LR, Miranda-Vilela AL, Silva IC, Akimoto AK, Klautau-Guimarães MN, Grisolia CK. Antioxidant effect of haptoglobin phenotypes against DNA damage induced by hydrogen peroxide in human leukocytes. *Genet Mol Res.* 2009;8(1):284–290.
45. Nielsen MJ, Moestrup SK. Receptor targeting of hemoglobin mediated by the haptoglobins: roles beyond heme scavenging. *Blood.* 2009;114(4):764–771.
46. Quaye IK. Haptoglobin, inflammation and disease. *Trans R Soc Trop Med Hyg.* 2008;102(8):735–742.
47. Friedrichs WE, Navarrijo-Ashbaugh AL, Bowman BH, Yang F. Expression and inflammatory regulation of haptoglobin gene in adipocytes. *Biochem Biophys Res Commun.* 1995;209(1):250–256.
48. Oliviero S, Cortese R. The human haptoglobin gene promoter: interleukin-6-responsive elements interact with a DNA-binding protein induced by interleukin-6. *EMBO J.* 1989;8(4):1145–1151.
49. Nielsen MJ, Andersen CB, Moestrup SK. CD163 binding to haptoglobin-hemoglobin complexes involves a dual-point electrostatic receptor-ligand pairing. *J Biol Chem.* 2013;288(26):18834–18841.
50. Møller N, Jørgensen JO. Effects of growth hormone on glucose, lipid, and protein metabolism in human subjects. *Endocr Rev.* 2009;30(2):152–177.
51. Trovato L, Riccomagno S, Prodam F, Genoni G, Walker GE, Moia S, Bellone S, Bona G. Isolated GHD: investigation and implication of JAK/STAT related genes before and after rhGH treatment. *Pituitary.* 2012;15(4):482–489.
52. Cruz-Topete D, Jørgensen JO, Christensen B, Sackmann-Sala L, Krusenstjerna-Hafstrøm T, Jara A, Okada S, Kopchick JJ. Identification of new biomarkers of low-dose GH replacement therapy in GH-deficient patients. *J Clin Endocrinol Metab.* 2011;96(7):2089–2097.
53. Tritos NA. Focus on growth hormone deficiency and bone in adults. *Best Pract Res Clin Endocrinol Metab.* 2017;31(1):49–57.
54. Sizonenko PC, Clayton PE, Cohen P, Hintz RL, Tanaka T, Laron Z. Diagnosis and management of growth hormone deficiency in childhood and adolescence. Part 1: diagnosis of growth hormone deficiency. *Growth Horm IGF Res.* 2001;11(3):137–165.
55. Wu X, Herndon DN, Wolf SE. Growth hormone down-regulation of interleukin-1beta and interleukin-6 induced acute phase protein gene expression is associated with increased gene expression of suppressor of cytokine signal-3. *Shock.* 2003;19(4):314–320.
56. Starr R, Willson TA, Viney EM, Murray LJ, Rayner JR, Jenkins BJ, Gonda TJ, Alexander WS, Metcalf D, Nicola NA, Hilton DJ. A family of cytokine-inducible inhibitors of signalling. *Nature.* 1997;387(6636):917–921.
57. Babon JJ, Kershaw NJ, Murphy JM, Varghese LN, Laktyushin A, Young SN, Lucet IS, Norton RS, Nicola NA. Suppression of cytokine signaling by SOCS3: characterization of the mode of inhibition and the basis of its specificity. *Immunity.* 2012;36(2):239–250.